Norwegian
Meteorological
Institute

MET report

no. 21/2013
Air Pollution

Atmospheric Transport of Radioactive Debris to Norway in Case of a Hypothetical Accident Related to the possible Recovery of K-27 Submarine

Jerzy Bartnicki, Heiko Klein, Ali Hosseini, Øystein Hov, Hilde Haakenstad, Ole Christian Lind, Brit Salbu and Cato C. Szacinski Wendel

Norwegian Meteorological Institute

MET report

Title	Date
Atmospheric Transport of Radioactive Debris to Norway in Case of a Hypothetical Accident Related to the possible Recovery of K-27 Submarine	December 16, 2013
Section	**Report no.**
KL	21/2013
Author(s)	**Classification**
Jerzy Bartnicki, Heiko Klein, Ali Hosseini, Øystein Hov, Hilde Haakenstad, Ole Christian Lind, Brit Salbu and Cato C. Szacinski Wendel	● Free ○ Restricted
Client(s)	**Client's reference**
NRPA	

Abstract

This project has been performed in close collaboration between Norwegian Meteorological Institute (MET), Norwegian Radiation Protection Authority (NRPA) and the Norwegian University for Life Sciences (NMBU) in the framework of CERAD - CoE (Centre of Environmental Radioactivity - Centre of Excellence). This is a sub-project within a Norwegian project lead by NRPA focusing on the possible consequences for Norway in case of a nuclear criticality accident related to the recovery of the Soviet K-27 nuclear submarine, which in September 1981 was scuttled at 30 m depth in the Stepovogo Bay, north-eastern coast of Novaya Zemlya. The main goal of this study is to analyse atmospheric transport and deposition of radioactive debris to Norwegian territory, in case of a nuclear accident related to the recovery of K-27.

Keywords

Nuclear accident, risk assessment, atmospheric dispersion, threat to Norway, submarine

H. Fagerli

Disciplinary signature
Hilde Fagerli

Øystein Hov

Responsible signature
Øystein Hov

Meteorologisk institutt
Meteorological Institute
Org.no 971274042
post@met.no

Oslo
P.O. Box 43 Blindern
0313 Oslo, Norway
T. +47 22 96 30 00

Bergen
Allégaten 70
5007 Bergen, Norway
T. +47 55 23 66 00

Tromsø
P.O. Box 6314
9293 Tromsø, Norway
T. +47 77 62 13 00

www.met.no
www.yr.no

Contents

1. Introduction

This study supports the Norwegian project lead by Norwegian Radiation Protection Authority (NRPA) assessing risks related to plans of salvaging and decommissioning of the Russian nuclear submarine, K-27. It is also a part of the research activity of the Centre for Environmental Radioactivity (CERAD). The Norwegian Meteorological Institute (MET) and Norwegian Radiation Protection Authority (NRPA) are member institutions of CERAD.

In September 1981, the K-27 submarine was scuttled at a very shallow depth of just 30 meters in the outer part of Stepovogo Bay, north-eastern coast of Novaya Zemlya. A map of the present location of K-27 submarine is shown in Fig. 1.

Figure 1: A map with the present location of K-27 submarine. Source: http://rt.com/news/k-27-submarine-arctic-oil-040/.

The nuclear submarine K-27 is one of several objects with spent nuclear fuel (SNF) which has been dumped in the Kara Sea . It contains two liquid metal reactors (LMRs) of 70 MW maximum thermal power each and Pb-Bi was used as the coolant. The reactors were loaded

with 180 kg of 90 % enriched U-235. In September 1981, the submarine was dumped in the shallow waters of Stepovogo Fjord at 30 m depth. Concerns have been expressed by various parties concerning radiological consequences of potential release of radionuclide from the submarine K-27 in the Kara Sea and in particular potential releases if a rescue operation of the submarine is initiated.

One of the possible scenarios that are included in the NRPA's assessment is the lifting the submarine and subsequently transporting it to Gremikha Bay in the Murmansk area for dismantling. A risk of accidents as a consequence of an uncontrolled chain reaction event cannot be ruled out. Such a hypothetical accident might pose a threat to Norwegian territory and has to be analysed from different perspectives. Here, we concentrate on the worst case meteorological scenario for Norway as a receptor, but the same approach can be applied for other Scandinavian countries and Russia. The main goal of this study was to analyse atmospheric transport and deposition of radioactive debris to Norwegian territory, in case of nuclear accident related to lifting and transporting the K-27 submarine. The operational SNAP (Severe Nuclear Accident Program) dispersion model was the main tool in the analysis, which has been performed in the following steps:

1. Compilation of large meteorological database for 30 years
2. Development of the preliminary sources term for selection procedure
3. SNAP runs for each day of two months of 30-year period
4. Selection of the worst case meteorological scenarios and statistical analysis
5. Development of the final source term for selected worst case SNAP runs
6. SNAP runs for selected meteorological scenarios
7. Analysis and discussion of the results and transfer of data to NRPA

As a first step in this study, a large database with meteorological data has been prepared for the period of thirty three years (1980-2012). This meteorological database is available for the domain of the size 4400 km $\times$ 2600 km which includes both the entire Norwegian territory and the region of Novaya Zemlya, as shown in Fig. 2.

The spatial resolution of the meteorological data is $0.1^\circ \times 0.1^\circ$. The temporal resolution is one hour for precipitation and three hours for all other elements. The vertical structure includes 40 layers. The most important meteorological elements are the 3-D velocity field, the surface precipitation field and the 3-D temperature field.

The second step in the study was the development of the preliminary source term for potential accidents which could be used by the dispersion model SNAP available at MET. Three locations for potential accidents with subsequent releases of radioactivity to the environment were assumed: 1) in the present location of K-27, 2) on the way to Murmansk and 3) in Gremikha Bay in the Murmansk region.

In the third step, the SNAP model was run starting twice a day (00UTC and 12UTC) for selected two months (August and September) of the entire 33 years period with meteorological data. These two months were selected, because these were the only ones with meteorological conditions good enough for lifting and transport of K-27 submarine. As a result of the model simulations, surface concentration fields and deposition fields were calculated for radioactive particles in the entire model area.

Based on these results, the worst case meteorological scenarios were selected. They were selected based on the highest levels of deposition on Norwegian territory. In addition, statis-

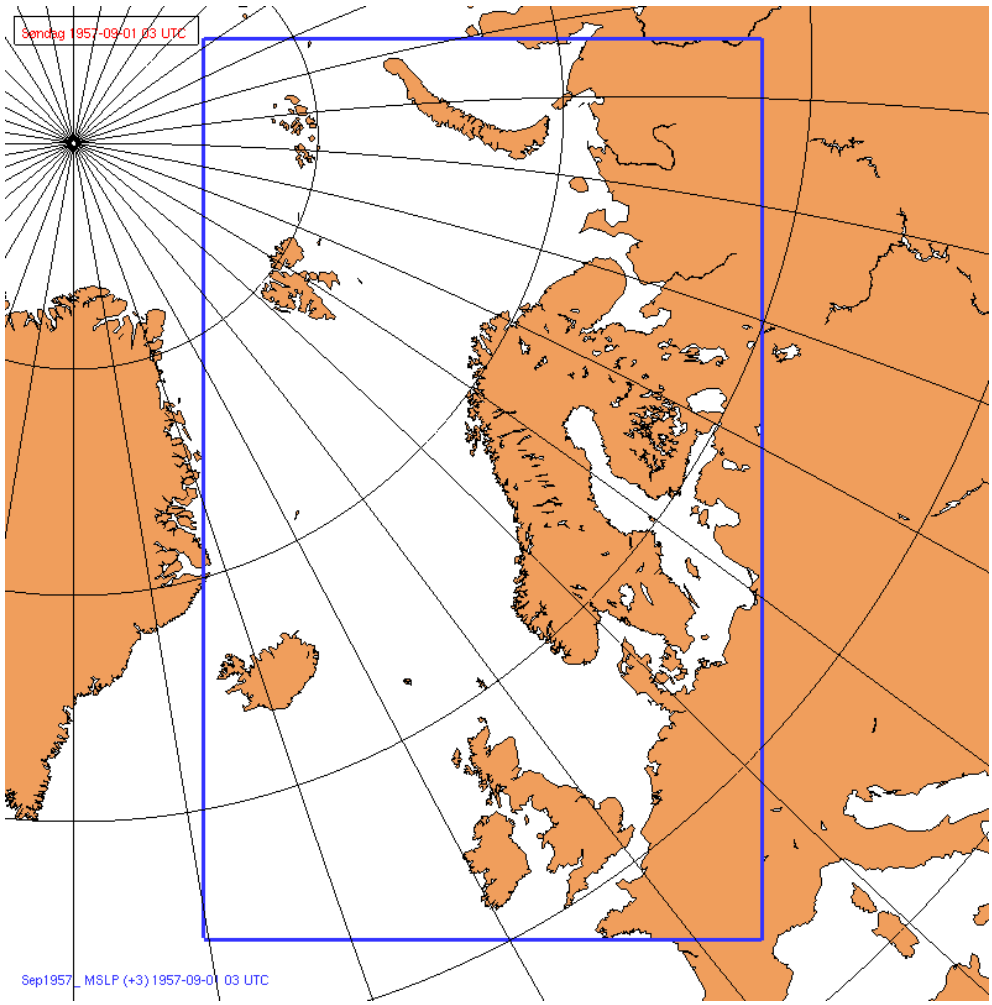

Figure 2: Domain (within blue frame) with meteorological data for the period 1980-2012 used in this study.

tical analysis was performed for the 33-year period. This analysis included calculation and discussion of the probability of arrival to arbitrary place in Norway and the calculation of shortest arrival time.

In the last two steps, the final source term corresponding to most likely accident scenario was developed and the SNAP model was run with this source term for selected worst case meteorological scenarios. The results of these runs are presented and discussed in the present report. These results were also transferred to NRPA in digital form.

The model results corresponding to the worst case scenario will feed into a subsequent impact assessment.

2. SNAP Model

The Severe Nuclear Accident Program (SNAP) model is a Lagrangian particle model, which has been developed at MET(former DNMI) for simulating atmospheric dispersion of radioactive debris, first from nuclear accidents and then from nuclear explosions. In addition to radioactive applications, SNAP was also used to simulate large fires in London and atmospheric dispersion of volcanic ash from Ejafjallajöokull eruption in 2010 [10].

The basic concept of a Lagrangian particle model is rather simple in principle. The emitted mass of radioactive debris is distributed among a large number of model particles. After the release, each model particle carries a given mass of selected pollutant which can be in the form of gas, aerosol or particulate matter. A model particle in this approach is given an abstract mathematical definition, rather than a physical air parcel containing a given pollutant. It is used in SNAP as a vehicle to carry the information about the pollutant emitted from the source. The model particle is not given a definite size and can be not subdivided or split into parts. On the other hand, the mass carried by the particle can be subdivided and partly removed during the transport.

As in case of many other models, the development of SNAP started after the Chernobyl accident which occurred in April 1986. The first, preliminary version of SNAP [33] was based on the early version of the NAME model [24]. This SNAP version became fully operational at DMNI in December 1995 [34], [32], [35] as a part of the major Management Project (MEMbrain), in the framework of EUREKA (EU-904) activity. This operational version of SNAP was tested against tracer measurements in the European Tracer Experiment (ETEX) [36], [37] and then improved [3]. In 1996, SNAP was compared with two other models, one of Lagrangian type (NAME model from UK meteorological Office) and one Eulerian (EMEP model modified for radioactive pollution from the Norwegian Meteorological Institute) [25]. These three models produced similar results concerning the location of radioactive cloud, but the differences in concentrations were larger. The SNAP model was compared with many other models and tested on measurements available from the tracer releases not only in the frame of ETEX experiments, but also ATMES experiment [39].

In the frame of joint project between met.nod NRPA, SNAP was used in analysis of potential threat from hypothetical accident in Kola nuclear power plant [4], [38], [40]. The results of SNAP calculations indicated that, in case of accident the radioactive cloud can reach Northern Norway already after six hours and Oslo after two days from the accident start.

In the early versions of the SNAP model only small (diameter below 1 μm) particles were taken into account in the model equations. Some measurements, performed by University of Life Sciences after Chernobyl accident, showed that in certain cases also much larger (of the order of 20 μm) particles, so called hot particles were transported for long distances reaching Norway. Therefore, parametrization of particles with arbitrary diameter and density was introduced into the SNAP model and this model version was applied to simulate the Chernobyl accident again [5], [6]. This version was also applied for simulating the potential release from Kola once again, this time focusing on radioactive particles of different size and density [7], [8].

SNAP has been an active member of the ENSEMBLE group [15] and project for the last 10 years. There are at least three important advantages of this on-going project: 1) possibil-

ity of comparing SNAP results with more than 20 other models in the same grid system, 2) possibility for the backup in case of problems with SNAP, and 3) possibility of creating the ensemble forecast giving a hint on uncertainty of the results, very important for the decision makers [16], [17].

Introduction of arbitrary particles into the SNAP equations made it possible to create a SNAP version for nuclear explosion [41], [6], [9]. This model version was also used as a basis for developing the source term for volcanic eruption and deposition of volcanic ash in SNAP, used to simulate atmospheric dispersion of volcanic ash from Ejafjallajöokull eruption in 2010 [10].

2.1. Meteorological input and model domain

The SNAP model is flexible concerning, both model domain and meteorological data. The spatial and vertical structure of the SNAP model domain is in fact defined by the meteorological input. The Hi Resolution Limited Area Model (HIRLAM) model version 7.1.3 [47] is used as the meteorological input provider for operational version of SNAP. However in this study, we have used a meteorological database especially developed for the project and described in details in Section 3.1. The model domain in this database was shown in Fig. 2. There are 40 vertical layers in the model grid system for this application.

For historical reasons the FORTRAN code of SNAP has been developed for a single processor computer and was implemented on several platforms at MET with the possibility of external use of the model by the NRPA. This solution creates some backup and security for operational applications in nuclear emergency, but at the same time it creates some limits for the operational model use in case of many different radionuclides and relatively long, over 10 days, release period. The main limits are: the available memory and the time of the computations.

2.2. Standard Source term and components

The source term can be specified individually for each SNAP application. The source geometry is time dependent in the SNAP model and can be specified differently for each time segment of the release. However, the number of model particles released at each model time step is the same for the entire period of the release. The source term can be also specified separately for each substance which is released into the atmosphere. Gases, noble gases and particles can be included for dispersion simulation in SNAP. The individual radionuclides are represented in the model by different model particles which can have different properties. The release rate is separate for each component included in the model run and can vary in time.

As in the earlier versions of SNAP [41], [6], there are two options for parametrizing geometry of the source: cylinder or two cylinders one above another (mushroom shape). This version assumes that all model particles are uniformly mixed and distributed in the cylinder volume immediately after release. Different model particles are used for each substance - pollutant and therefore the trajectories of these model particles can also differ. The radius of the cylinder, as well as the bottom and top of the cylinder are specified in the input file for the model run.

The arbitrary radionuclides released into the air can be simulated by SNAP, but there is also a standard list of possible radionuclides which is used by NRPA within the ARGOS system. The list of isotopes which are included in the ARGOS system and can be run by SNAP is shown in Appendix A. This list includes the name of isotope, type (noble gas, aerosol and Iodine) and decay rate for each isotope.

2.3. Mixing height

As good as possible determination of the mixing height, which represents in the model the depth of atmospheric boundary layer (ABL), is very important for modelling atmospheric transport and deposition of air pollution. The turbulent diffusion is significantly more intensive in the ABL and only pollution in the boundary layer is a subject of dry deposition.

The procedure to identify and calculate the mixing height h is based on critical Richardson Number formulation R_{iC}. The gradient Richardson Number, R_i, is calculated for a given model layer from

$$R_i = \frac{g\Delta\theta_i/\Delta z}{\bar{T}(\Delta\mathbf{u}/\Delta z)^2} \tag{1}$$

where $\Delta\theta_i/\Delta z$ and $\Delta\mathbf{u}/\Delta z$ are the gradients of potential temperature and wind speed, g is the acceleration due to gravity and $\bar{T}$ is the mean temperature of the layer. It is assumed that the mixing height can be determined from the meteorological input data at which a small positive number of R_i is reached, below which turbulent motion tends to persists and above which it is suppressed. The critical value R_{iC} is used to identify the top of the ABL that is, the mixing height h. The model gradients of potential temperature and wind, $\Delta\theta/\Delta z$ and $\Delta\mathbf{u}/\Delta z$, are used to search for R_{iC} layer by layer, starting from the surface and stepping upward trough the model layers. The value $R_{iC} = 1.8$ is used for determining the mixing height in the SNAP model.

2.4. Advection and diffusion

The advective displacement of each model particle is calculated at each model time step, Δt, which is equal to 5 minutes (300 s) in the present SNAP version. For this calculation, three-dimensional velocity is interpolated to particle position from the eight nearest nodes in the model grid. Bilinear interpolation in space is applied to horizontal components of the velocity field and linear interpolation for the vertical component. In addition, linear interpolation in time is applied between sequential meteorological input fields. The advective displacement of each particle in one model time step is calculated according to

$$\mathbf{x}'_{t+\Delta t} = \mathbf{x}_t + [\mathbf{u}(\mathbf{x}_t) + \mathbf{u}_g(\mathbf{x}_t)]\Delta t \tag{2}$$

where $\mathbf{x}_t = (x, y, \eta, t)$ is the position of particle, $\mathbf{u} = (x, y, \eta, t)$ is velocity from the numerical weather prediction model and $\mathbf{u}_g = \mathbf{u}_g(x, y, \eta, t)$ is the gravitational setting velocity for the given model particle, all at time t. The intermediate position of the particle after advection is denoted by the vector $\mathbf{x}'_{t+\Delta t}$.

The calculation of gravitational settling velocity included in Eq. 2 is described in the next Section. A relatively simple iterative procedure developed by Petersen [27] is used for numerical solution of Equation 2. This procedure is using velocity fields at time levels t and $t+\Delta t$. We have found two iterations in this procedure to be entirely sufficient for calculating the new position of the model particle. So, the final position of the model particle after advection can be calculated directly as:

$$\mathbf{x}_{t+\Delta t} = \mathbf{x}_t + \frac{1}{2}[\mathbf{u}(\mathbf{x}_t) + \mathbf{u}(\mathbf{x}_{t+\Delta t}) + \mathbf{u}_g(\mathbf{x}_t) + \mathbf{u}_g(\mathbf{x}_{t+\Delta t})]\Delta t \tag{3}$$

Eq. 3 is used for all model particles and at each model time step for calculating a new position after advection.

2.4.1. Gravitational settling velocity

For conditions when the Stokes law is valid, gravitational settling velocity with spherical shape of particles is a function of particle size, particle density and air density [45]:

$$v_g = \frac{d_p^2 g(\rho_p - \rho_a)C(d_p)}{18\nu} \tag{4}$$

where:
d_p is the particle diameter,
g is the acceleration due to gravity,
ρ_p is the particle density,
$\rho_a = \rho_a(p,T)$ is the density of the air at particle location,
$C(d_p)$ is Cunningham correction factor,
$\nu = \nu(T)$ is the dynamic molecular viscosity of the air at particle location.

The density of the air is calculated from the equation of state

$$\rho_a = \frac{p}{RT} \tag{5}$$

where
p is the atmospheric pressure,
T is the absolute temperature,
$R = 287.04$ is the gas constant for dry air ($Jkg^{-1}K^{-1}$)

Viscosity of the air is a function of temperature [28]:

$$\nu = 1.72 \times 10^{-5} \frac{393}{T+120}\left(\frac{T}{273}\right)^{\frac{3}{2}} \tag{6}$$

and Cunningham correction factor for small particles [45] is calculated as:

$$C(d_p) = 1 + \frac{2\lambda}{d_p}(1.257 + 0.4e^{-0.55\frac{d_p}{2\lambda}}) \tag{7}$$

where $\lambda = 6.53 \times 10^{-8}$m is the mean free path of air molecules. Eq. 4 is not valid for particles with the radius larger than 10-15 μm. In case of the larger particle classes, correction to account for high Reynolds numbers is necessary. Such a correction was introduced in the SNAP model [6] leading to the following set of equations [45]:

$$\begin{array}{ll} v_g(1+\frac{3}{16}Re+\frac{9}{160}Re^2\ln 2Re) = \frac{d_p^2 g(\rho_p-\rho_a)C(d_p)}{18\nu} & 0.1 < Re \leq 2 \\ v_g(1+0.15Re^{0.578}) = \frac{d_p^2 g(\rho_p-\rho_a)C(d_p)}{18\nu} & 2 < Re \leq 500 \end{array} \tag{8}$$

where $Re = v_g d_p \rho_a / \nu$ is the Reynolds Number. Eq. 8 is non-linear and requires a numerical solution, which may significantly slow down the model performance, if it is applied to each individual particle at each model time step. In the present version of SNAP, there is an option for using the tabulated values of gravitational settling velocities for each of the selected particle class. This table is calculated only once at the beginning of each model run, so that application of these equations did not significantly reduced the model performance.

2.4.2. Random walk method

Random walk techniques giving effect to diffusion are described in detail in [31]. The Wiener-type of process used here is governed by a length scale, the sequence of steps following the description by Mayron [24]. A slightly different parametrization is used for particles located within boundary layer and for those above, but can be described by the same equations. The new particle position is calculated as:

$$\begin{array}{l} x'' = x' + r_x l \\ y'' = y' + r_y l \\ \eta'' = \eta' + r_\eta l_\eta \end{array} \tag{9}$$

where $\mathbf{x}''_{t+\Delta t} = (x'', y'', \eta'')$ is the particle position vector at time $t + \Delta t$ after application of the diffusion algorithm; r_x,r_y,r_η are randomly sampled numbers from the range (-0.5,+0.5), generated from uniform distribution; l and l_η are the length scales from the horizontal and vertical turbulent motion. Horizontal diffusion above the ABL in SNAP is parametrized in the same way as for the particles below, but the value of the coefficient of proportionality is different for two regions. We assume horizontal length-scale for the turbulent motion, defining horizontal diffusion:

$$l = ax^b \tag{10}$$

where $x = |\mathbf{u}|\Delta t$, $|\mathbf{u}| = \sqrt{u^2+v^2}$ is the wind speed in m/s, $b = 0.875$, $a = 0.5$ in ABL and $a = 0.25$ above.

The scale of vertical diffusion is $l_\eta = 0.08$ within ABL and $l_\eta = 0.001$ above the boundary layer. Parametrization of vertical diffusion in the present version of SNAP is relatively simple, probably too simple especially in the ABL. We plan to improve this part of the model and implement more accurate ABL parametrization available already in the EEMEP and EMEP [46] models which are operational at MET. It should be also mentioned that in most of the dispersion models, vertical diffusion is very week above the ABL and in some models it is even neglected [23].

2.4.3. Boundary conditions

When displaced, particles can reach the boundaries of the model domain. Since SNAP is a model of the Lagrangian type, formulation of boundary conditions is relatively simple.

For particles with larger diameter like 10 μm and above, the mechanism of gravitational settling can be effective in moving them quickly to the ground. If the position of model particle, representing the size 10 μm and above, is lower than the ground level $\eta > 1.0$, the entire particle is removed from the further computations and its entire mass is added to dry deposition matrix. In the random walk process, the model particles representing the size below 10 μm cannot penetrate the surface - the bottom boundary of the model domain. If the "small" particle hits the ground in the random walk procedure, it is reflected back into the boundary layer.

A similar procedure is applied to the model particles reaching the upper boundary of the model domain. At the top of the model domain, there is no exchange of particles. This assumption implies the closed upper boundary conditions.

Particles can flow out of the lateral boundaries of the model domain, but they cannot enter the model domain from the outside. This implies open lateral boundary conditions.

2.5. Dry deposition

Gases and many particles of different size are released into the atmosphere during nuclear accident and especially during nuclear explosion. For relatively large particles, the dry deposition process is dominated by the gravitational settling. However, for the relatively small particles with the diameter below 3 μm, other processes are dominating the removal of particles from the air. Therefore, not only gravitational settling, but also other surface related processes are included in the parametrization of dry deposition.

A key parameter in the dry deposition process is the dry deposition velocity v_d, which can be calculated based on the resistance analogy [45]. In this approach, dry deposition of gases is governed by steady-state mass conservation equation:

$$F = K(z)\frac{\partial c}{\partial z} \tag{11}$$

where $K(z)$ is the diffusion coefficient and c is the concentration. Integration of the Eq. 11 gives:

$$F = K(z)\frac{c(z)}{r(z)} \tag{12}$$

where $r(z) = \int_0^z \frac{dz}{K(z)}$ is the resistance to vertical transport. The Eq. 12 has the same form as equation for an electrical circuit with voltage corresponding to concentration, current to flux and electrical resistance to transport resistance.

The dry deposition velocity v_d is defined as an inverse of resistance, and the dry deposition flux can be calculated as:

$$F = v_d(z)c(z) \tag{13}$$

According to Seinfeld [45] Eq. 11 can be also applied for particles with the following formulation of dry deposition velocity:

$$v_d = \frac{1}{r_a + r_s + r_a r_s v_g} + v_g \tag{14}$$

In Eq. 14, the aerodynamic resistance r_a accounts for turbulent diffusion from the free atmosphere to surface laminar sub-layer and it is a function of meteorological parameters such as wind speed, atmospheric stability and surface roughness. The surface layer resistance r_s is related to diffusion trough a laminar sub-layer and is more dependent on molecular than turbulent properties. For the latest version of SNAP, we have assumed the total resistance in Equation 14 to be 200 s m^{-1}. The gravitational settling velocity is dominating dry deposition process for large particles. For very large particles, emitted into the atmosphere during nuclear accident or explosion, this leads to the simplification $v_d \approx v_g$.

Venkatram and Pleim [49] pointed out that Eq. 14 is not strictly valid for particles because dry deposition flux associated with particles does not depend on the concentration gradient. Assuming that turbulent transport and particle settling can be added together, the vertical flux can be calculated as follows [12]:

$$F = K(z)\frac{c}{r} + v_g c = v_d c \tag{15}$$

The dry deposition velocity in Eq. 15 has the following form [49]:

$$v_d = \frac{v_g}{1 - e^{-r v_g}} \tag{16}$$

where r is the total resistance for particles. Since the differences between dry depositions calculated with Eq. 17 and Eq. 16 are small [49], we still use Eq. 17 in operational version of SNAP.

In our calculations, we assumed that the model particles located above the surface layer h are not affected by the dry deposition process. The height of the surface layer is defined as 10% of the mixing height. Reduction of the particle activity, A, due to dry deposition in one time step Δt, for each model particle located within the surface layer can be calculated as:

$$A(t + \Delta t) = A(t) exp(-\frac{v_d}{h_s}\Delta t) \tag{17}$$

where h_s is the height of the surface layer. In addition to mass reduction of the model particles in dry deposition process, the particles reaching the ground in due to gravitational settling are entirely eliminated from the model and their mass is added to dry deposition matrix.

The above parametrization of dry deposition is relatively simple, except gravitational settling velocity calculations. This simple approach can affect the deposition field and concentrations in the ABL. However, in SNAP applications for nuclear accidents and explosions, the uncertainty introduced by simplifications in dry deposition parametrization is much lower than the uncertainty due to unknown source term.

The present version of SNAP can be remotely applied from NRPA both for nuclear accidents and nuclear explosions. In case of nuclear explosion, relatively large particles, with diameter up to 300 μm are injected into the air. For these large particles, not dry deposition but

gravitational settling is the most effective mechanism for removing them from the dry air. To take this fact into account, we first calculate vertical transport of model particles governed by the sum of large scale vertical velocity and gravitational settling velocity. If the model particle hits the ground, its activity is in 100% deposited to the surface and stored in the deposition matrix. In this way we can make consistent parametrization of dry deposition with calculation of gravitational settling and vertical transport.

2.6. Wet deposition

Wet deposition is the most effective process in removing soluble gases and particles of different size from the atmosphere. This process includes absorption of particles into the droplets in the clouds (rain-out) and then droplet removal by precipitation (washout). Wet deposition process depends on many complicated factors, which are difficult to take into account, like for example occult deposition related to fog, scavenging by snow, effect of convective precipitation and orographic effects.

In the present version of the model, we have assumed that the mass of particle, m affected by precipitation is reduced during one model time step Δt in the following way:

$$m(t+\Delta t) = m(t)e^{-k_w \Delta t} \tag{18}$$

Following Baklanov and Sørensen [2], the coefficient of wet deposition k_w is a function of the particle radius r (in μm) and the precipitation intensity q (in mm per hour). For below cloud scavenging, the coefficient of wet deposition is calculated differently for three classes of particles:

$$k_w(r,q) = \begin{cases} a_0 q^{0.79} & r \leq 1.4 \\ (b_0 + b_1 r + b_2 r^2 + b_3 r^3) f(q) & 1.4 < r \leq 10.0 \\ f(q) & 10.0 < r \end{cases} \tag{19}$$

where
$f(q) = a_1 q + a_2 q^2$,
$a_0 = 8.4 \times 10^{-5}$, $a_1 = 2.7 \times 10^{-4}$, $a_2 = -3.618 \times 10^{-6}$,
$b_0 = -0.1483$, $b_1 = 0.3220133$, $b_2 = -3.0062 \times 10^{-2}$, $b_3 = 9.34458 \times 10^{-4}$.

In Equation 19, the wet deposition coefficient for small particles ($r \leq 1.4\mu m$) and for large particles ($10.0\mu m < r$) does not depend on the particle size, but on precipitation intensity. Only for particles in the range ($1.4\mu m < r \leq 10.0\mu m$), wet deposition coefficient is a function of both particle size and precipitation intensity.

Wet deposition process between cloud base and cloud top (rain-out) depends on the type of precipitation - dynamic or convective. Wet deposition coefficient for dynamic precipitation is close to wet deposition coefficient below the cloud and can be also estimated by Eq. 19. The wet deposition is more effective for convective than dynamic precipitation. Therefore, wet deposition coefficient for convective precipitation between cloud base and top is estimated according to Maryon et. al. [26] in the following way:

$$k_w(r,q) = a_0 q^{0.79} \tag{20}$$

where $a_0 = 3.36 \times 10^{-4}$. The wet deposition coefficient within the cloud is not dependent on the particle size as it was suggested by Crandall et. al. [11].

In many cases and in convective situation especially, precipitation does not occur in the entire model grid square. The area of the model grid square covered by precipitation as a function of precipitation intensity was originally estimated in [18]. In the SNAP model we use a probability curve Fig. 3 based on this estimation. From the probability curve we can find the probability of the model particle to be affected by precipitation in a given model grid as a function of precipitation intensity. If the probability ϕ of precipitation for a given location of the model particle is above zero, we replace the precipitation intensity q in Equation 19 by the effective precipitation intensity $q_{eff} = q/\phi$.

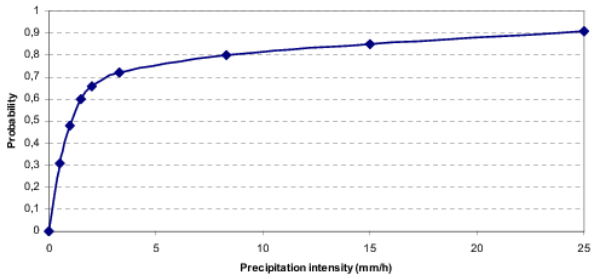

Figure 3: The probability curve for precipitation used in the SNAP, model and taken from [18].

In addition, there is an elevation limit for model particles to be a subject of wet deposition. In the present version of SNAP, we have assumed that only those particles located below the model level $\eta = 0.76$ are losing mass due to wet deposition. This η level corresponds roughly to 2000 m.

2.7. Radioactive decay

All isotopes included in the SNAP model are subject to radioactive decay. The half-life time for arbitrary radionuclide can be specified in input file for the model run. For remote applications of SNAP from NRPA the radionuclides specified in Appendix A are used in the model runs. This specification also includes information about the decay constant. The relation between half-life time $T_{1/2}$ and decay constant λ is the following:

$$T_{1/2} = \frac{ln2}{\lambda} = \frac{0.693}{\lambda} \tag{21}$$

The activity of any isotope remaining in the air after time t is calculated according to the following equation:

$$A(t) = A_0 e^{-\lambda t} \tag{22}$$

where $A(t)$ is the activity at time T and A_0 is the initial activity of the considered isotope. The calculations are performed at every time step Δt, so:

$$A(t+\Delta t) = A(t)e^{-\lambda t} \tag{23}$$

The radioactive decay is also affecting a part of each isotope already deposited to the ground, so the same approach is applied to matrices of wet and dry deposition for each isotope at each model time step.

$$\begin{aligned} D_{dry}(i,j,t+\Delta t) &= D_{dry}(i,j,t)e^{-\lambda t} \\ D_{wet}(i,j,t+\Delta t) &= D_{wet}(i,j,t)e^{-\lambda t} \end{aligned} \tag{24}$$

where $D_{dry}(i,j,t)$ and $D_{wet}(i,j,t)$ are matrices of dry and wet deposition respectively.

3. Selection of the worst case meteorological scenario

In order to find out the worst case meteorological scenarios for Norway, first of all, we needed a large database with historical meteorological fields as input for the SNAP runs. This database was compiled for a 33-year period: 1980-2012 and this was a time demanding tasks. The next important question was related to the selection procedure for the worst case meteorological scenario. A preliminary analysis showed, that we could not apply the final accident scenario described in Section 4.2, because of too long computational time needed. A simplification was necessary and we were forced to use only one radionuclide in the preliminary source term for selecting meteorological situations of interest. A large meteorological database was also used for statistical analysis of the radioactivity transport to Norway in case of release from K-27 submarine. In this analysis the probability of arrival was of the main interest.

3.1. Meteorological database

The European Medium Range Weather Forecast Centre (ECMWF) in Reading is a valuable source of not only meteorological forecasts, but a long term historical meteorological data, as well. The comprehensive earth-system model has been developed at ECMWF and forms the basis for all the data assimilation and forecasting activities. All the main applications required are available through one integrated computer software system (a set of computer programs written in FORTRAN) called the Integrated Forecast System or IFS.

The ECMWF ReAnalysis 40 - ERA40 [48] is a well known, first historical database developed at ECMWF. This is a 45-year global re-analysis carried out with the goal of producing the best possible set of meteorological data from the past. Later on, a second historical database was developed at ECMWF: ERA-Interim [14]. The aim of this new global re-analysis was to improve and replace ERA40. It was called interim, because the original project started as a test and ended up as a success.

For the specific Norwegian needs, a historical meteorological database NORA10 was developed [29] by downscaling the HIRLAM model ERA40 reanalysis and the ECMWF-IFS operational analysis. The spatial resolution of NORA10 data was approximately 11 km.

In this study, a new meteorological database called NORA10-EI has been used. The database NORA10-EI has been produced by dynamical downscaling with the same HIRLAM model as in the production of NORA10, but with downscaling the ERA-Interim reanalysis instead of the two datasets; the ERA40 re-analysis and the ECMWF-IFS operational analysis. The advantage of using the ERA-Interim re-analysis, is that this reanalysis is produced with a single assimilation and forecast system version and is therefore not affected by changes in the method as the ECMWF-IFS operational analyses are. ERA-Interim also uses better input data and better assimilation method compared to ERA40 and has also an increased spatial resolution of approximately 80 km, compared to ERA40 which has approximately 125 km resolution.

The NORA10-EI covers the same area as NORA10; the north-eastern North Atlantic and the Nordic mainlands. The NORA10-EI has also the same horizontal resolution as NORA10; approximately 11 km. Surface fields are stored every hour, while model level fields are stored every third hour. This database covers the period January 1980 and up to December 2012.

The dynamical downscaling is performed with the NWP model, HIRLAM version 6.4.2 [47], running series of short prognostic runs initialized form a blend of ERA-Interim and the previous prognostic run. The blending is responsible for preserving the fine-scale surface features obtained in the hindcast, while maintaining the large scale synoptic field from ERA-Interim as well. Main features of the HIRLAM NWP model used for producing NORA10-EI database are given in Table 1.

3.2. Selection procedure

It is difficult to formulate a set of objective criteria for selecting the worst case meteorological scenario for the atmospheric transport of radioactive pollutants to Norway. Such attempt was made in the past for Kola NPP as a source [4], [39], but anyway the 'objective criteria' became quite subjective at the and of this process, depending on individual judgement.

A semi-natural ecosystem in the Northern Norway can be very sensitive to depositions of radioactive substances with relatively slow decay. We also know that wet deposition is the most effective mechanism responsible for significant depositions far away from the original source. Therefore the wet meteorological situation is one important aspect of the worst case scenario. especially, the situation with the long atmospheric transport without precipitation on the way and strong precipitation on arrival point is of interest.

If we look at the problem from a health-administrative perspective, we should concentrate more on large population centres and the cumulative doses to the population by inhalation. This perspective will make the dry meteorological situations most important. Transport from the source with calm winds and stable atmosphere will create high concentrations at the receptor which might last relatively long. Such conditions may cause maximum exposure and radiological dosage to the population.

An additional aspect deserves some attention if we see the problem from the point of view of the Norwegian Nuclear Preparedness Organization namely short travel time. It can be a serious problem for this organization since, notifying and assembling the key members of the decision making team, then making decisions and implementing the proper measures are all time consuming. Short travel time for the debris to reach Norway requires a state of high preparedness for the organization as a whole.

The selection of the worst case meteorological scenario from 33-year database is a time demanding task for any chosen criteria. It has to be done by performing SNAP model runs for given accident scenario twice a day for the entire considered period. There are three accident locations which have to be taken into account: 1) the initial - present location of K-27, 2) the location on the way to Murmansk region and 3) final location at the receptor at Gremikha Bay. A map with all three locations of the potential accidents is shown in Fig. 4.

The accident can happen only during two months of each year (August and September) at the initial location and on the way to Gremikha Bay. At the final location, accident can happen any time of the year, however in the present calculations, we have only used the same two months as for other locations. With the above assumptions more than 12000 model runs are required in the selection procedure.

Table 1: Main features and parameters of the HIRLAM NWP model used for producing NORA10-EI long term meteorological database.

Parameters	
Horizontal grid points	248 × 400
Number of vertical levels	40
Horizontal resolution (deg)	0.1 × 0.1
Large scale forcing method	Blending: [51]
Initialization	IDFI
Host model	ERA-Interim: [14]
Boundary forcing interval	6 hours
Forecast length	9 hours
Cycle interval	6 hours
Time step	240 s
Parametrisation schemes	
Micro physics and convection	Soft TRAnsition COndensation (STRACO) - gradual transitions between the condensation types. Convection: [21], [22]. Microphysics for large scale condensation and precipitation: [42].
Radiation scheme	Savijärvi radiation scheme [44] which provides the net radiative fluxes plus the temperature tendency of air resulting from terrestrial (long-wave) and solar (short-wave) radiation. [43], [50]
Land surface model	Mosaic of tiles [1] Detailed classification into surface types. The different land use patches evolve independently and couple directly to the atmosphere of the model
Surface layer physics	ISBA (Interaction Soil Biosphere Atmosphere), [**?**] is used for the land surface types. Soil temperature and soil water content are treated with force-restore models. The soil is divided in two layers: one surface layer with a depth of 1 cm and a total layer extending down to a depth of about 1 m.
Planetary boundary layer	TKE-l turbulence scheme based on prognostic turbulent kinetic energy combined with a diagnostic length scale built on the CBR-scheme [13].
Static data	HIRLAM Static data (19 categories). Global 30 Arc Second Elevation data (GTOPO30), USGS, 1998. The Global Land Cover Characteristics (GLCC), USGS, 1997.

Figure 4: Three accident locations which have been taken into account in the selection procedure: 1) the initial - present location of K-27, 2) the location on the way to Murmansk region and 3) final location at the receptor at Gremikha Bay.

3.2.1. Source term for the selection procedure

The conditions for hypothetical accident are slightly different at three selected potential locations and in principle three different accident scenarios should be created corresponding to each accident location. However, mainly because of computational time limit, we have used only one and simplified source term for all accident locations. Assuming only one accident scenario, the simplified source term is summarised in Table. 2.

The simplified source-term defined in Table. 2 has been used only for the selection of the worst case meteorological scenarios. The size and density are taken from ARGOS database included in Appendix A used by radiation protection authorities in Scandinavian countries: Norway, Denmark Sweden and Finland. This is more or less the smallest particle size in this database, which is a subject of the longest atmospheric transport and the least effective wet deposition on the way. The release rate and period as well as vertical range are in a good

Table 2: Specification of the preliminary source term used for the selection procedure

Parameter	**Value**
Initial Location Intermediate Location Final Location	72.5N 55.5E 69.5N, 47.0E 68.04N,39.33E
Radionuclide Particle size	Cs-137 in the particle form 0.55 μm
Particle density	2.3 g cm^{-3}
Release rate	2.0×10^{11} Bq s^{-1} (Total release - 8.64×10^{15} Bq)
Release period	12 hours
Vertical range	0-500 m

agreement with what was typically used in the MetNet exercises (five Scandinavian countries).

We have run the the SNAP model for all three accident locations. The model has been run twice a day at 00:00UTC and 12:00 UTC, in the months of August and September for the entire period of 33 years available in our meteorological database. This means 12078 model runs in total. For such a large number of runs, it was not possible to examine the results of each individual run visually, so we have used a simple automatic algorithm for the selection purpose. It was applied to each of three accident locations separately. In the algorithm, we calculated the total deposition of Cs-137 to Norwegian territory for each model run and assigned it to the release date. Initially, we included Svalbard as Norwegian territory in the selection procedure. This choice created some strange results concerning worst case scenarios and we decided to exclude Svalbard from further calculations and concentrate on the ”main” territory of Norway without Svalbard. In the next step of the selection procedure, we sorted the output file according to deposition values and picked up the situations with largest depositions. The top cases on the sorted list were then inspected visually for selection of the worst case meteorological scenarios. The results of the selection procedure for all three release locations are shown in Table 3. Top for cases and the last case - with lowest average deposition over Norway are shown in Table. 3.

The number of cases with deposition above zero is decreasing with the distance between the release location and Norway. For releases at initial location, on the way and at final destination, probability of reaching Norwegian Territory is 17%, 25% and 37%, respectively. Also, the average deposition over Norway is clearly dependant on the distance from the release location, with the largest depositions for the source at final destination. There is en exception however with largest deposition for the source located on the transport route and case from from 7 September 1986 at 12 UTC. This exceptional case is discussed in Section 3.3.2.

The final selection of the worst case meteorological scenarios is discussed in the following sections.

Table 3: Results of the selection procedure for the worst case meteorological scenarios for all three releases locations. The time of accident start is shown as year, month, day and hour (UTC). Average deposition over Norway is given in Bq m^{-2}.

Initial location		
Rank	**Date**	**Av. Dep.**
1	1986 09 06 00	4877.7
2	1986 09 05 12	3271.8
3	1998 08 26 00	3145.9
4	1986 09 06 12	2933.4
.	. . . . .	. . . . .
620	1983 09 19 12	0.0003
On the way		
Rank	**Date**	**Av. Dep.**
1	1986 09 07 12	6424.9
2	1986 09 07 00	4970.1
3	1998 09 17 00	4277.8
4	1999 08 15 12	4257.6
.	. . . . .	. . . . .
930	2009 08 20 00	0.0003
Final destination		
Rank	**Date**	**Av. Dep.**
1	2009 08 23 12	6184.8
2	2004 09 22 00	6000.5
3	2004 09 22 12	5992.6
4	2006 08 16 00	5644.5
.	. . . . .	. . . . .
1342	1983 09 07 12	0.0007

3.3. Worst case meteorological scenarios

The results of the selection procedure - worst case meteorological scenarios are discussed separately for each location of the hypothetical accident. When selecting the worst case meteorological scenario we took into account not only absolute values of the average deposition for Norway, as listed in Table. 3, but the spatial distribution over Norwegian territory as well.

3.3.1. Worst case for the initial location

Deposition maps corresponding to top four meteorological cases listed in Table. 3, for accident at the initial location of K-27 in Novaya Zemlya, are shown in Fig. 5. For three out of top four meteorological cases, only northern and central part of Norway is covered by the deposition with strong maximum in the North. Average deposition in case number three is approximately 35% lower than average deposition in case number one, but almost entire territory of Norway, including Oslo is covered by the deposition in this case. The maximum above 3000 Bq m^{-2} is again located far North, but deposition in the South is still significant, above 300 Bq m^{-2}. Therefore, we have selected the case number three as the worst case meteorological scenario for hypothetical accident at the initial destination of K-27 with the accident start on 26 August 1998 at 00 UTC.

3.3.2. Worst case on the way to Gremikha Bay

Deposition maps corresponding to top four meteorological cases listed in Table. 3, for accident on the way from Novaya Zemlya to Gremikha Bay near Murmansk, are shown in Fig. 6. For this accident location, all four cases do not reach the south of Norway, but the top case in Table. 3, with the accident start on 7 September 1986 at 12 UTC, covers the entire coast of Western Norway and a large part of Central Norway. This is also the case with absolute maximum of average deposition over Norway for all three accident locations - 6425 Bq m^{-2}. These were the main reasons for selecting this case as the worst case meteorological scenario for accident on the way. It is interesting to notice the case number three with the accident start on 17 September 1998. In this case the radioactive cloud is passing only through the very northern part of Norway and then turning North towards Svalbard. Deposition is very large in the north of Norway, reaching Bq m^{-2}, but there is no deposition in the remaining territory of Norway.

3.3.3. Worst case for the final destination

For accident located at the final destination, all four cases in Table. 3 show very high level of average deposition, close to 6000 Bq m^{-2}. The spatial pattern of the deposition in cases two and three is quite similar, however in case three, deposition in southern Norway is larger, above 1000 Bq m^{-2}. Since the average deposition in case three (with the accident start on 22 September 2004 at 12 UTC) is only 5% lower than the average deposition in top case, it was selected as the worst case meteorological scenario for accident located at the final destination.

It should be mentioned that this meteorological worst case scenario is also the worst case among three accident locations from the Norwegian perspective. Additional factor confirming

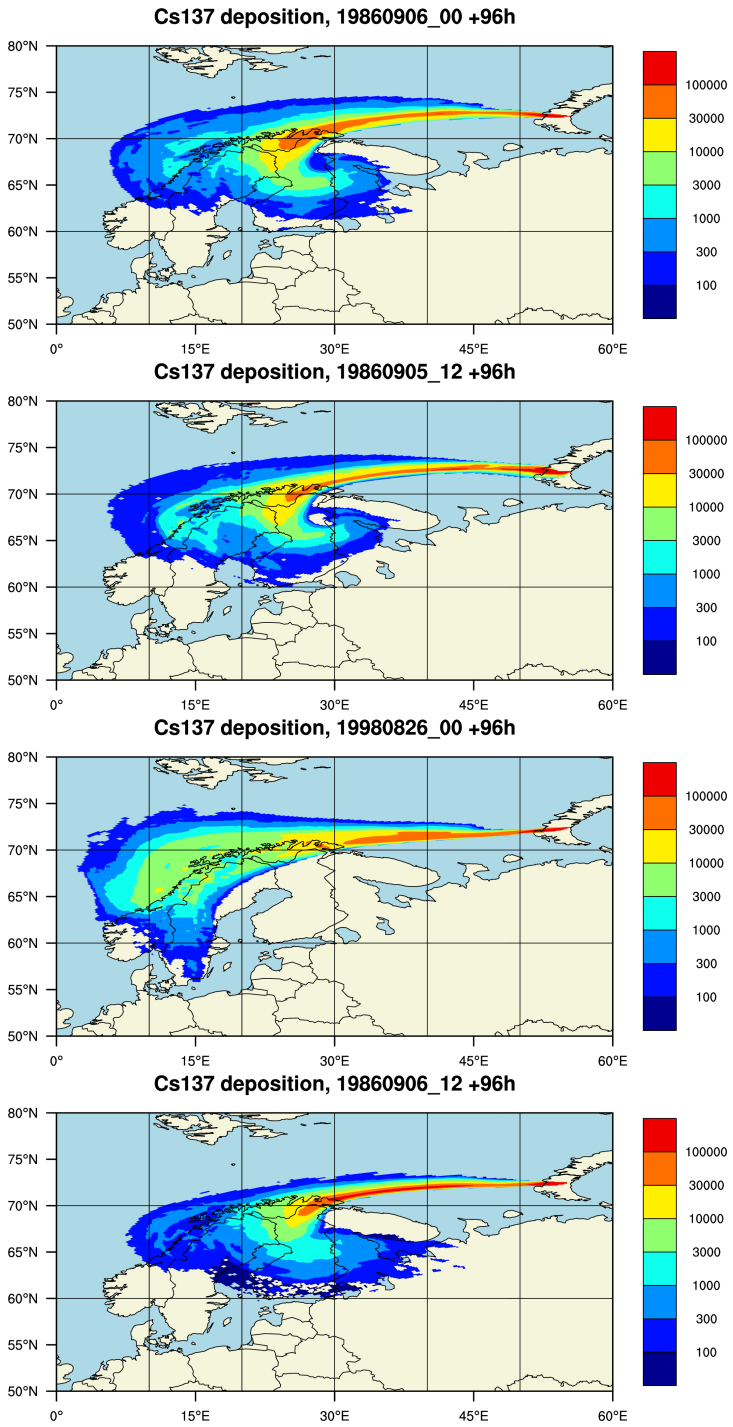

Figure 5: Deposition maps of Cs-137 for accident at the initial location of K-27, 96 hours after the accident start. The date and hour of the accident start are shown above each map. Top four meteorological cases from Table. 3. Units: Bq m^{-2}

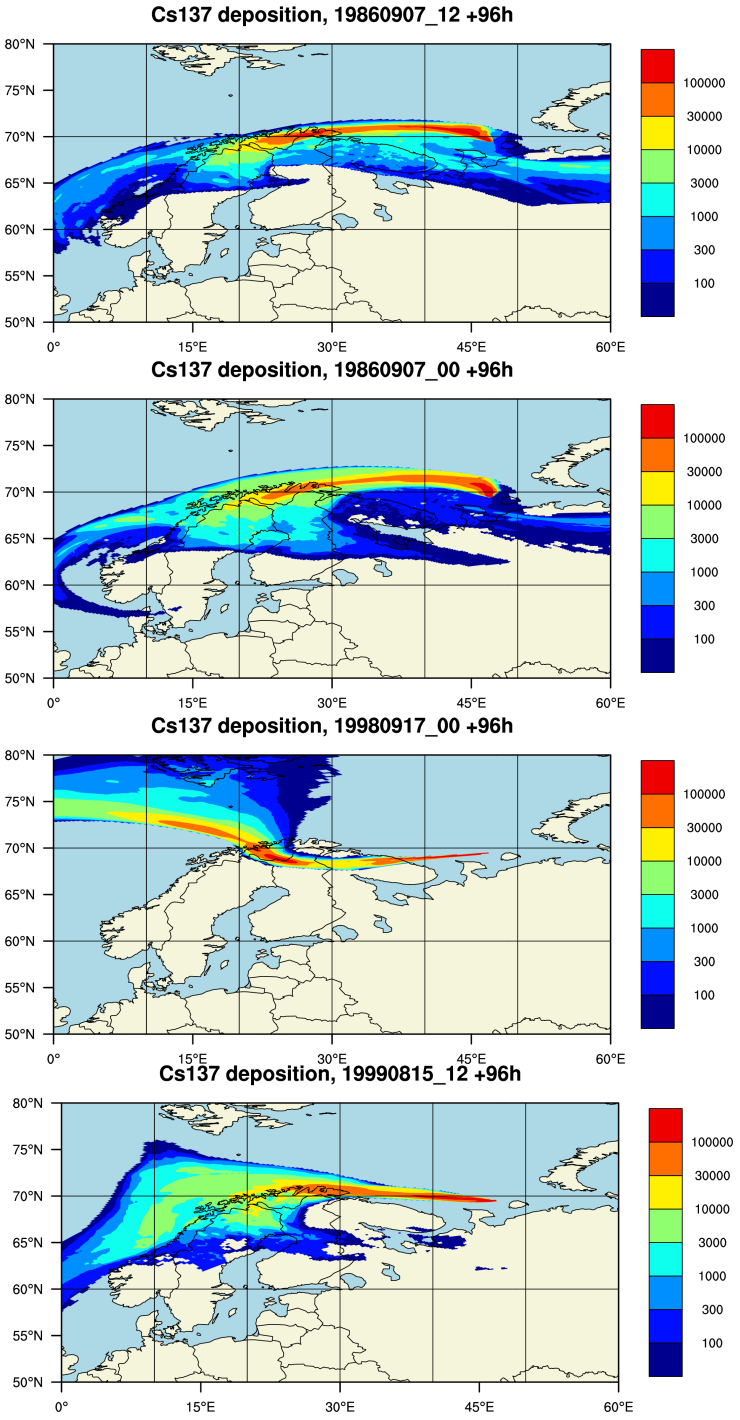

Figure 6: Deposition maps of Cs-137 for accident during the transport, 96 hours after the accident start. The date and hour of the accident start are shown above each map. Top four meteorological cases from Table. 3. Units: Bq m^{-2}

this statement is a possibility of potential accident during the entire year and not only during two months like for remaining two accident locations.

It should be also stressed that for the complete analysis of the transport to Norway from the potential accident at the final destination at Gremikha Bay, all months of each year from the meteorological database should be used. It was not possible during 2013, because of a very limited time for the project. However, we plan to continue in 2014 and to perform the complete analysis of the worst case meteorological scenarios in the frame of CERAD activities.

3.4. Statistical analysis of threat to Norway

Statistical analysis of the threat to Norway is based on the results of all model runs in August and September of each year of the entire thirty three year period. It includes calculations of total deposition and probability of arrival for the entire period and for each model grid belonging to the territory of Norway. This analysis was performed only for one radionuclide Cs-137, because of a very long computational time it requires. However, the source term for Cs-137 is very close to the worst case accident scenario and we do not expect worse results for other radionuclides. Statistical analysis was performed separately for each of the three accident locations.

3.4.1. Cases with arrival to Norway

The first question to be answered concerning results of the statistical analysis is: in how many cases the radioactive pollutants released during hypothetical K-27 accident are coming to Norway and what is the deposition level for each of this case? The answer to this questions is illustrated in Fig. 8 with average depositions for all cases with arrival to Norway and from all accident locations. The blue colour dominates in the upper part of Fig. 8 indicating much larger number of the cases arriving to Norway from Gremikha Bay than from other two locations. This not a surprise, because the release source in Gremikha is located much closer to Norway than the two remaining accident sources. There are less cases of arrival from the source on the way to Gremikha (shown in red) and less again from the sources at initial location of K-27 at Novaya Zemlya (shown in yellow). Also the values of average deposition over Norway are highest for the source in Gremikha Bay and lowest for the source at initial locations. In three cases of the transport from Gremikha Bay and in one case of the transport from the source on the way to Gremikha the average deposition over Norway exceeded 6000 Bq m^{-2}.

The percentiles for the deposition to Norwegian territory (excluding Svalbard) is also shown in Fig. 8. Also in this chart the dominance of Gremikha over two other locations concerning number of arrivals to Norway is quite clear. The results are very similar for the sources located at the initial location and on the way to Gremikha. Compared to other accident locations, there is significantly more transport to Norway and with higher average deposition over Norway, from the final destination of K-27 in Gremikha Bay. It should be noticed that only 37% of the releases at any location are coming to Norway in the model simulations.

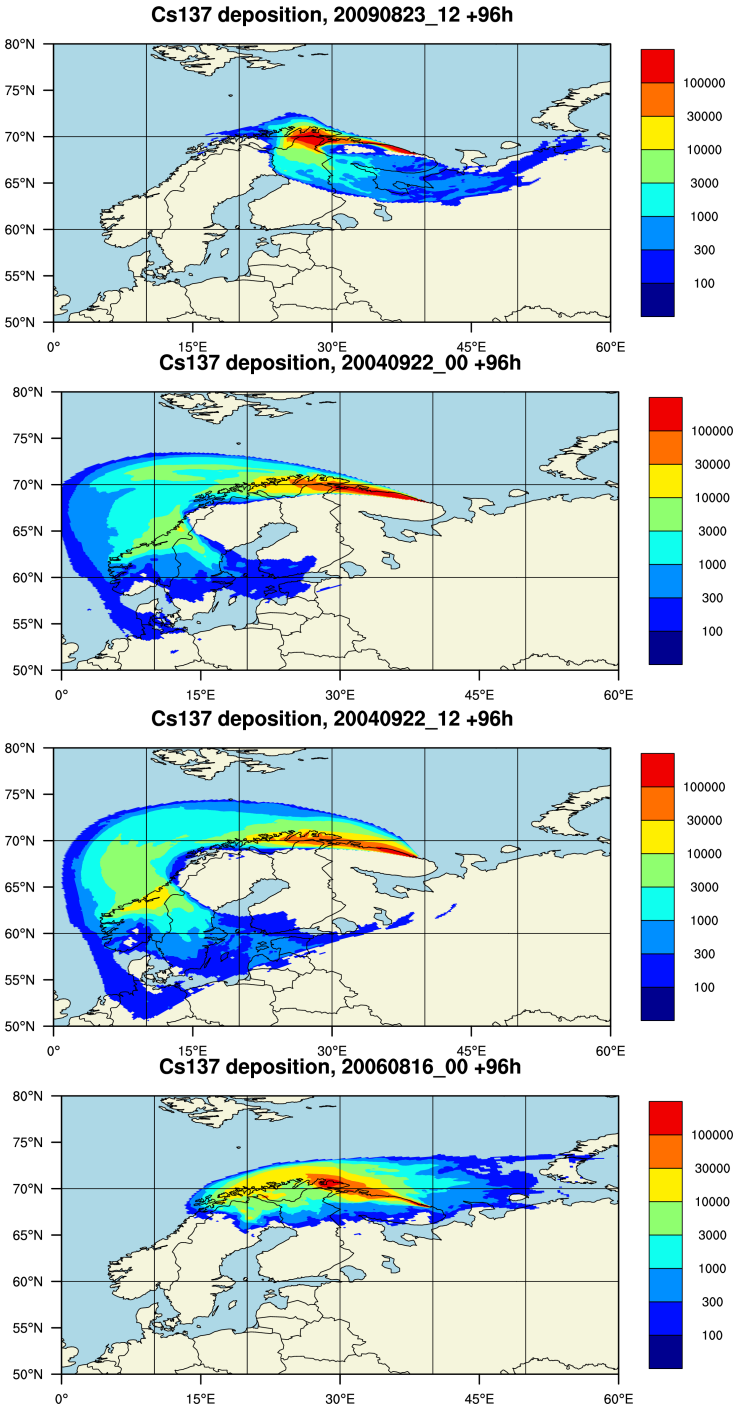

Figure 7: Deposition maps of Cs-137 for release at the final destination, 96 hours after the accident start. The date and hour of the accident start are shown above each map. Top four meteorological cases from Table. 3. Units: Bq m^{-2}

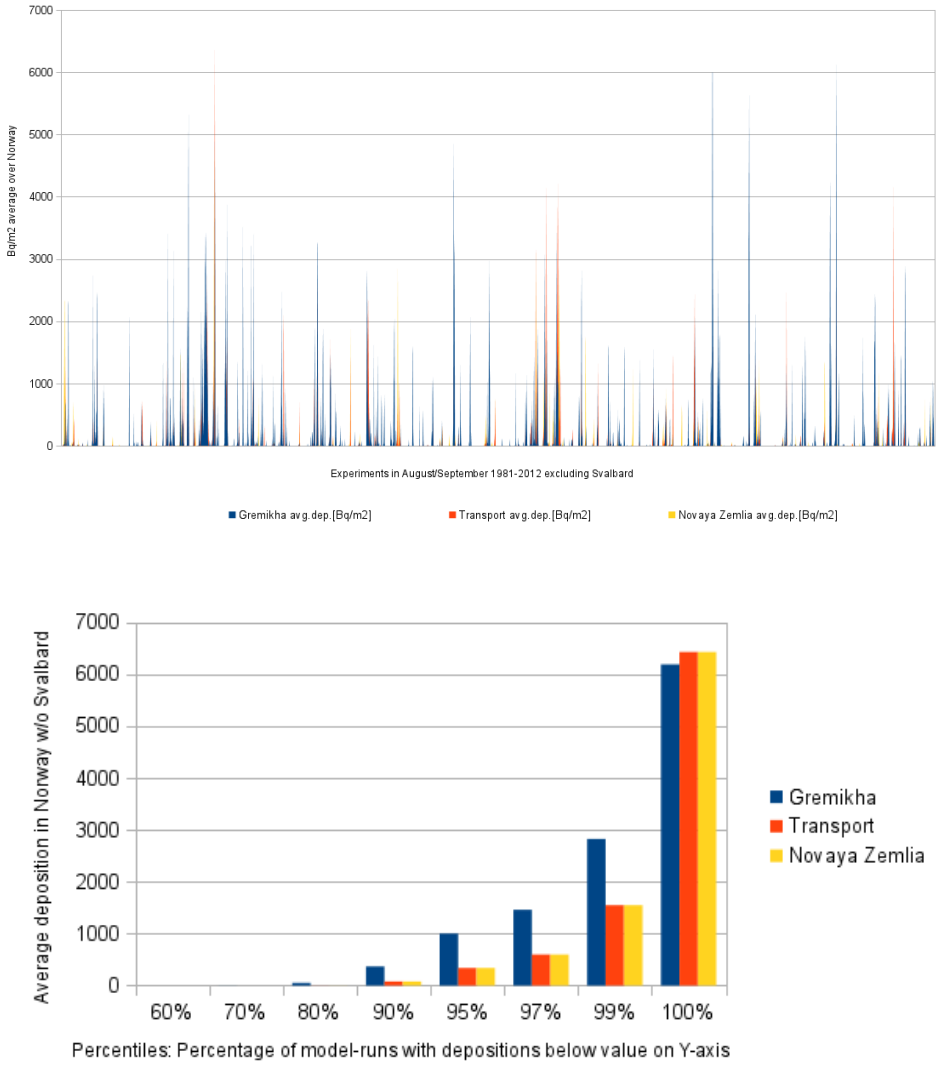

Figure 8: Cases with positive deposition to Norway from all model runs in the entire period - above and percentiles of the deposition - at the bottom. The territory of Svalbard was excluded in these calculations. Deposition units: Bq m^{-2}

3.4.2. Probability of arrival

Probability of arrival is another piece of information important for the threat estimation. Probability of arrival to given model grid was calculated as the ratio of model runs with non-zero concentrations in given grid to total number of model runs. The maps of probability of arrival to each model grid are shown in Fig. 9 for all three accident locations.

Probability of arrival to Norway is clearly higher for the hypothetical accident in Gremikha

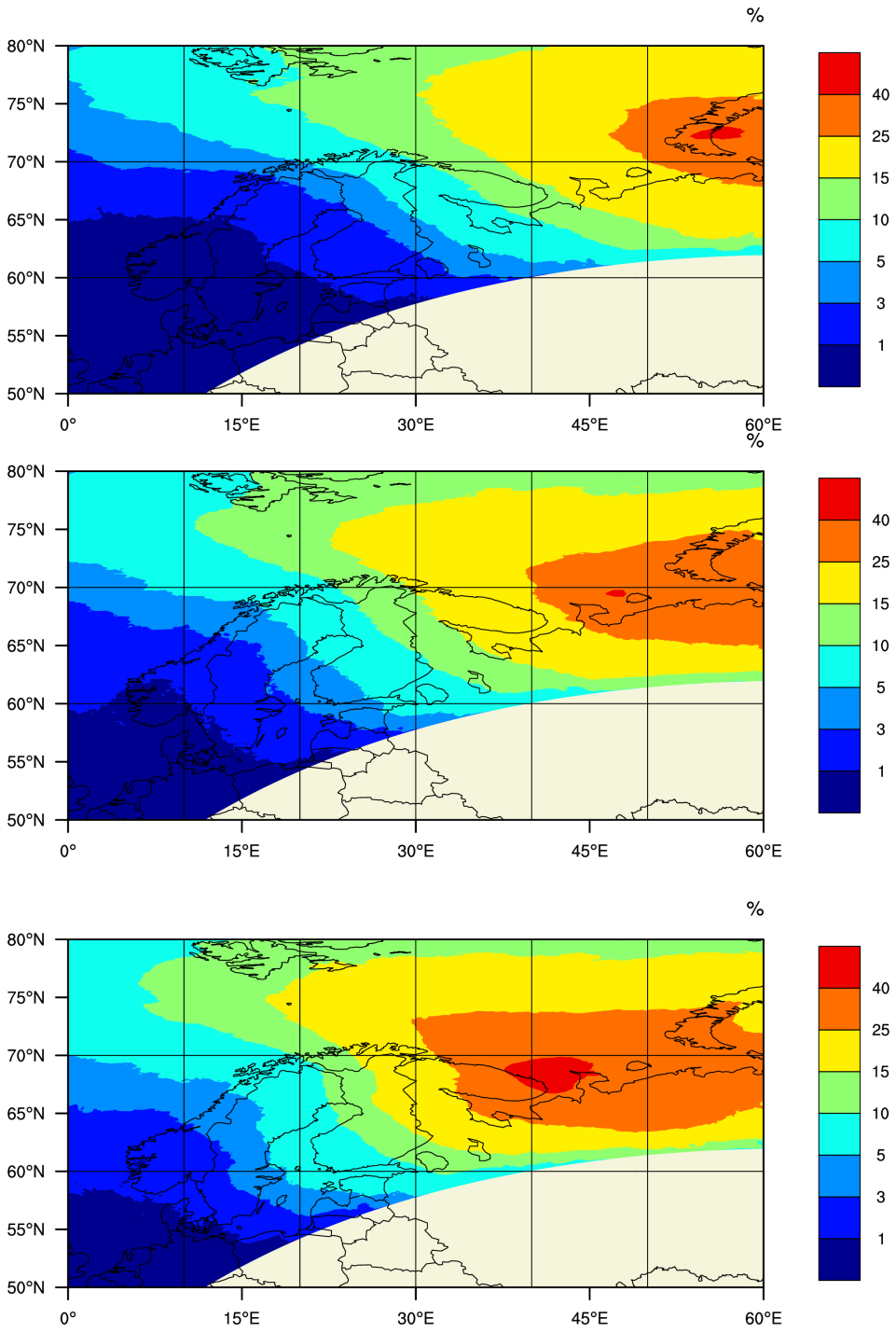

Figure 9: Maps of probability of arrival to each model grid from releases: at initial location - top, on the way to Gremikha Bay - in the middle and at the final destination - bottom.

Bay then for accidents in two other locations. This probability has a maximum in the very northern part of Norway with the ranges 10-15%, 15-25% (but closer to 15%) and 15-25% again (but closer to 25%) for accident in the initial location, on the way and at the final destination, respectively. These probabilities are much lower in southern Norway, below 1% for accident at the initial location and below 3% for accident at the remaining locations.

4. Soure term for selected scenarios

The simplified, preliminary source term was used for the model runs in the selection procedure. A more advanced and complicated source term was developed for the final SNAP runs with the selected worst case meteorological scenarios. This source term took into account properties of the K-27 submarine and especially the properties of the reactors. It is the source term for the worst case accident scenario of K-27 submarine. For general information, the main properties of the K-27 submarine are summarized in Table. 4.

Table 4: General characteristics of K-27 submarine.

Class and type:	November class submarine
Displacement:	3,420 tons surface; 4,380 tons submerged
Length:	109.8 m
Beam:	8.3 m
Draft:	5.8 m
Propulsion:	two VT-1 nuclear reactors with lead-bismuth liquid-metal coolants, capable of producing about 73 megawatts a piece)
Speed:	14.7 knots surface; 30.2 knots submerged
Range:	unlimited

A liquid metal cooled nuclear reactors used in K-27 were the advanced type of nuclear reactors with liquid metal as a primary coolant. These reactors had theoretical safety advantages because they did not need to be kept under pressure, and allowed a much higher power density than traditional coolants. Disadvantages included difficulties associated with the inspection and repair of reactors, as well as, corrosion and/or production of radioactive activation products.

4.1. Main assumptions

At present, the K-27 remains at the bottom of the Kara Sea Fig. 10, near the eastern coast of Novaya Zemlya at 72°31'N, 55°30'E. Before sinking, the reactor compartment was filled with a mixture of furfuryl alcohol and bitumen to seal the compartment and to avoid radioactive pollution of the ocean. There are four alternatives related to the handling of this sub-marine. (i) So called "zero alternative", when no action is taken, the submarine remains at current location and potential accident happens 20-30 m under the sea surface. In this case most of the radioactive pollution is released directly into the water. (ii) The second alternative is the potential accident during the lifting submarine to the surface. In this case the potential accident can take place also under water or on the sea surface. Depending on the depth, the release can be directly into the water or directly into the air. (iii) The third alternative

involves the accident during transportation of the submarine from Novaya Zemlya to the final destination at Gremikha Bay. (iv) Finally, the fourth alternative is a potential accident at the final destination at Gremikha Bay. The potential accident can take place on the water surface or on shore. In both cases most of the radionuclides will be released directly into the air.

In our study we only take into account last three alternatives. All of them involve direct release of most of radionuclides into the air. There is also a possibility for the accident under water. Close to the surface it will create a secondary release into the air, but the magnitude of such a release is assumed to be much lower than in case of a direct release into the air.

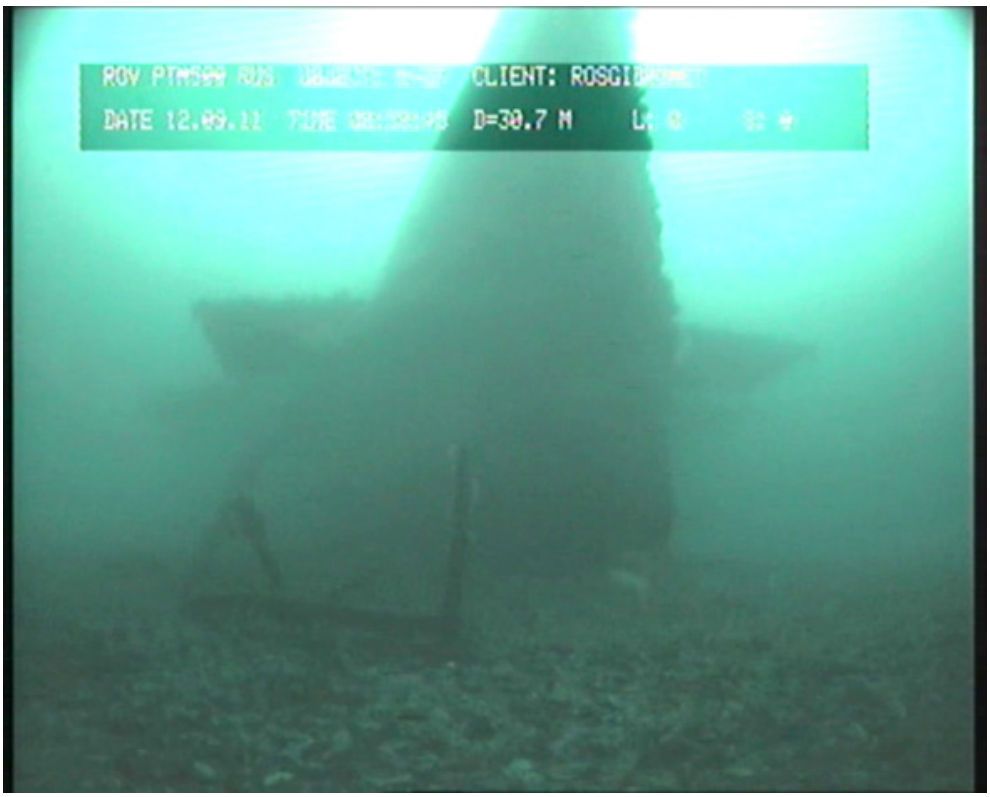

Figure 10: Picture of the K-27 submarine on the bottom of Stepovogo Bay, close to the coast of Novaya Zemlya [30].

For the compilation of the potential source term it is necessary to estimate residual activities in the submarine located in different places and related to different radionuclides. There are several estimates available from the past [19] [20], but in the present work we have used the residual activities for 2013 which have been provided to NRPA by the Kurchatov Institute in Russia (Table. 5).

Because of the possible changes in the reactors concerning criticality, the possibility of the Spontaneous Chain Reaction (SCR) must be taken into account. There are two possible conditions for SCR to take place: (1) water penetration to the core, and (2) relative displacement of fuel and absorbers resulting in reduction of the compensation capacity of the CPS operating elements. The reactor compartment of K-27 was sealed before dumping to reduced releases

Table 5: The latest estimates, with 2013 as a reference year, of residual activities for nuclear submarine K-27.

Activity source	**Main radionuclides currently present in the reactor core**	**Activity (TBq)**
Fission products	Cs137 + Ba-137m, SR-90 + Y-90	270
Control rods	Eu-152, Eu-154	40
Reactor shell constructions	Ni-63, Co-60	11
Actinides	Pu-238, Pu-239, Pu-240, Pu-241, Am-241	4.6
Tritium	H-3	34

of radionuclides in the marine environment. In addition, the measures were taken to prevent displacement of fuel and absorbers that ensured the lowest sub-criticality of the system. Because of these measures, sea water penetration into the core would be the only likely condition under which the SCR may take place.

The specification of the source term for the final model runs was developed with all above facts in mind. In the final model runs, with the worst case meteorological scenarios, the same source term was used for all three locations of the potential accident. Activities for the present study were calculated at the release time assuming 20% of the original reactor inventory plus the activity generated during potential criticality. Four particle classes with different densities and sizes and Iodine gas were taken into account in determining the source term for the final model run. In addition the Iodine gas was also included. There were some common features of the source for all classes of particles and Iodine gas. These were:

- the release time of one hour
- the release hight of 100 m,
- the release radius of 25 m.

Specification of the source term for four classes of particles and for Iodine gas is shown in Table. 6.

4.2. Source term for the SNAP runs

In the SNAP model the properties of real particles and gases are included in the so called ”model particles” explained in Chapter 2. According to specification in Table. 6, if each real particle and gas is represented, we would need 24 model particles for the UO2-Be group, 32 in Bitumen group, 24 in Metal group and 6 in Ru-106 group. In addition, two model particles should represent I-131 and I-133. Altogether this approach would require 86 model particles. However, a closer inspection of Table. 6 indicates that the properties of the real radioactive particles in each group are quite similar. In fact they are similar enough to include several real particles in each group in the same model particles. The most important similarities are the same density and the same size for the components in each group. There are some small differences in the half-life time, but for the 96 hours SNAP simulation, it is long enough to

Table 6: Source term for the worst case accident scenario for K-27 submarine.

UO2-Be, density=2.1 g cm^{-3}, size classes: 0.1, 0.5, 1.0, 5.0, 10.0, 20.0, 50.0, 100.0 μm		
Component	**Half-time**	**Total release (Bq)**
Cs-137	30.17 years	7.1×10^{12}
Sr-90	28.8 years	6.2×10^{12}
Pu-238	no decay	1.6×10^{11}
Bitumen, density=1 g cm^{-3}, size classes: 0.1, 0.5, 1.0, 5.0, 10.0, 20.0, 50.0, 100.0 μm		
Component	**Half-time**	**Total release (Bq)**
Cs-137	30.17 years	4.4×10^{11}
Sr-90	28.8 years	3.9×10^{11}
Pu-238+Pu240	no decay	1.0×10^{10}
I-131	8.04 days	1.4×10^{11}
Metal coolant, density=10.5 g cm^{-3}, size classes: 0.1, 0.5, 1.0, 5.0, 10.0, 20.0, 50.0, 100.0 μm		
Component	**Half-time**	**Total release (Bq)**
Cs-137	30.17 years	4.4×10^{11}
Sr-90	28.8 years	3.9×10^{11}
Pu-238	no decay	1.0×10^{10}
Ru-106, density=3.3 g cm^{-3}, size classes: 0.1, 0.5, 1.0, 5.0, 10.0, 20.0 μm		
Component	**Half-time**	**Total release (Bq)**
Ru-106	1.02 years	1.9×10^{9}
I-131, gas, density=0.0113 g cm^{-3}		
Component	**Half-time**	**Total release (Bq)**
I-131	8.04 days	1.4×10^{11}
I-133	20.04 hours	5.2×10^{12}

neglect the entire decay process. The only exception is I-131 in the Bitumen group, but I-131 is included anyway in the model particle representing I-131 gas, where the decay process is taken into account. In this way the number of model particles for simulating the source term specified in Table. 6 can be reduced. The specification of the model particles used in the SNAP runs for the worst case scenarios is presented in Table. 7.

Table 7: Specification of the model particles representing the real particles and gases for the worst case SNAP model runs. The symbol "•" indicates the type of the model particle used in the simulations.

Group	**Density**	**Size in μm**								**Release**	**Decay**
	g cm^{-3}	0.1	0.5	1.0	5.0	10	20	50	100	Bq	hrs
UO2-Be	2.1	•	•	•	•	•	•	•	•	1.35×10^{13}	No
Bitumen	1.0	•	•	•	•	•	•	•	•	9.8×10^{11}	No
Metal	10.5	•	•	•	•	•	•	•	•	8.4×10^{11}	No
RU-106	3.3	•	•	•	•	•	•			1.9×10^{9}	No
I-131	0.0113	• (gas)								1.4×10^{11}	192.96
I-133	0.0113	• (gas)								5.2×10^{12}	20.04

Altogether, 32 model particles were used in the SNAP runs with the final source term. The release rate for each model particle was specified in the snap.input file according to Table. 7. We assume that the accident starts as an explosion and the release of radionuclides to the atmosphere is quite fast, especially at the beginning of the process. Because of its intensity this process is not assumed to last long and therefore we have used one hour as the total period of release.

Not much information is available about the radioactivity distribution among different size clasess. Therefore, we have assumed an equal distribution for each of the size class used in the SNAP runs.

The heat generated during the explosion lifts the radioactive pollutants into the air. Usually the upper limit for vertical distribution of pollutants in such case is the top of the mixing layer. For the chosen locations and the time of the year when the potential accidents can happen, the typical range of the mixing layer is 200 m. Therefore, we have assumed the release to be placed in the middle of this typical mixing layer - 100 m.

The horizontal spread of radionuclides during the release was assumed to take place in the cylinder with the radius of 25 m. There is some uncertainty in this assumption, but for the long range transport like in our case, the calculated depositions are rather insensitive to this parameter.

5. Model runs for the worst case scenarios

In this Chapter we present the results of the SNAP model runs with the final model source term as specified in Table. 7. These results are presented separately for each of three locations of the hypothetical accident. However, we also chose the final worst case scenario among different release locations. This final worst case is discus in more detail at the end of this Chapter, in Section 5.3. As expected, the final worst case scenario is related to potential accident in Gremikha Bay.

5.1. Accident at the initial location

To simulate the worst case scenario for accident at the initial location, the SNAP model was run with the final model source term, as presented in Table. 7, with the accident start on 26 August 1998 at 00 UTC. The model simulation was performed for 96 hrs, which means that deposition and concentration fields were calculated for 30 August 1998 at 00 UTC. In Fig. 11 the results of the model simulation are shown as maps of dry, wet and total deposition. These depositions were calculated as a sum of depositions from all particle classes and Iodine gas. Usually, wet deposition dominates over dry deposition in the atmospheric transport of radioactive particles. However, in this meteorological scenario, with accident at the initial location of K-27 submarine, Norway is more affected by dry than wet deposition, except for a very northern part of Finmark where both types of depositions contribute almost equally to total deposition. There is also a second area with visible deposition located between Nordland and Troms counties, but this time only dry deposition is present. The maximum values of total deposition in the northern part of Finmark are in the range of 10-30 Bq m^{-2}. A range of maximum total deposition in the region between Nordland and Troms is is slightly lower, 3-10 Bq m^{-2}.

These results of the model run with the final source term are quite different from those with the model run with preliminary source term and Cs-137 deposition, when almost entire Norway was covered by total deposition. For easier comparison, we have used the same scale on the maps. The reasons for a large difference will be discusses in Section 5.3.

5.2. Accident on the way

For simulation of the hypothetical accident on the way from Novaya Zemlya to Gremikha Bay, the worst case meteorological scenario No. 1 from Table 3 was selected, with the start of accident on 7 September 1986 at 12 UTC. Also for this meteorological scenario the SNAP model was run for 96 hours with the final source term specified in Table. 7. The calculated maps of dry wet and total depositions - 96 hours later, on 11 September 1986 at 12 UTC are shown in Fig. 12. These maps also include complete deposition, as a sum from all particle classes and Iodine gas.

Compared to previous simulation (accident at initial location), we have completely different picture here concerning proportions between dry and wet deposition. The dry deposition shape is very narrow indicating relatively low turbulence and lateral mixing close to the ground. The pattern of wet deposition is much wider indicating more mixing in the upper parts of

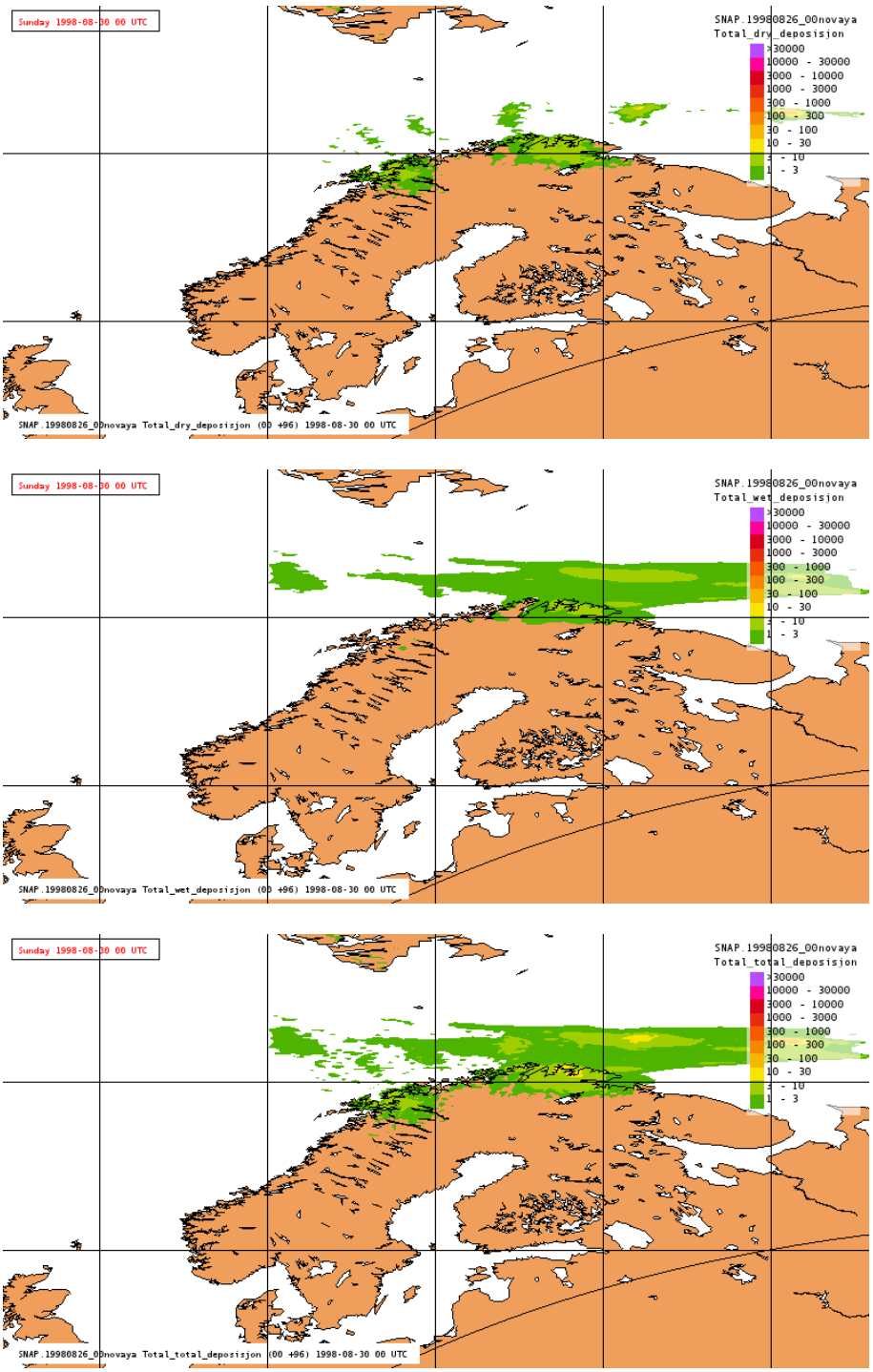

Figure 11: Deposition maps from SNAP run with the final source term specified in Table. 7 and accident at the initial location. Dry deposition - at the top, wet deposition - in the middle and total deposition (dry+wet) at the bottom. Units: Bq m^{-2}

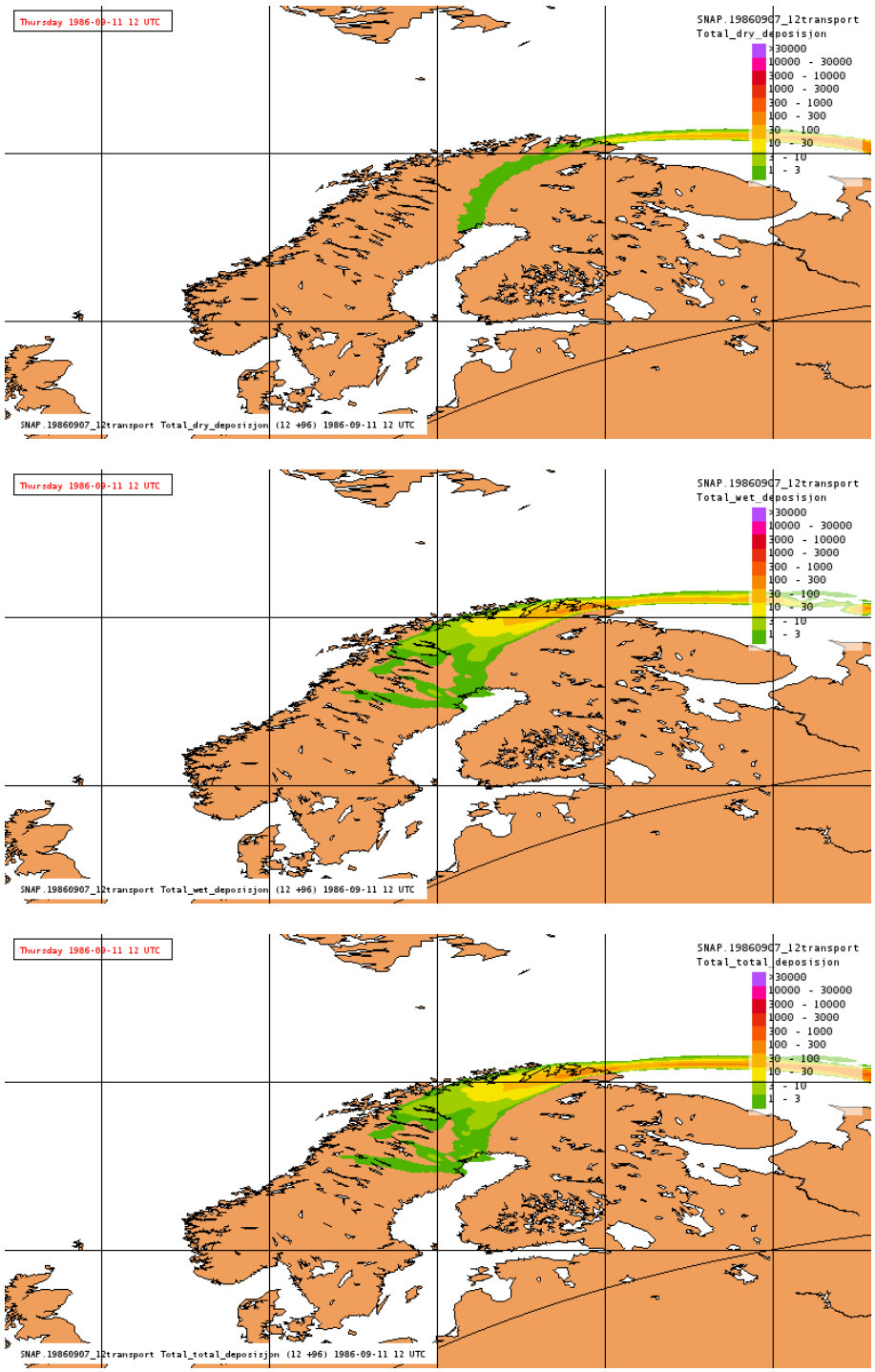

Figure 12: Deposition maps from SNAP run with the final source term specified in Table. 7 and accident on the way to Gremikha. Dry deposition - at the top, wet deposition - in the middle and total deposition (dry+wet) at the bottom. Units: Bq m^{-2}

the atmosphere. Dry deposition is visible only in Finmark with relatively low values of 1-3 Bq m^{-2}. Wet deposition has maximum values also in Finmark, with much higher range of 100-300 Bq m^{-2}), but it is also present in Troms and Nordland counties. The shape of total (dry+wet) deposition is very similar to the wet deposition pattern with maximum in the northern part of Finmark close to 300 Bq m^{-2}. Also in this case, the central and southern part of Norway is not affected by the accident.

Comparison with the results of model simulations with the preliminary source term shows more similarities in this case, but the level of depositions is clearly lower in the results of the model runs with the final source term.

5.3. Accident at final destination - general worst case scenario

The SNAP model was run again with the final source term as specified in Table. 7 to simulate the worst case meteorological scenario for accident at the final destination, in Gremikha bay. The case No. 2 from from Table 3 was selected, with the start of accident on 22 September 2004 at 12 UTC. Depositions and concentrations were calculated 96 hours from the accident start on 22 September 2004 at 12 UTC. In Figure 13 the maps with dry, wet and total depositions are shown. These depositions were calculated as a sum from all particle classes and Iodine gas.

The range of the deposition and Norwegian area covered by the deposition is significantly larger in this case compared to two previous cases. It applies to dry, wet and total deposition. The dry deposition pattern is in the form of relatively narrow and long tongue reaching the coast of central Norway, but affecting only Finmark Troms and to very small extent Nordland counties. The maximum of dry deposition close to 30 Bq m^{-2} can be found in the far North, close to Kirkenes.

The wet deposition pattern is much wider and more irregular compared to dry deposition. There are two local maxima, one in the North reaching 300 Bq m^{-2} and one central Norway (Nord Trondelag county) in the range 10-30 Bq m^{-2}.

The same local maxima are also visible in the pattern of total (dry+wet) deposition, which affects three counties in the North (Finmark, Troms and Nordland), but in addition several counties in central Norway (Nord Trondelag, Sør Trondelag, Møre og Romsdal, Opland and Hedmark). The levels of local maxima are similar to the levels of wet deposition 100-300 Bq m^{-2} in the North and 10-30 Bq m^{-2} in central Norway.

This is the worst case among three locations of the potential accident. However, for all locations, the results with the final source term are quite different from those with with the preliminary source term and Cs-137 deposition, when almost entire Norway was covered by total deposition. The main reason for this dramatic difference is the difference in total releases in case of preliminary and the final source term. The total release of the final source term is almost 100 times lower than the total release used in the preliminary source term.

5.3.1. Deposition from individual components

Total deposition from all components together was presented and discussed in the previous section. Here we will discuss the individual impact of all 32 model particles or components

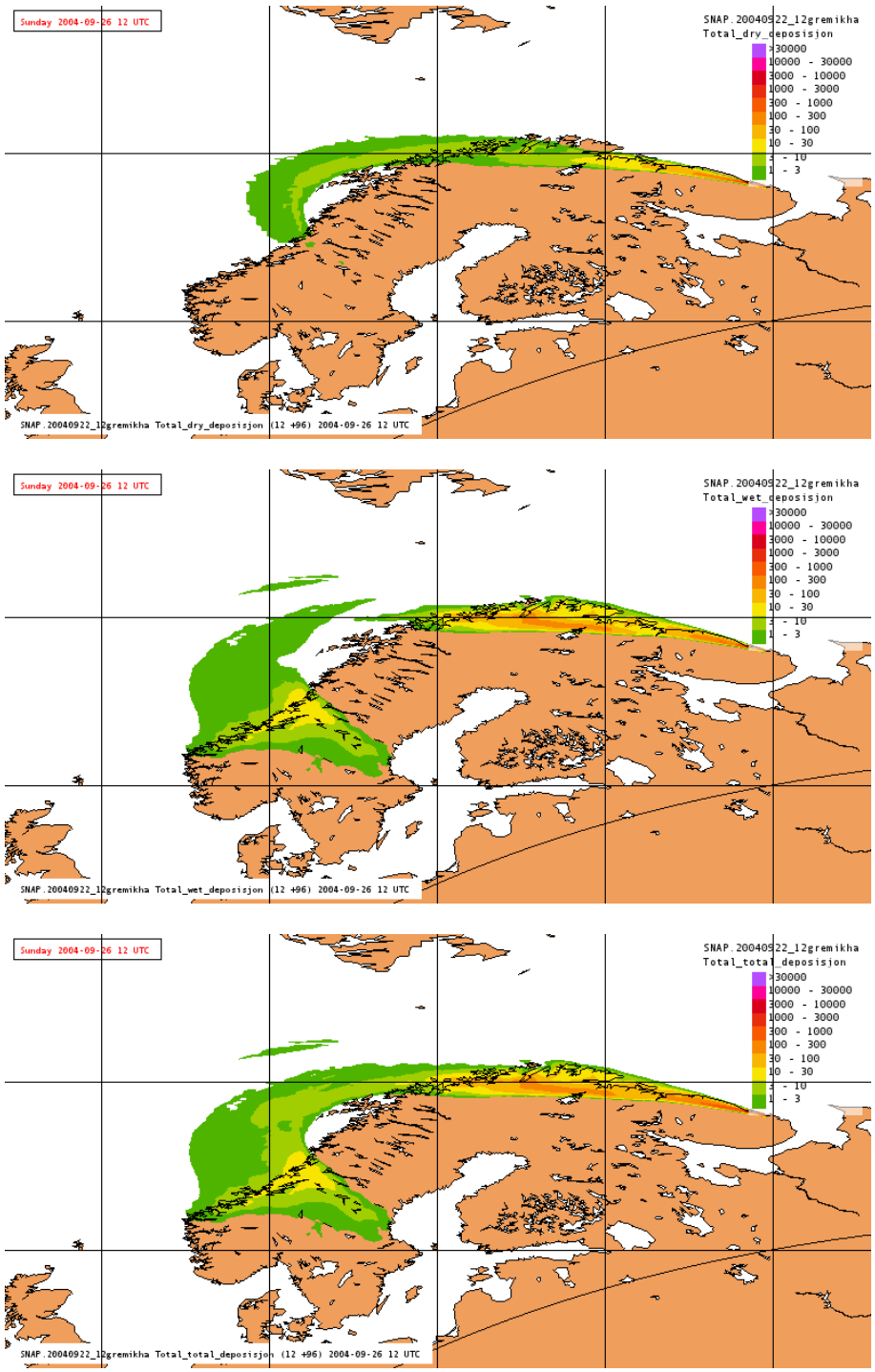

Figure 13: Deposition maps from SNAP run with the final source term specified in Table. 7 and accident at the final destination. Dry deposition - at the top, wet deposition - in the middle and total deposition (dry+wet) at the bottom. Units: Bq m^{-2}

included in Table. 7. The results of the model run for all individual components are shown in Appendix B as maps of dry, wet and total deposition after 96 hours from the accident start. Among four groups of particles which were included in the SNAP run for the worst case scenario, the total release was highest for the UO2-Be group. It was two order of magnitude higher than the releases for two next groups (Bitumen and Metal). The total release in the last group (RU-106) was again much lower, more than four orders of magnitude lower compared to UO2-Be group. The total releases of Iodine gases were one and two order of magnitude lower, for I-133 and I-131 respectively.

These differences in total releases for the groups are clearly reflected in the deposition maps. Also, differences in particle sizes for individual components within each group are quite significant and probably the most important. Deposition from UO2-Be components is higher than deposition from the Bitumen group and slightly lower deposition from the Metal group. The main reason for lower deposition from the Metal group, despite of very similar level of release is higher density of particles in the metal group compared to the Bitumen group. The difference in total release is so large that deposition from the last group RU-106 is hardly visible on the maps and only close to the source, since the same deposition scale is used for all groups.

There are some similarities for all groups of particles. Namely, long range transport is most effective when the particle size is below 1 μm. For UO2-Be group deposition fields for particles with the size 0.1, 0.2 and 1.0 μm, deposition fields are very similar. Above 1 μm, the transport range is rapidly decreasing and for particles with the size above 20 um (50 and 100 μm) only local area is affected in practice. Deposition fields for Iodine and especially for I-133 are similar to those with particle size below 1 μm.

5.3.2. Dynamics of the transport

The radioactive cloud resulting from the K-27 potential accident originating in Gremikha Bay is travelling fast towards Norway in in the worst case scenario. In Appendix C we show the evolution in time of the total deposition for the period of 96 hours with maps of total deposition for the worst case scenario and accident at the final destination in Gremikha Bay. The maps are shown with 3 hours interval and the same scale is used for the deposition in all maps.

Already after 8-9 hours from the accident start, Norwegian cities Vadsø, Vardø and Kirkenes are contaminated with the deposition. In the next 1-2 hours also Mehamn and Hammerfest are contaminated. After 18-20 hours of the transport, Tromsø is also covered by the deposition. Later on, in the next 15-16 hours, deposition from the radioactive cloud is only expanding over the sea. Approximately 35-36 hours from the accident start Namsos and Steinkjer are affected by the deposition and a bit later, after next 9 hours, Trondheim as well. In the next stage, the radioactive cloud is travelling to Sweden reaching the Baltic Sea after 51 hours of the transport.

Because of the scale used, Oslo is not covered by the deposition, however with the source term involving higher release we can expect that the radionculides released from potential K-27 accident will be also deposited in the Oslo area. If it happens the travel time can be estimated to be approximately 40-45 hours from the accident start which means less than two days.

5.3.3. Time integrated concentrations

The doses to population can be calculated from the time integrated concentrations at the surface level. A map of time integrated concentration form all components together is shown in Fig. 14. The integration period starts with the beginning of accident. The range of time integrated concentration is shorter than the range of deposition. This is not a surprise since the wind speed is much lower at the surface than in the upper part of the mixing layer and above. In addition, wet deposition is a major contributor to total deposition and radionuclides can be subject to washout from a high elevation. Very often wet deposition from the nuclear accident can be observed before a significant increase of ground concentration.

Mainly northern part of Norway is affected by time integrated concentration and cities like Vadsø, Vardø and Kirkenes. Theoretically also some ships on the Norwegian Sea can be affected. In addition, the level of time integrated concentration can be slightly elevated in Namsos.

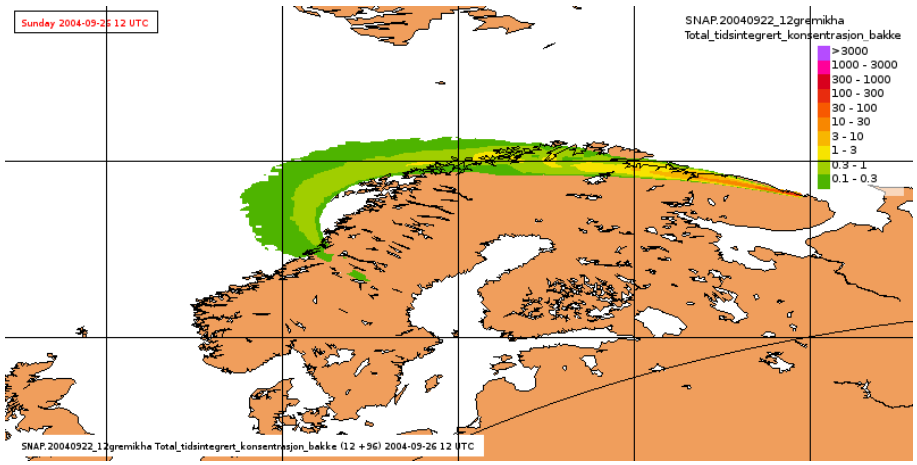

Figure 14: Map of time integrated concentration from the SNAP run with the final source term specified in Table. 7 and accident at the final destination. Units: Bq hr m^{-3}

5.3.4. Comparison with the Chernobyl Accident

The relatively low level of total deposition over Norway from the potential K-27 accident is also confirmed in the comparison with total deposition from the Chernobyl accident shown in Fig. 15. In case of Chernobyl accident the entire Western Norway and especially mountain regions show high levels of deposition. The maximum, above 30000 Bq m^{-2} is visible in the Jotunheimen and in southern Norway in general. The maximum deposition from the potential K-27 accident is two order of magnitude lower (100-300 Bq m^{-2}) and can be found in northern Norway. In case of release from K-27, deposition in southern Norway is at least 100 times lower and is of no radio ecological concern.

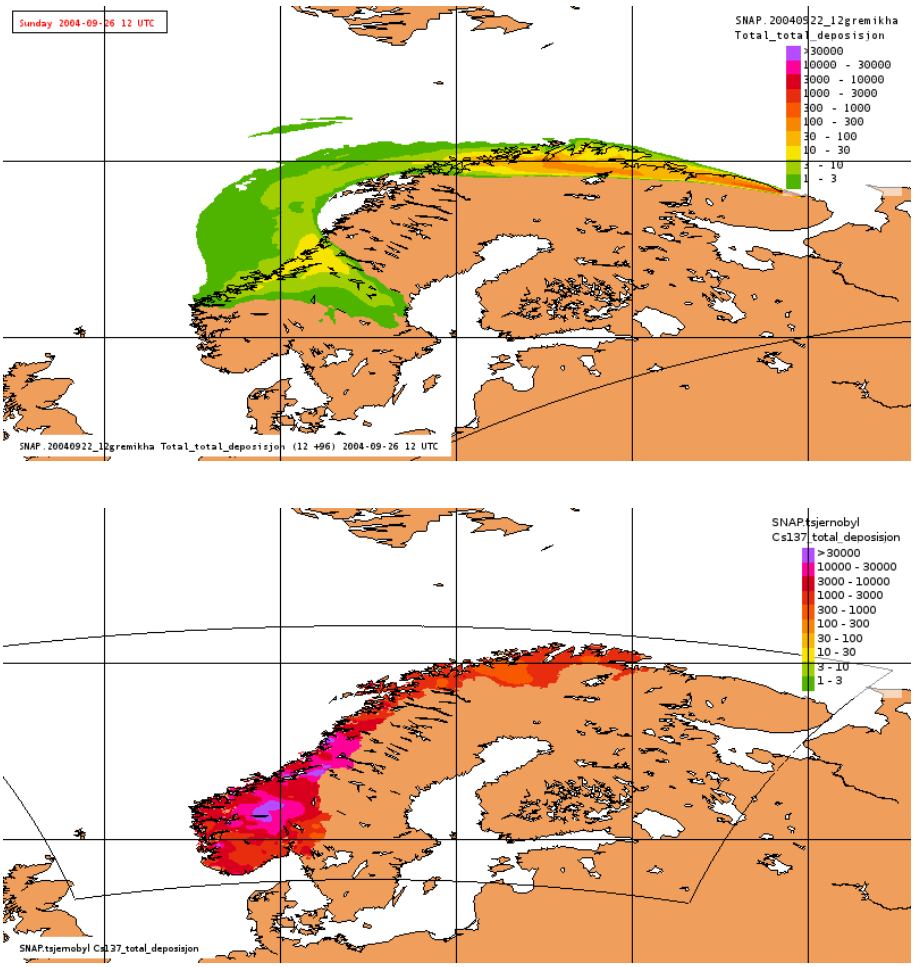

Figure 15: Comparison of a deposition map from the worst case K-27 scenario with a deposition map from the Chernobyl accident. The same scale is used on both maps. Deposition data for Norway from Chernobyl accident were provided by NRPA.

6. Summary and conclusions

The main goal of this study was to analyse the atmospheric transport and deposition of radioactive debris to Norwegian territory, in case of nuclear accident related to lifting and transporting the K-27 submarine. We have used the SNAP model and large meteorological data base in order to find the worst case meteorological scenario. The development of meteorological database for the period 1980-2012 was the first step in the study. All meteorological elements necessary as input to the SNAP model, of which the latest version is described in the report, are included in the database. Once the long-term meteorological input for the SNAP model was ready, we could start the selection procedure for finding the worst case meteorological scenarios. We assumed three locations of the accident, but only one accident scenario in the selection procedure. This was a simplified scenario with release of Cs-137 particles of small size and typical density, having in mind very long computational time of the selection procedure. The main conclusions from the selection procedure are the following:

- The number of cases with deposition above zero over Norwegian territory is decreasing with the distance between the release location and Norway. For releases at initial location, on the way and at final destination, probability of reaching Norwegian territory is 17%, 25% and 37%, respectively.

- The average deposition over Norway is clearly dependent on the distance from the release location, with the largest depositions for the source at final destination of K-27.

Statistical analysis of the threat to Norway was based on the results of all model runs in August and September of each year of the entire thirty three year period. It included calculations of total deposition and probability of arrival for the entire period and for model grids belonging to the territory of Norway. The main conclusions from the statistical analysis are the following:

- Concerning percentile of the model runs with deposition exceeding specified values, in 70% of cases from all locations there is no transport to Norway in practice. The results are similar for the sources located at the initial location and on the way to Gremikha. Compared to other accident locations, there is significantly more transport to Norway and with higher average deposition over Norway, from the final destination of K-27 in Gremikha Bay.

- As a result of the selection procedure, the worst case meteorological scenarios were selected for the dates: 26 August 1998, 7 September 1986 and 22 September 2004, for hypothetical accident locations at the initial destination, on the way and at the final destination, respectively.

- The worst meteorological case among all destinations is the one in Gremikha Bay. It should be noticed that the accident at final destination can happen any time during the year and therefore additional analysis will be necessary for this location. We plan to perform this additional analysis at the end of 2014 in the frame of CERAD activities.

An important part of the study was a development a source term for potential K-27 accident, as close as possible to most likely real situation. In this source term only potential release into the air was taken into account and therefore it was the same for all selected locations. In this process, we have used the latest available information from 2013 about residual activities of K-27, which have been provided to NRPA by Kurchatov Institute in Russia. Because of possible change in the reactors concerning criticality, the possibility of Spontaneous Chain Reaction was taken into account in the inventory. The source term for SNAP model included 32 individual components in four particle groups (UO2-Be, Bitumen, Metal and RU-106) and in two Iodine components (I-131 and I-133). Different particle sizes and densities were used ranging from 0.1 to 100 μm and from 1 to 10.5 g cm^{-3}. Also the total release was different for each particle group with highest release for UO2-Be and lowest for RU-106 with four orders of magnitude difference between them.

It should be stressed that the total release in the final source term for the worst case meteorological scenarios is relatively low (two orders of magnitude lower) compared to typical source term used by Scandinavian countries in case of hypothetical nuclear ship accident [19]. This fact has a large influence on calculated depositions which are also lower than those calculated with the preliminary source term used in the selection procedure. Nevertheless, this final source term was used to calculate deposition for the worst case meteorological scenarios.

The main conclusions from model runs with the finals source term and worst case meteorological scenarios are the following:

- The range and values of depositions calculated with the final source term are much lower compared to the model results obtained with the preliminary source term.
- For all locations of the potential accident mainly northern part of Norway is affected and all maxima of he deposition are located there with the range 10-300 Bq m^{-2}.
- Only for the potential accident located at Gremikha Bay, also central Norway is affected by total deposition and an additional local maximum in the range 10-30 Bq m^{-2} can be found there.
- The contribution of wet deposition to total deposition is much higher than the contribution of dry deposition. It applies to all available results.
- The differences in total release for individual particle groups are clearly visible in calculated depositions. Deposition from the UO2-Be group is higher than depositions from Bitumen and Metal groups and much higher than deposition from RU-106 group.
- There are some similarities for all groups of particles. Namely, long range transport is most effective when the particle size is below 1 μm. For UO2-Be group deposition fields for particles with the size 0.1, 0.2 and 1.0 μm, deposition fields are very similar. Above 1 μm, the transport range is rapidly decreasing and for particles with the size above 20 um (50 and 100 μm) only local area is affected in practice.
- Deposition fields for Iodine and especially for I-133 are similar to those with particle size below 1 μm.

- The radioactive cloud resulting from the K-27 potential accident originating in Gremikha Bay is travelling fast towards Norway in in the worst case scenario. Already after 8-9 hours from the accident start, Norwegian cities Vadsø, Vardø and Kirkenes are contaminated with the deposition. In the next 1-2 hours also Mehamn and Hammerfest are contaminated. After 18-20 hours of the transport, Tromsø is also covered by the deposition. Later on, in the next 15-16 hours, deposition from the radioactive cloud is only expanding over the sea. Approximately 35-36 hours from the accident start Namsos and Steinkjer are affected by the deposition and a bit later, after next 9 hours, Trondheim as well.

- Because of the scale used, Oslo is not covered by the deposition, however with the source term involving higher release we can expect that the radionculides released from potential K-27 accident will be also deposited over Oslo. If it happens the travel time can be estimated to be approximately 40-45 hours from the accident start which means less than two days.

- The range of time integrated concentration is shorter than the range of deposition. Mainly northern part of Norway is affected by time integrated concentration and cities like Vadsø, Vardø and Kirkenes.

- Compared to Chernobyl accident, maximum of the deposition from K-27 accident (300 Bq m^{-2}) is a factor of 100 lower than the maximum deposition in Norway from the Chernobyl accident (above 30000 Bq m^{-2}). Also the area of Norway affected is different in both cases, mostly northern Norway from the K-27 accident and mostly central Norway from the Chernobyl accident.

One important general conclusion from this study is that calculated depositions are very sensitive to the magnitude of the source term used. Therefore it is very important to develop as accurate as possible estimation of the source term in case of the potential accident involving K-27 submarine.

References

[1] Avissar, R., and R. A. Pielke (1989) A parametrization of heterogeneous land surfaces for atmospheric numerical models and its impact on regional meteorology. Mon. Wea. Rev., 117, 2113-2136.

[2] Baklanov A. and J. H. Sørensen (2001) Parameterization of radionuclide deposition in atmospheric long-range transport modeling. Physics of the Chemistry of the Earth (B) 26(10), 787-799.

[3] Bartnicki, J. and J. Saltbones (1996) Severe Nuclear Accident Program (SNAP) - A real time dispersion model. In: Development and Application of Computer Techniques to Environmental Studies VI. (P. Zannetti and C.A. Brebbia, eds.), pp. 17-26. Computational Mechanics Publications, Southampton, Boston.

[4] Bartnicki, J. and J. Saltbones (1997) Analysis of Atmospheric Transport and Deposition of Radioactive Material Released During a Potential Accident at Kola Nuclear Power Plant. Research Report No. 43, ISSN 0332-9879. Norwegian Meteorological Institute, Oslo, Norway.

[5] Bartnicki J., Salbu B., Saltbones J., Foss A. and O. C. Lind (2001) Gravitational settling of particles in dispersion model simulations using the Chernobyl Accident as a test case. DNMI Research Report No. 131. Norwegian Meteorological Institute, Oslo, Norway.

[6] Bartnicki J., B. Salbu, J. Saltbones, A. Foss and O. C. Lind (2003) Long-range transport of large particles in case of nuclear accident or explosion. Preprints of 26th NATO/CCMS International Technical Meeting on Air Pollution Modelling and its Application, 26-30 May 2003. Istanbul Technical University, Istanbul, Turkey, pp. 53-60.

[7] Bartnicki, J., Salbu B., Saltbones J. and A. Foss (2005) Analysis of Atmospheric Transport and Deposition of Radioactive Material Released During a Potential Accident at Kola Nuclear Power Plant. Research Report No. 10, ISSN 1503-8025. Norwegian Meteorological Institute, Oslo, Norway.

[8] Bartnicki J., B. Salbu, J. Saltbones, A. Foss and O. C. Lind (2006) Long-range transport and deposition of radioactive particles from potential accidents at Kola Nuclear Power Plant. Proceedings of 1st Joint Emergency Preparedness and Response/Robotic and Remote Systems Topical Meeting. February 11-16, 2006 Salt Lake City, Utah, USA

[9] Bartnicki J. and J. Saltbones (2008) Atmospheric dispersion of radioactive debris released in case of nuclear explosions using the Norwegiain SNAP model. Proceedings of The 12th International Conference on Harmonization within Atmospheric Dispersion Modelling for Regulatory Purposes HARMO12. 6-10 October 2008 - Cavtat, Croatia. pp. 111-115.

[10] Bartnicki J., H. Haakenstad and Ø. Hov (2010) Volcano version of the SNAP model. Met.no report No. 15/2010. Norwegian Meteorological Institute, Oslo, Norway.

[11] Crandall W.K., Molenkamp C.R., Wiliams A.L., Fulk M.M., Lange R. and J.B. Knox (1973) An investigating of scavenging of radioactivity from nuclear debris clouds: research in progress. lavrence Livermore National Laboratory, california, USA, Report UCRL-51328.

[12] Csanady G.T. (1973) Turbulent Diffusion in the Environment. Reidel, Dordrecht, Holland.

[13] Cuxart, J., P. Bougeault, and J. L. Redelsberger (2000) A turbulence scheme allowing for mesoscale and large-eddy simulations. Quart. J. Roy. Met. Soc., 126, 1-30.

[14] Dee, D. P., S. M. Uppala, A. J. Simmons, P. Berrisford, P. Poli, S. Kobayashi,U. Andrae, M. A. Balmaseda, G. Balsamo, P. Bauer, P. Bechtold, A. C. M. Beljaars,L. van de Berg, J. Bidlot, N. Bormann, C. Delsol, R. Dragani, M. Fuentes, A. J. Geer,L. Haimberger, S. B. Healy, H. Hersbach, E. V. Holm, L. Isaksen, P. Kållberg, M. Kohler, M. Matricardi, A. P. McNally, B. M. Monge-Sanz , J.-J. Morcrette, B.-K. Park, C. Peubey, P. de Rosnay, C. Tavolato, J.-N. Thepaut and F. Vitart, 2011, The ERA-Interim reanalysis: configuration and performance of the data assimilation system. Q.J.R. Meteorol.Soc. 137, pp.553-597.

[15] ENSEMBLE web-site (2010) http://ensemble.jrc.ec.europa.eu/

[16] Galmarini, S., Bianconi, R., Klug, W., Mikkelsen, T., Addis, R., Andronopoulos, S., Astrup, P., Baklanov, A., Bartnicki, J., Bartzis, J.C., Bellasio, R., Bompay, F., Buckley, R., Bouzom, M., Champion, H., D'Amours, R., Davakis, E., Eleveld, H., Geertsema, G.T., Glaab, H., Kollax, M., Ilvonen, M., Manning, A., Pechinger, U., Persson, C., Polreich, E., Potemski, S., Prodanova, M., Saltbones, J., Slaper, H., Sofiev, M.A., Syrakov, D., SÃ¸rensen, J.H., Van der Auwera, L., Valkama, I., Zelazny, R., 2004a. Ensemble dispersion forecasting, part 1: concept, approach and indicators. Atmos. Environ. 38 (28): 4607-4617.

[17] Galmarini S., Bianconi R., Klug W., Mikkelsen T., Addis R., Andronopoulos S., Astrup P., Baklanov A., Bartnicki J., Bartzis J. C., Bellasio S., Bompay F., Buckley R., Bouzom M., Champion H., D'amours R., Davakis E., Eleveld H., Geertsema G. T., Glaab H., Kollax M., Ilvonen M., Manning A., Pechinger U., Persson C., Polreich E., Potempski S., Prodanova M., Saltbones J., Slaper H., Sofiev M. A., Syrakov D., Sørensen J. H., Van der Auvera L., Vaikama I. and R. Zelazny (2004) Can the confidence in long range atmospheric transport models be increased? The Pan-European experience on ENSEMBLE. Radiation Protection Dosimetry, 109 (1-2), pp. 19-24.

[18] Haga P.E. (1991) Hvordan influerer nedbørprocesser tids- og romskala på langtransport av svoveldioksyd og partiklataert sulfat? (in Norwegian). Thesis, Oslo University.

[19] IAEA 1997. Predicted radionuclide release from marine reactors dumped in the Kara Sea. Report of the Source Term Working Group of the International Arctic Seas Assessment Project (IASAP). International Atomic Energy Agency, VIENNA, 1997, TECDOC-938.

[20] ISTC 1999. Lavkovsky S.A. Overview of the Project 101B-96 ISTC (Kurgan). International Seminar on ISTC projects Radiation Legacy in the CIS. Brussels, March 1999.

[21] Kuo, H. L. (1965) On the formation and intensification of tropical cyclone through latent heat release by cumulus convection. J. Atm. Sci., 22, 40-63.

[22] Kuo, H. L. (1974) Further Studies of the Parameterization of the Influence of Cumulus Convection on Large-Scale Flow. J. Atm. Sci., 31, 1232-1240.

[23] Langner, J., Robertson, L., Persson, C. and Ullerstig, A. (1998:) Validation of the operational emergency response model at the Swedish meteorological and hydrological institute using data from ETEX and the Chernobyl accident. Atmos. Environ. 32, 4325-4333.

[24] Maryon R.H., Smith J.B., Convay B.J., and D.M Godard (1991) The United Kingdom Nuclear Accident Model. Prog. Nucl. Energy, 26:85-104.

[25] Maryon R.H., J. Saltbones, D.B. Ryall, J. Bartnicki, H.A. Jakobsen and E. Berge (1996) An intercomparison of three long range dispersion models developed for the UK Meteorological Office, DNMI and EMEP. UK Met Office Turbulence and Diffusion Note 234. UK Meteorological Office, Bracknell, United Kingdom.

[26] Maryon R.H. and D. B. Ryall (1996) Developments of the UK nuclear accident response model (NAME). Department of Environment, UK Met Office Turbulence and Diffusion Note 234. UK Meteorological Office, Bracknell, United Kingdom.

[27] Pettersen S. (1956) Weather Analysis and Forecasting. McGraw-Hill, New York.

[28] RAFF (1999) Properties of nuclear fuel particles and release of radionuclides from carrier matrix. RAFF final report. A research programme carried out with the financial support from the Commision of EC - DG XII. Contract No. FICCT960007.

[29] Reistad M., Ø. Breivik, H. Haakenstad, O. J. Aarnes, B. R. Furevik and J-R Bidlo (2011) A high-resolution hindcast of wind and waves for The North Sea, The Norwegian Sea and The Barents Sea. J. Geophys. Res., 116, C05019, doi:10.1029/2010JC006402.

[30] JOINT NORWEGIAN-RUSSIAN EXPERT GROUP for investigation of Radioactive Contamination in the Northern Areas (2012) INVESTIGATION INTO THE RADIOECOLOGICAL STATUS OF STEPOVOGO FJORD. The dumping site of the nuclear submarine K-27 and solid radioactive waste. Results from the 2012 research cruise. JOINT NORWEGIAN-RUSSIAN EXPERT GROUP for investigation of Radioactive Contamination in the Northern Areas. J.P. Gwynn and A.I. Nikitin - editors.

[31] Ryall D.B. and Maryon R.H. (1996) The NAME2 dispersion model: a scientific overview. UK Meteorological Office. MetO(Apr) Turbulence and Diffusion note 217b.

[32] Saltbones J.(1995) Real-time dispersion model calculations as part of NORMEM-WP19. Safety Science 20, 51-59.

[33] Saltbones J. and A. Foss (1994) Real-time dispersion model calculations of radioactive pollutants at DNMI. Part of Norwegian preparedness against nuclear accidents. Preprints of the XIX Nordic Meteorologists Meeting, June 1994, Kristiansand, Norway.

[34] Saltbones J., Foss A. and J. Bartnicki (1995) Severe Nuclear Accident Program. Technical Description. Research Report No. 15. Norwegian Meteorological Institute. Oslo, Norway.

[35] Saltbones J., Foss A. and J. Bartnicki (1995) Severe Nuclear Accident Program (SNAP) - A real time dispersion model. In: Proceedings of Oslo Conference on International Aspects of Emergency management and Environmental Technology. (K.H. Drager ed.), pp. 177-184.

[36] Saltbones J., Foss A. and J. Bartnicki (1995) ETEX - the European Tracer Experiment - DNMI's participation in an international program for evaluation of real time dispersion models. In: Proceedings of Oslo Conference on International Aspects of Emergency management and Environmental Technology. (k:H: drager ed.), pp. 129-138.

[37] Saltbones J., Foss A. and J. Bartnicki (1996) A real time dispersion model for severe nuclear accidents tested in the European Tracer Experiment. Systems Analysis Modelling Simulation 25, 263-279.

[38] Saltbones J. and J. Bartnicki (1997) Atmospheric transport of radioactive material from potential accident in Kola nuclear power plant (in Norwegian). Naturen 4, 178-188.

[39] Saltbones J., Foss A. and J. Bartnicki (1998) Norwegian Meteorological Institute's Real-Time Dispersion Model SNAP (Severe Nuclear Accident Program). Runs for ETEX and ATMES II Experiments with Different Meteorological Input. Atmospheric Environment 32(24), 4277-4283.

[40] Saltbones J., Foss A. and J. Bartnicki (2000) Threat to Norway from potential accidents at the Kola nuclear power plant. Climatological trajectory analysis and episode studies. Atmospheric Environment 34, 407-418.

[41] Saltbones J., Bartnicki J. and A. Foss (2003) Handling of Fallout Processes from Nuclear Explosions in Severe Nuclear Accident Program - SNAP. Research Report No. 157. Norwegian Meteorological Institute. Oslo, Norway.

[42] Sundqvist, H. (1993) Inclusion of Ice Phase of Hydrometeors in Cloud Parameterization for Mesoscale and Largescale Models. Contr. Atm. Phys., 66, 137-147.

[43] Sass, B. H., L. Rontu, and P. Räisänen (1994) HIRLAM-2 Radiation Scheme: Documentation and Tests. Technical Report 16, The HIRLAM-3 Project, SMHI, S-60176 Norrköping, Sweden.

[44] Savijärvi H.(1990) Fast radiation parameterization schemes for mesoscale and short-range forecast models. J. Appl. Meteor., 29, 437-447.

[45] Seinfeld J.H. (1986) Atmospheric Chemistry and Physics of Air Pollution. John Wile & Sons. New York. 738 pp.

[46] Simpson, D., H., Bergström, R., Emberson, L. D., Fagerli, H., Flechard, C. R., Hayman, G. D., Gauss, M., Jonson, J. E., Jenkin, M. E., Nyiri, A., Richter, C., Semeena, V. S., Tsyro, S., Tuovinen, J.-P., Valdebenito, Á., and Wind, P. (2012) The EMEP MSC-W chemical transport model - technical description Atmos. Chem. Phys., 12 (16), 7825-7865.

[47] Undén, P., Rontu, L., Järvinen, H., Lynch, P., Calvo, J., Cats, G., Cuaxart, J., Eerola, K., Fortelius, C., Garcia-Moya, J.A., Jones, C., Lenderlink, G., McDonald, A., McGrath, R., Navascues, B., Nielsen, N.W., Ødegaard, V., Rodriguez,E., Rummukainen, M., Rööm, R., Sattler, K., Sass, B.H., Savijärvi, H., Schreur, B.W., Sigg, R., The, H. and Tijm,A. (2002) HIRLAM-5 Scientific Documentation, HIRLAM-5 Project. Available from SMHI, S-601767 Norrköping, Sweden.

[48] Uppala, S.M., Kållberg, P.W., Simmons, A.J., Andrae, U., da Costa Bechtold, V., Fiorino, M., Gibson, J.K., Haseler, J., Hernandez, A., Kelly, G.A., Li, X., Onogi, K., Saarinen, S., Sokka, N., Allan, R.P., Andersson, E., Arpe, K., Balmaseda, M.A., Beljaars, A.C.M., van de Berg, L., Bidlot, J., Bormann, N., Caires, S., Chevallier, F., Dethof, A., Dragosavac, M., Fisher, M., Fuentes, M., Hagemann, S., Hólm, E., Hoskins, B.J., Isaksen, L., Janssen, P.A.E.M., Jenne, R., McNally, A.P., Mahfouf, J.-F., Morcrette, J.-J., Rayner, N.A., Saunders, R.W., Simon, P., Sterl, A., Trenberth, K.E., Untch, A., Vasiljevic, D., Viterbo, P., and Woollen, J., 2005, The ERA-40 re-analysis. Quart. J. R. Meteorol. Soc. 131, 2961-3012.

[49] Venkatram A. and J. Pleim (1999) Atmospheric Environment, 33, 3075-3076.

[50] Wyser, K., L. Rontu, and H. Savijärvi (1999) Introducing the effective radius into a fast radiation scheme of a mesoscale model. Contr. Atm. Phys., 72, 205-218.

[51] Yang, X. (2005) Background blending using an incremental spatial filter. Hirlam Newsletter,49, pages 3-11.

A. List of Isotopes used in Remote Simulations from NRPA

In this Appendix we show the list of isotopes used for remote SNAP runs from NRPA. Altogether there are 382 isotopes which can be used in remote applications of SNAP from NRPA. Identification number of each isotope is given in the first column and name of the isotope in the second coulmn. There can be three forms of the isotope specified by one digit number: 0-noble gas, 1-gas and 2-aerosol. This information is included in the third column. The radioactive decay constant is given in column four with the unit s^{-1}.

Identification number	Name	Type	Decay constant
1	H - 3	0	0.178E-08
2	Na- 24	2	0.128E-04
3	Ar- 41	0	0.105E-03
4	Co- 58	2	0.113E-06
5	Co- 60	2	0.416E-08
6	Zn- 72	2	0.414E-05
7	Ga- 72	2	0.137E-04
8	Ga- 73	2	0.395E-04
9	Ge- 75	2	0.140E-03
10	Ge- 77m	2	0.128E-01
11	Ge- 77	2	0.170E-04
12	Ge- 78	2	0.133E-03
13	As- 77	2	0.496E-05
14	As- 78	2	0.127E-03
15	Se- 79	2	0.338E-12
16	Se- 81m	2	0.202E-03
17	Se- 81	2	0.625E-03
18	Se- 83m	2	0.990E-02
19	Se- 83	2	0.513E-03
20	Br- 82m	2	0.189E-02
21	Br- 82	2	0.544E-05
22	Br- 83	2	0.802E-04
23	Br- 84m	2	0.193E-02
24	Br- 84	2	0.363E-03
25	Kr- 83m	0	0.104E-03
26	Kr- 85m	0	0.438E-04
27	Kr- 85	0	0.203E-08
28	Kr- 87	0	0.152E-03
29	Kr- 88	0	0.686E-04
30	Kr- 89	0	0.364E-02
31	Rb- 86m	2	0.114E-01
32	Rb- 86	2	0.430E-06
33	Rb- 87	2	0.470E-18
34	Rb- 88	2	0.642E-03
35	Rb- 89	2	0.760E-03
36	Sr- 89	2	0.154E-06
37	Sr- 90	2	0.787E-09
38	Sr- 91	2	0.203E-04
39	Sr- 92	2	0.711E-04
40	Y - 90m	2	0.604E-04

Identification number	Name	Type	Decay rate
41	Y - 90	2	0.301E-05
42	Y - 91m	2	0.232E-03
43	Y - 91	2	0.137E-06
44	Y - 92	2	0.545E-04
45	Y - 93	2	0.189E-04
46	Y - 94	2	0.608E-03
47	Y - 95	2	0.110E-02
48	Zr- 93	2	0.231E-13
49	Zr- 95	2	0.123E-06
50	Zr- 97	2	0.115E-04
51	Nb- 94m	2	0.185E-02
52	Nb- 94	2	0.110E-11
53	Nb- 95m	2	0.222E-05
54	Nb- 95	2	0.228E-06
55	Nb- 96	2	0.823E-05
56	Nb- 97m	2	0.128E-01
57	Nb- 97	2	0.157E-03
58	Nb- 98	2	0.227E-03
59	Mo- 99	2	0.289E-05
60	Mo-101	2	0.791E-03
61	Mo-102	2	0.104E-02
62	Tc- 99m	2	0.320E-04
63	Tc- 99	2	0.103E-12
64	Tc-101	2	0.814E-03
65	Tc-102m	2	0.269E-02
66	Tc-102	2	0.131E+00
67	Tc-104	2	0.642E-03
68	Ru-103	2	0.203E-06
69	Ru-105	2	0.434E-04
70	Ru-106	2	0.219E-07
71	Rh-103m	2	0.206E-03
72	Rh-105m	2	0.182E-01
73	Rh-105	2	0.542E-05
74	Rh-106m	2	0.883E-04
75	Rh-106	2	0.232E-01
76	Rh-107	2	0.532E-03
77	Pd-107m	2	0.325E-01
78	Pd-107	2	0.338E-14
79	Pd-109	2	0.143E-04
80	Pd-111m	2	0.350E-04

Identification number	Name	Type	Decay rate
81	Pd-111	2	0.525E-03
82	Pd-112	2	0.958E-05
83	Ag-109m	2	0.175E-01
84	Ag-110m	2	0.297E-07
85	Ag-111m	2	0.937E-02
86	Ag-111	2	0.107E-05
87	Ag-112	2	0.615E-04
88	Ag-113m	2	0.105E-01
89	Ag-113	2	0.363E-04
90	Ag-115m	2	0.408E-01
91	Ag-115	2	0.550E-03
92	Cd-111m	2	0.237E-03
93	Cd-113m	2	0.151E-08
94	Cd-113	2	0.244E-23
95	Cd-115m	2	0.180E-06
96	Cd-115	2	0.360E-05
97	Cd-117m	2	0.566E-04
98	Cd-117	2	0.741E-04
99	Cd-118	2	0.230E-03
100	In-113m	2	0.116E-03
101	In-115m	2	0.428E-04
102	In-115	2	0.431E-23
103	In-116m	2	0.213E-03
104	In-116	2	0.488E-01
105	In-117m	2	0.993E-04
106	In-117	2	0.263E-03
107	In-118m	2	0.263E-02
108	In-118	2	0.139E+00
109	In-119m	2	0.642E-03
110	In-119	2	0.462E-02
111	Sn-117m	2	0.573E-06
112	Sn-119m	2	0.328E-07
113	Sn-121m	2	0.440E-09
114	Sn-121	2	0.718E-05
115	Sn-123m	2	0.289E-03
116	Sn-123	2	0.622E-07
117	Sn-125	2	0.831E-06
118	Sn-126	2	0.220E-12
119	Sn-127	2	0.908E-04
120	Sn-128	2	0.196E-03

Identification number	Name	Type	Decay rate
121	Sn-130	2	0.312E-02
122	Sb-124m	2	0.569E-03
123	Sb-124	2	0.133E-06
124	Sb-125	2	0.805E-08
125	Sb-126m	2	0.608E-03
126	Sb-126	2	0.647E-06
127	Sb-127	2	0.211E-05
128	Sb-128m	2	0.111E-02
129	Sb-128	2	0.214E-04
130	Sb-129	2	0.444E-04
131	Sb-130m	2	0.175E-02
132	Sb-130	2	0.312E-03
133	Sb-131	2	0.502E-03
134	Te-125m	2	0.138E-06
135	Te-127m	2	0.736E-07
136	Te-127	2	0.205E-04
137	Te-129m	2	0.240E-06
138	Te-129	2	0.165E-03
139	Te-131m	2	0.642E-05
140	Te-131	2	0.462E-03
141	Te-132	2	0.247E-05
142	Te-133m	2	0.209E-03
143	Te-133	2	0.924E-03
144	Te-134	2	0.275E-03
145	I -129	1	0.138E-14
146	I -130m	1	0.130E-02
147	I -130	1	0.155E-04
148	I -131	1	0.994E-06
149	I -132	1	0.836E-04
150	I -133m	1	0.770E-01
151	I -133	1	0.921E-05
152	I -134m	1	0.321E-02
153	I -134	1	0.222E-03
154	I -135	1	0.288E-04
155	Xe-129m	0	0.100E-05
156	Xe-131m	0	0.680E-06
157	Xe-133m	0	0.355E-05
158	Xe-133	0	0.152E-05
159	Xe-134m	0	0.239E+01
160	Xe-135m	0	0.743E-03

Identification number	Name	Type	Decay rate
161	Xe-135	0	0.210E-04
162	Xe-137	0	0.296E-02
163	Xe-138	0	0.815E-03
164	Cs-134m	2	0.664E-04
165	Cs-134	2	0.107E-07
166	Cs-135m	2	0.218E-03
167	Cs-135	2	0.956E-14
168	Cs-136	2	0.617E-06
169	Cs-137	2	0.729E-09
170	Cs-138	2	0.359E-03
171	Ba-135m	2	0.671E-05
172	Ba-137m	2	0.453E-02
173	Ba-139	2	0.139E-03
174	Ba-140	2	0.627E-06
175	La-140	2	0.456E-05
176	La-141	2	0.498E-04
177	La-142	2	0.125E-03
178	La-143	2	0.825E-03
179	Ce-141	2	0.243E-06
180	Ce-142	2	0.440E-24
181	Ce-143	2	0.584E-05
182	Ce-144	2	0.282E-07
183	Ce-146	2	0.814E-03
184	Pr-142m	2	0.791E-03
185	Pr-142	2	0.101E-04
186	Pr-143	2	0.591E-06
187	Pr-144m	2	0.161E-02
188	Pr-144	2	0.669E-03
189	Pr-145	2	0.322E-04
190	Pr-146	2	0.477E-03
191	Pr-147	2	0.963E-03
192	Nd-144	2	0.105E-22
193	Nd-147	2	0.730E-06
194	Nd-149	2	0.111E-03
195	Nd-151	2	0.932E-03
196	Nd-152	2	0.101E-02
197	Pm-147	2	0.838E-08
198	Pm-148m	2	0.194E-06
199	Pm-148	2	0.149E-05
200	Pm-149	2	0.363E-05

Identification number	Name	Type	Decay rate
201	Pm-150	2	0.718E-04
202	Pm-151	2	0.678E-05
203	Pm-152m	2	0.642E-03
204	Pm-152	2	0.282E-02
205	Sm-147	2	0.205E-18
206	Sm-148	2	0.275E-23
207	Sm-149	2	0.220E-23
208	Sm-151	2	0.236E-09
209	Sm-153	2	0.414E-05
210	Sm-155	2	0.520E-03
211	Sm-156	2	0.205E-04
212	Eu-154	2	0.256E-08
213	Eu-155	2	0.458E-08
214	Eu-156	2	0.528E-06
215	Eu-157	2	0.127E-04
216	Eu-158	2	0.252E-03
217	Eu-159	2	0.638E-03
218	Gd-159	2	0.104E-04
219	Gd-162	2	0.116E-02
220	Tb-160	2	0.111E-06
221	Tb-161	2	0.116E-05
222	Tb-162m	2	0.863E-04
223	Tb-162	2	0.155E-02
224	Tb-163	2	0.592E-03
225	Dy-165	2	0.819E-04
226	Hg-206	2	0.144E-02
227	Tl-206	2	0.276E-02
228	Tl-207	2	0.241E-02
229	Tl-208	2	0.373E-02
230	Tl-209	2	0.525E-02
231	Tl-210	2	0.889E-02
232	Pb-207m	2	0.866E+00
233	Pb-209	2	0.583E-04
234	Pb-210	2	0.105E-08
235	Pb-211	2	0.320E-03
236	Pb-212	2	0.181E-04
237	Pb-213	2	0.116E-02
238	Pb-214	2	0.431E-03
239	Bi-209	2	0.110E-25
240	Bi-210	2	0.160E-05

Identification number	Name	Type	Decay rate
241	Bi-211	2	0.537E-02
242	Bi-212	2	0.191E-03
243	Bi-213	2	0.246E-03
244	Bi-214	2	0.586E-03
245	Bi-215	2	0.165E-02
246	Po-210	2	0.580E-07
247	Po-211	2	0.133E+01
248	Po-212	2	0.228E+07
249	Po-213	2	0.165E+06
250	Po-214	2	0.423E+04
251	Po-215	2	0.389E+03
252	Po-216	2	0.462E+01
253	Po-217	2	0.693E-01
254	Po-218	2	0.379E-02
255	At-215	2	0.693E+04
256	At-216	2	0.231E+04
257	At-217	2	0.217E+02
258	At-218	2	0.347E+00
259	At-219	2	0.128E-01
260	Rn-218	2	0.198E+02
261	Rn-219	2	0.173E+00
262	Rn-220	2	0.126E-01
263	Rn-221	2	0.462E-03
264	Rn-222	2	0.210E-05
265	Rn-223	2	0.269E-03
266	Fr-221	2	0.241E-02
267	Fr-222	2	0.781E-03
268	Fr-223	2	0.525E-03
269	Ra-222	2	0.182E-01
270	Ra-223	0	0.702E-06
271	Ra-224	0	0.220E-05
272	Ra-225	0	0.542E-06
273	Ra-226	0	0.137E-10
274	Ra-227	0	0.280E-03
275	Ra-228	0	0.328E-08
276	Ra-229	0	0.693E+12
277	Ac-225	2	0.802E-06
278	Ac-226	2	0.664E-05
279	Ac-227	2	0.102E-08
280	Ac-228	2	0.314E-04

Identification number	Name	Type	Decay rate
281	Ac-229	2	0.175E-03
282	Th-226	2	0.374E-03
283	Th-227	2	0.441E-06
284	Th-228	2	0.115E-07
285	Th-229	2	0.299E-11
286	Th-230	2	0.275E-12
287	Th-231	2	0.755E-05
288	Th-232	2	0.156E-17
289	Th-233	2	0.520E-03
290	Th-234	2	0.333E-06
291	Pa-230	2	0.453E-06
292	Pa-231	2	0.676E-12
293	Pa-232	2	0.612E-05
294	Pa-233	2	0.297E-06
295	Pa-234m	2	0.987E-02
296	Pa-234	2	0.285E-04
297	U -230	2	0.386E-06
298	U -231	2	0.187E-05
299	U -232	2	0.305E-09
300	U -233	2	0.136E-12
301	U -234	2	0.889E-13
302	U -235	2	0.309E-16
303	U -236	2	0.919E-15
304	U -237	2	0.119E-05
305	U -238	2	0.487E-17
306	U -239	2	0.492E-03
307	U -240	2	0.134E-04
308	Np-235	2	0.196E-07
309	Np-236m	2	0.170E-15
310	Np-236	2	0.875E-05
311	Np-237	2	0.103E-13
312	Np-238	2	0.382E-05
313	Np-239	2	0.341E-05
314	Np-240m	2	0.158E-02
315	Np-240	2	0.183E-03
316	Pu-235	2	0.444E-03
317	Pu-236	2	0.771E-08
318	Pu-237	2	0.176E-06
319	Pu-238	2	0.255E-09
320	Pu-239	2	0.900E-12

Identification number	Name	Type	Decay rate
321	Pu-240	2	0.334E-11
322	Pu-241	2	0.166E-08
323	Pu-242	2	0.580E-13
324	Pu-243	2	0.387E-04
325	Pu-244	2	0.275E-15
326	Pu-245	2	0.193E-04
327	Am-240	2	0.378E-05
328	Am-241	2	0.480E-10
329	Am-242	2	0.495E+02
330	Am-242m	2	0.145E-09
331	Am-242	2	0.120E-04
332	Am-243	2	0.276E-11
333	Am-244m	2	0.444E-03
334	Am-244	2	0.191E-04
335	Am-245	2	0.917E-04
336	Cm-241	2	0.229E-06
337	Cm-242	2	0.492E-07
338	Cm-243	2	0.686E-09
339	Cm-244	2	0.125E-08
340	Cm-245	2	0.236E-11
341	Cm-246	2	0.399E-11
342	Cm-247	2	0.137E-14
343	Cm-248	2	0.467E-13
344	Cm-249	2	0.181E-03
345	Cm-250	2	0.318E-11
346	Bk-249	2	0.255E-07
347	Bk-250	2	0.598E-04
348	Cf-249	2	0.610E-10
349	Cf-250	2	0.169E-08
350	Cf-251	2	0.275E-10
351	Cf-252	2	0.829E-08
352	Cf-253	2	0.456E-06
353	Cf-254	2	0.133E-06
354	Es-253	2	0.392E-06
355	Es-254m	2	0.491E-05
356	Es-254	2	0.291E-07
357	Es-255	2	0.209E-06
358	C - 11	0	0.567E-03
359	N - 13	0	0.116E-02
360	O - 15	0	0.567E-02

Identification number	Name	Type	Decay rate
361	F - 18	0	0.115E-03
545	I -129e	1	0.138E-14
645	I -129o	1	0.138E-14
745	I -129a	1	0.138E-14
547	I -130e	1	0.155E-04
647	I -130o	1	0.155E-04
747	I -130a	1	0.155E-04
548	I -131e	1	0.994E-06
648	I -131o	1	0.994E-06
748	I -131a	1	0.994E-06
549	I -132e	1	0.836E-04
649	I -132o	1	0.836E-04
749	I -132a	1	0.836E-04
551	I -133e	1	0.921E-05
651	I -133o	1	0.921E-05
751	I -133a	1	0.921E-05
553	I -134e	1	0.222E-03
653	I -134o	1	0.222E-03
753	I -134a	1	0.222E-03
554	I -135e	1	0.288E-04
654	I -135o	1	0.288E-04
754	I -135a	1	0.288E-04

B. Deposition fields for the worst case scenario - individual components

Here we present the maps of dry, wet and total deposition of individual components for the worst case scenario and accident at the final destination in Germikha Bay. The maps are shown after 96 hours from the accident start. The same scale is used for all maps and the units are Bq m^{-2}.

UO2-Be 0.1 μm - dry deposition after 96 hrs

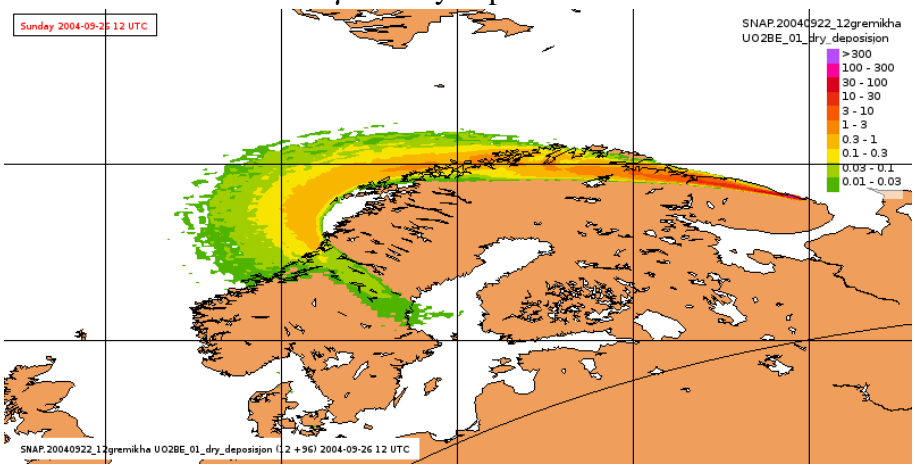

UO2-Be 0.1 μm - wet deposition after 96 hrs

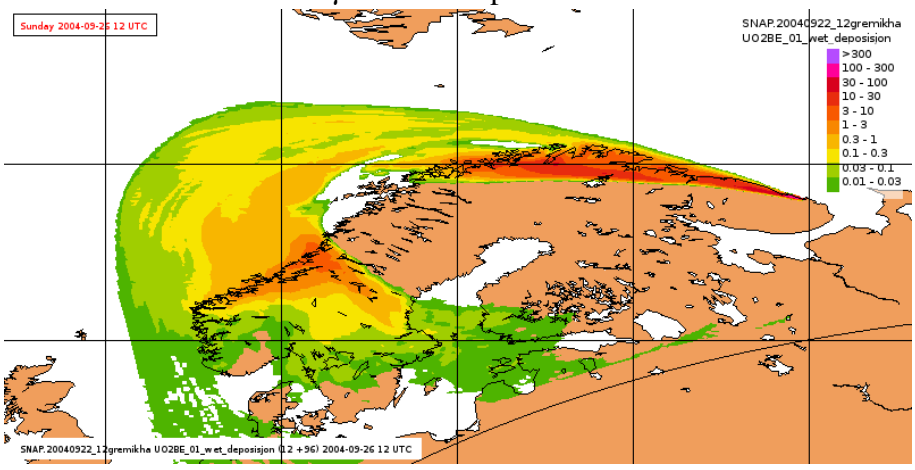

UO2-Be 0.1 μm - total deposition after 96 hrs

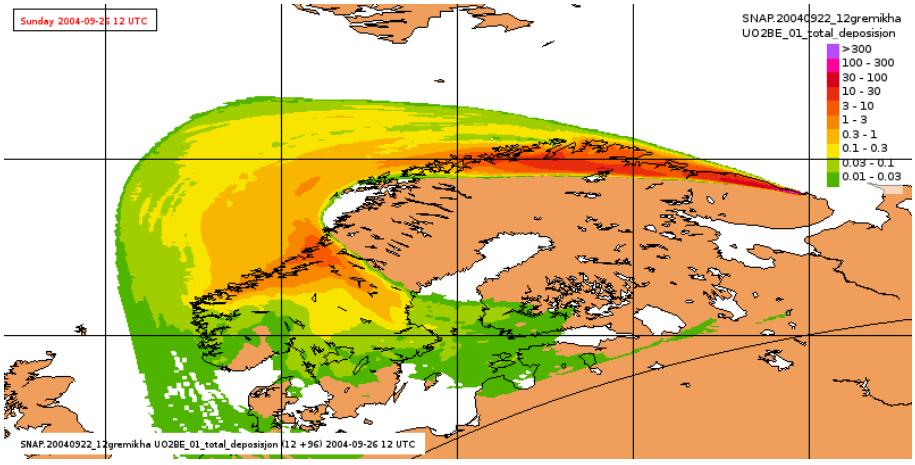

B. *Deposition fields for the worst case scenario - individual components*

UO2-Be 0.5 μm - dry deposition after 96 hrs

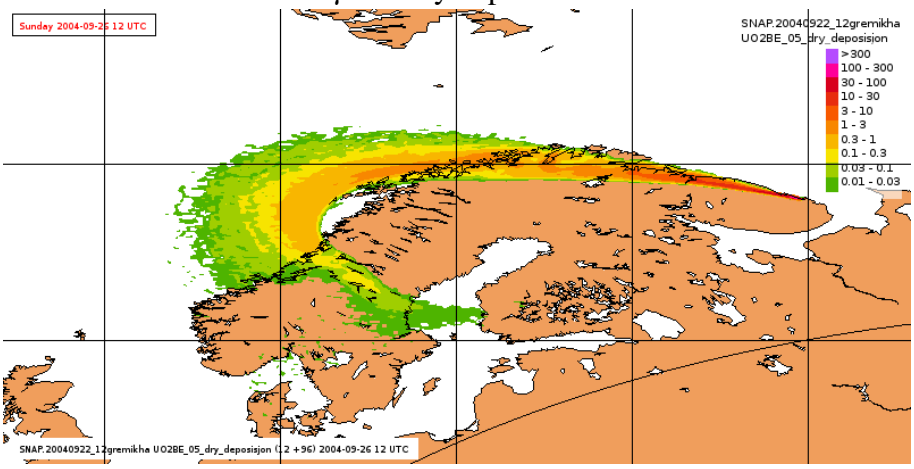

UO2-Be 0.5 μm - wet deposition after 96 hrs

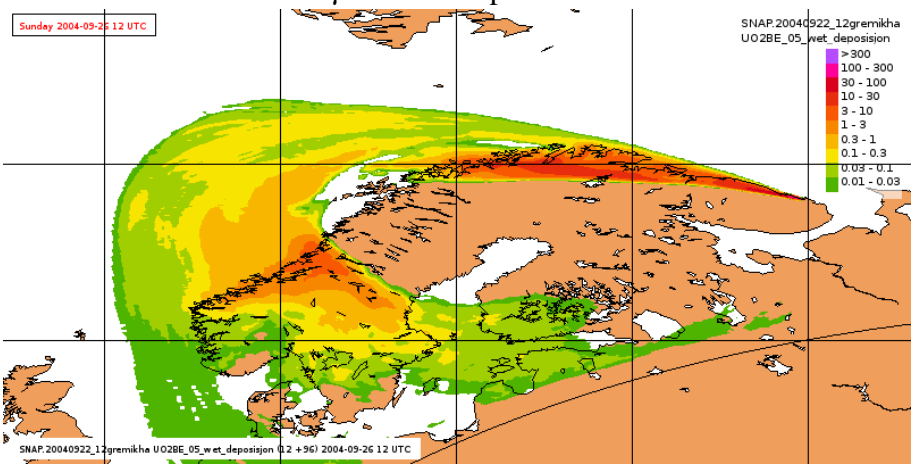

UO2-Be 0.5 μm - total deposition after 96 hrs

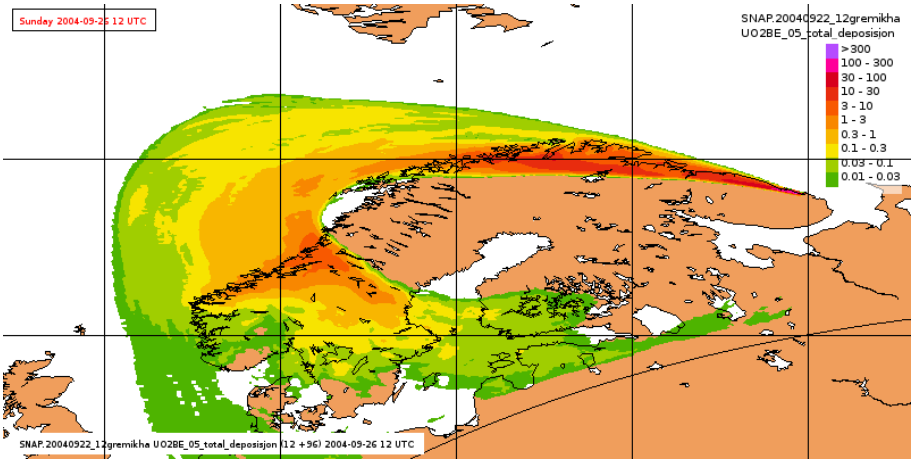

UO2-Be 1 μm - dry deposition after 96 hrs

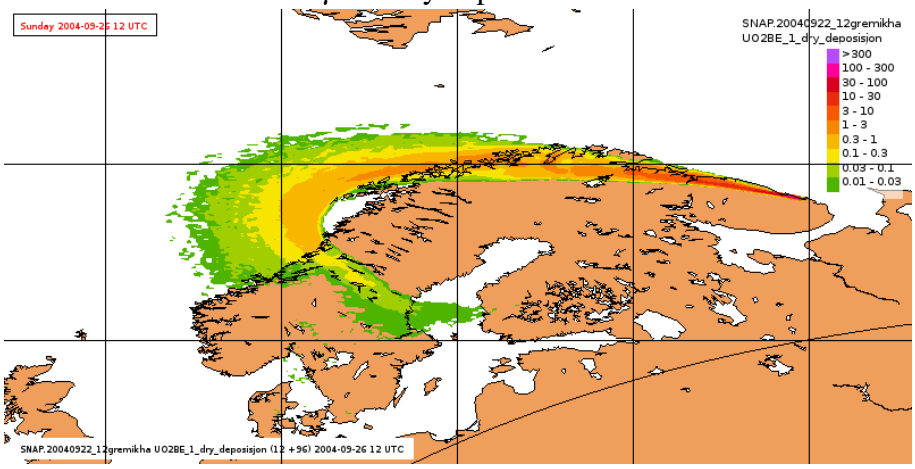

UO2-Be 1 μm - wet deposition after 96 hrs

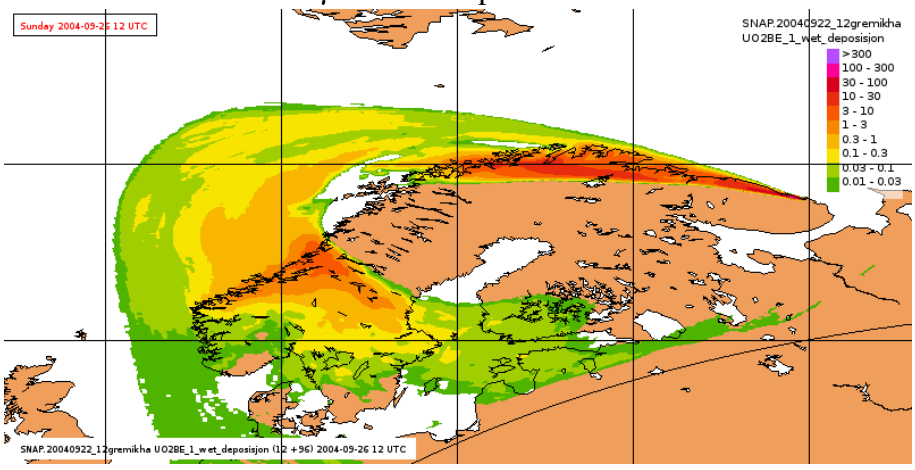

UO2-Be 1 μm - total deposition after 96 hrs

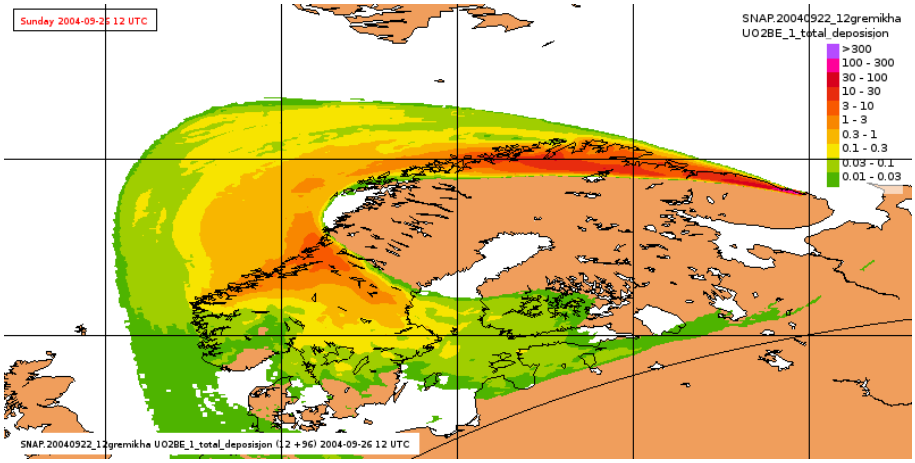

B. Deposition fields for the worst case scenario - individual components

UO2-Be 5 μm - dry deposition after 96 hrs

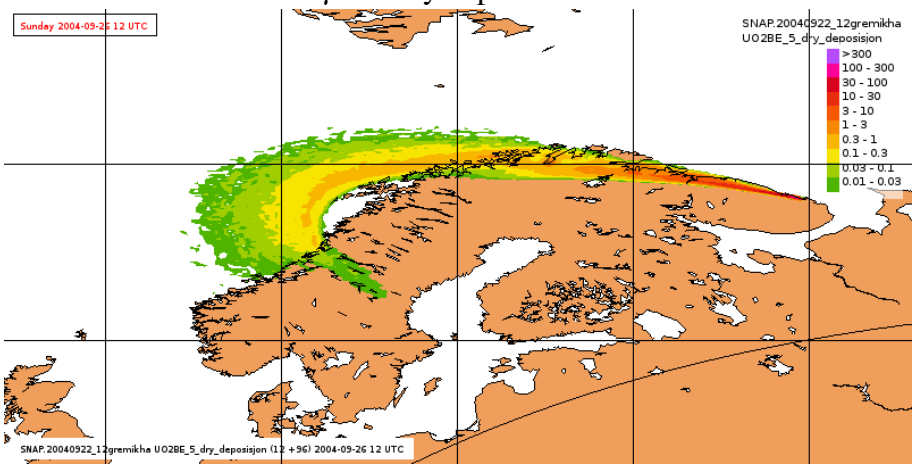

UO2-Be 5 μm - wet deposition after 96 hrs

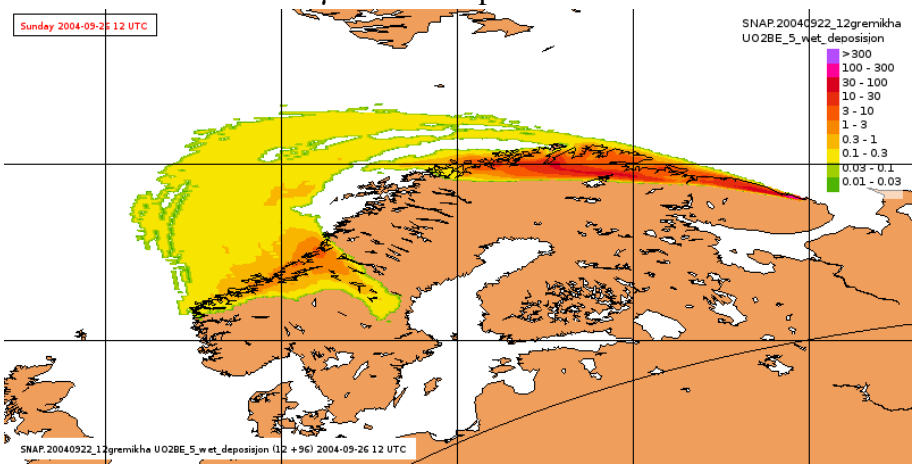

UO2-Be 5 μm - total deposition after 96 hrs

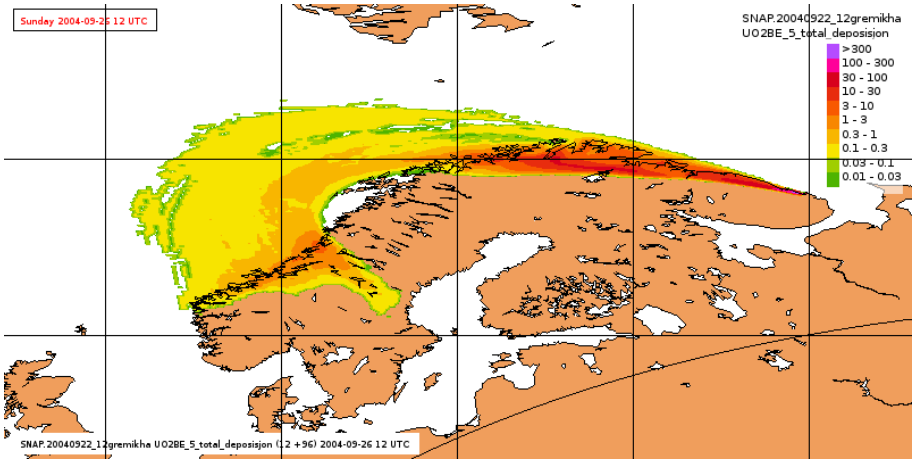

UO2-Be 10 μm - dry deposition after 96 hrs

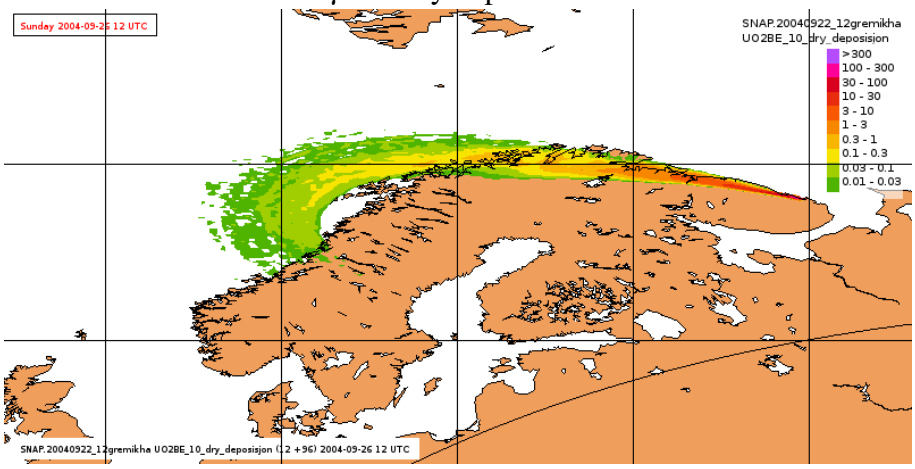

UO2-Be 10 μm - wet deposition after 96 hrs

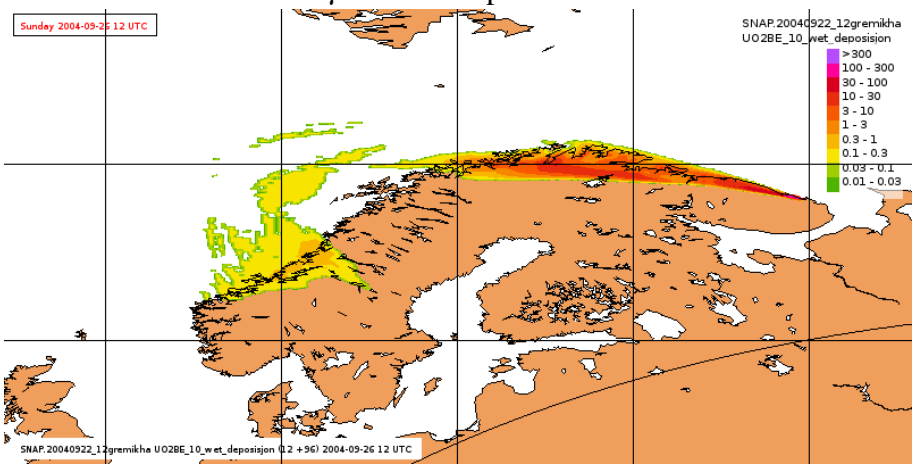

UO2-Be 10 μm - total deposition after 96 hrs

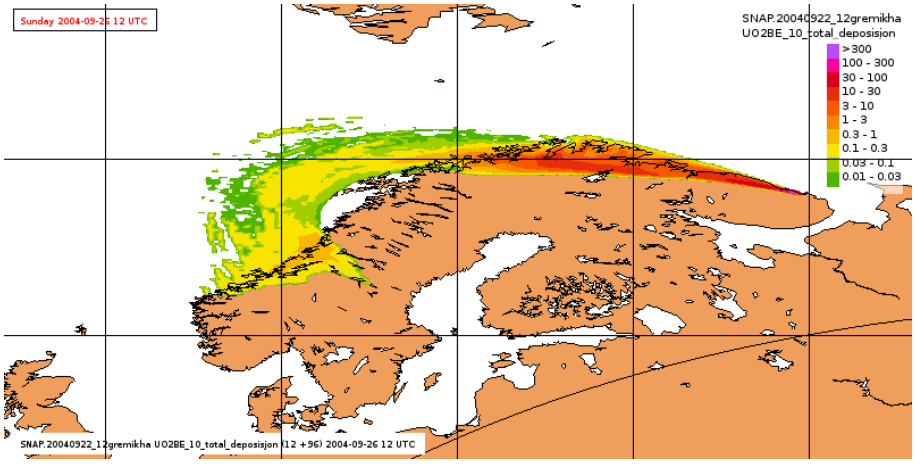

UO2-Be 20 μm - dry deposition after 96 hrs

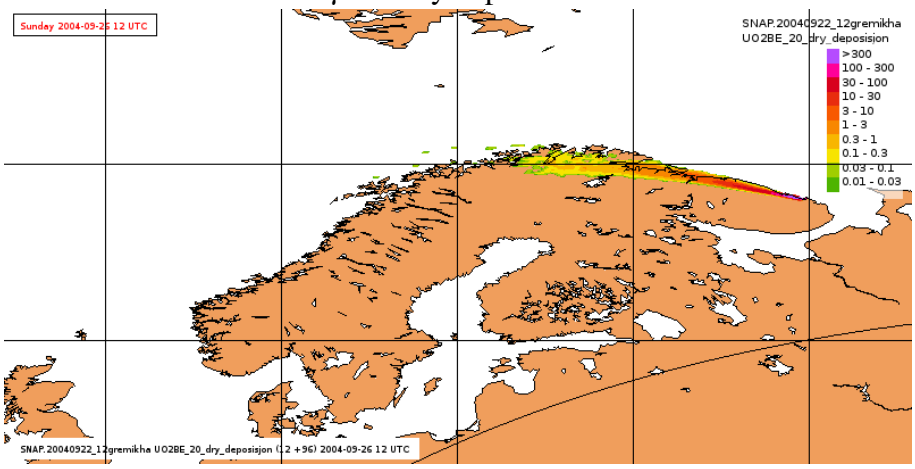

UO2-Be 20 μm - wet deposition after 96 hrs

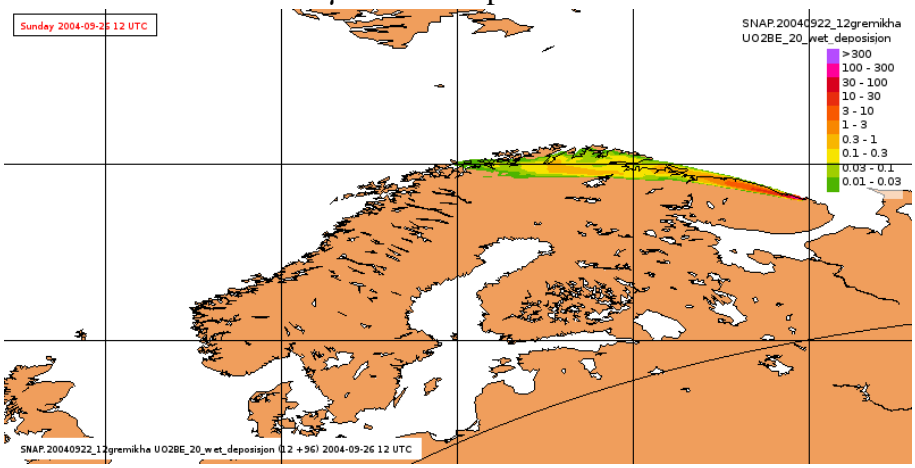

UO2-Be 20 μm - total deposition after 96 hrs

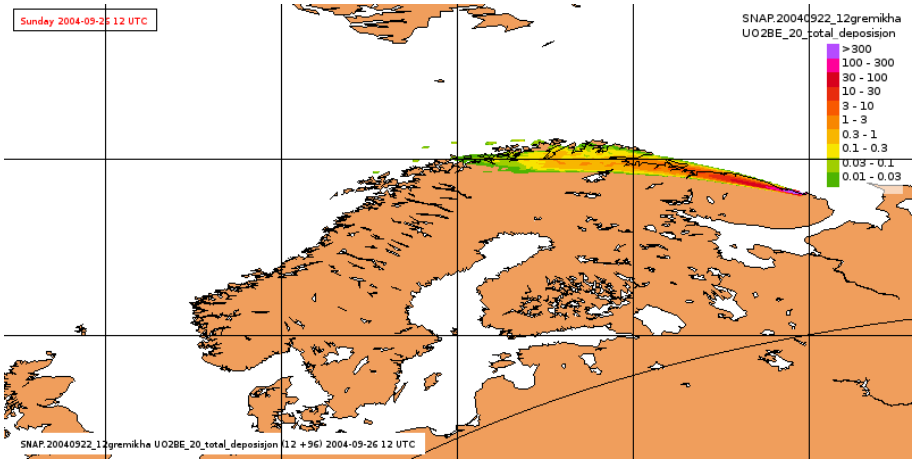

UO2-Be 50 μm - dry deposition after 96 hrs

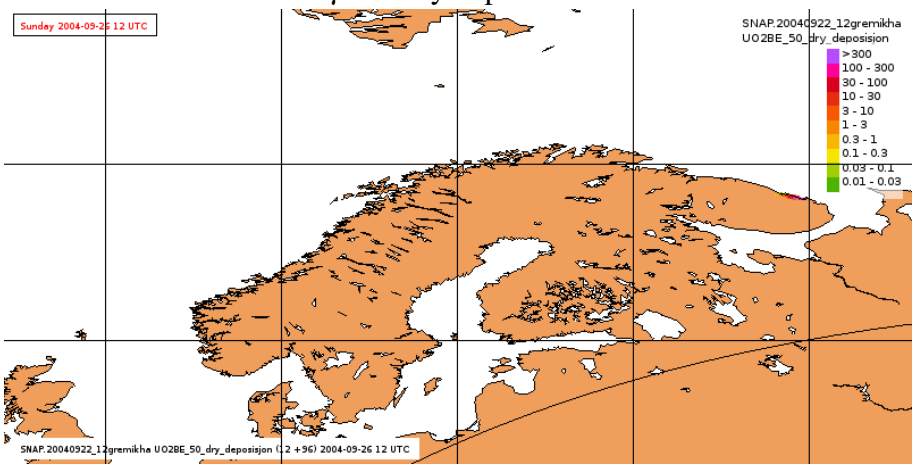

UO2-Be 50 μm - wet deposition after 96 hrs

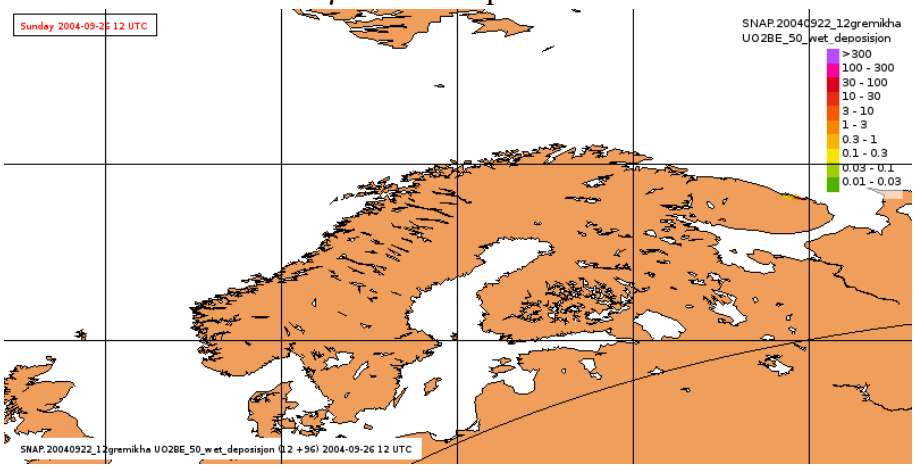

UO2-Be 50 μm - total deposition after 96 hrs

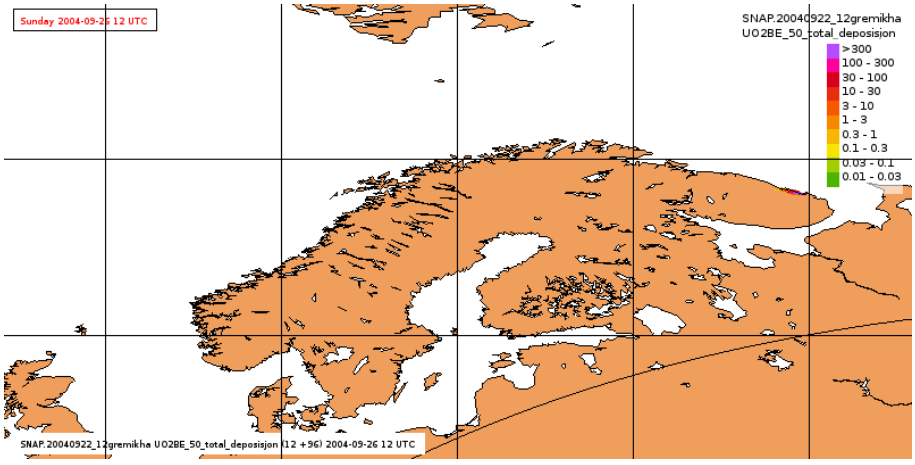

B. Deposition fields for the worst case scenario - individual components

UO2-Be 100 μm - dry deposition after 96 hrs

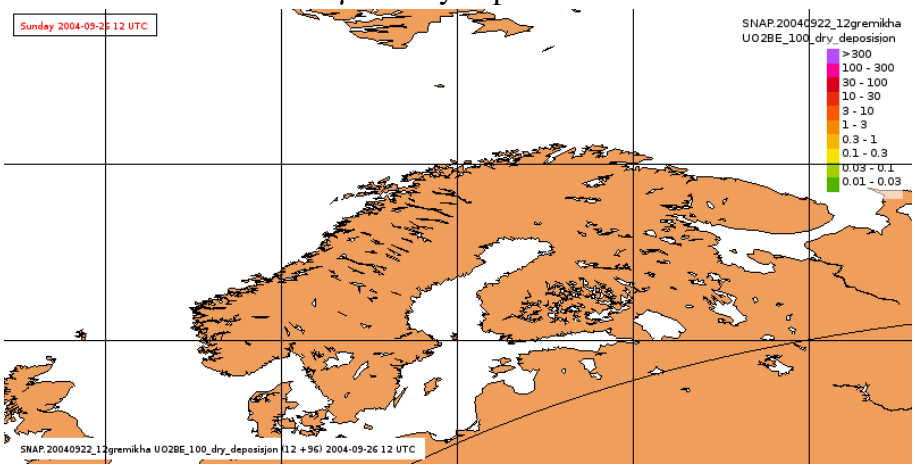

UO2-Be 100 μm - wet deposition after 96 hrs

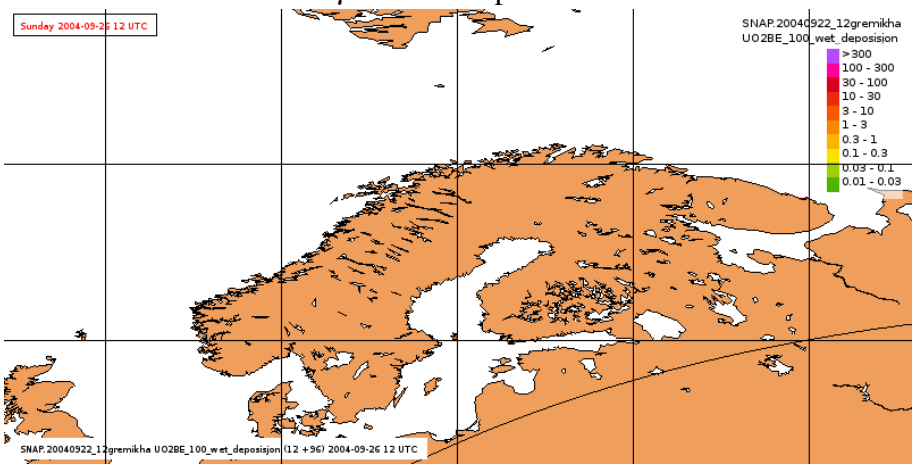

UO2-Be 100 μm - total deposition after 96 hrs

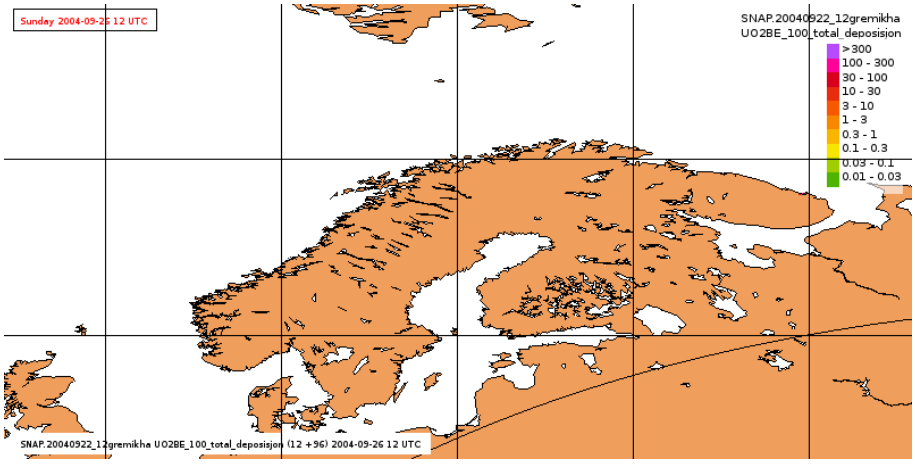

Bitumen 0.1 μm - dry deposition after 96 hrs

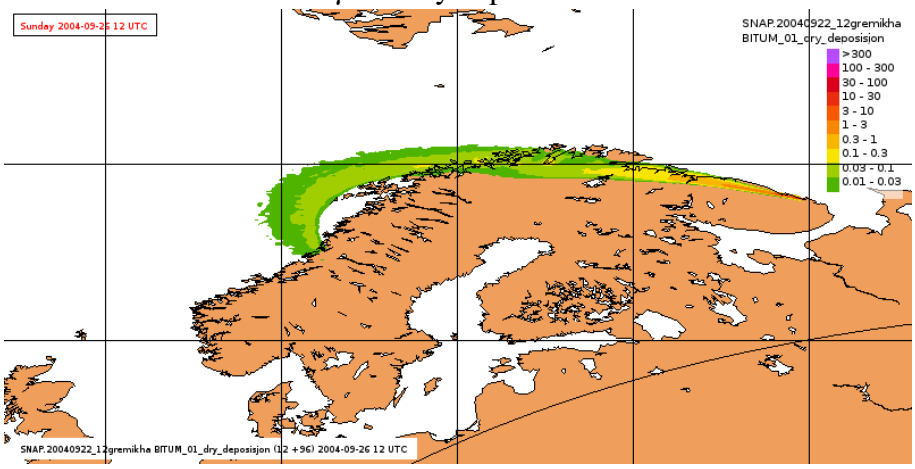

Bitumen 0.1 μm - wet deposition after 96 hrs

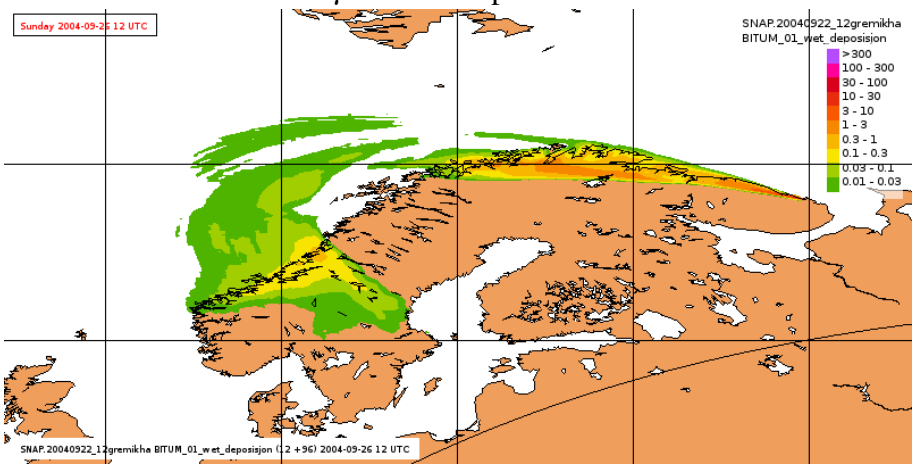

Bitumen 0.1 μm - total deposition after 96 hrs

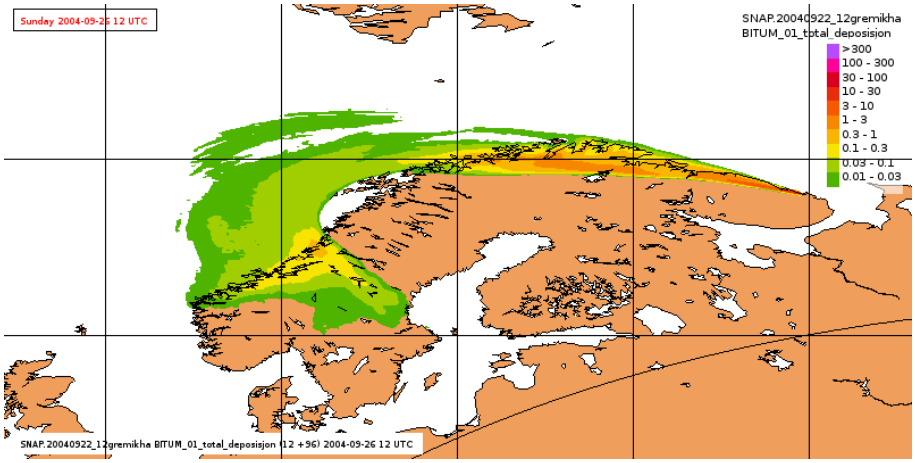

B. *Deposition fields for the worst case scenario - individual components*

Bitumen 0.5 μm - dry deposition after 96 hrs

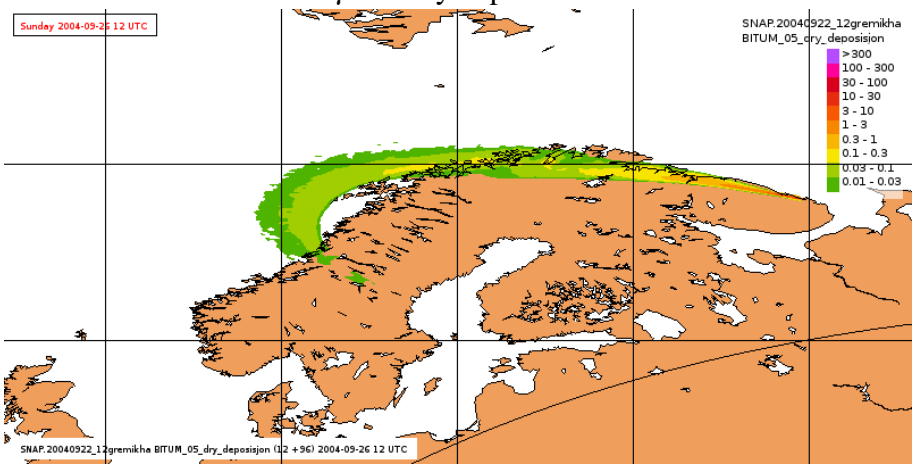

Bitumen 0.5 μm - wet deposition after 96 hrs

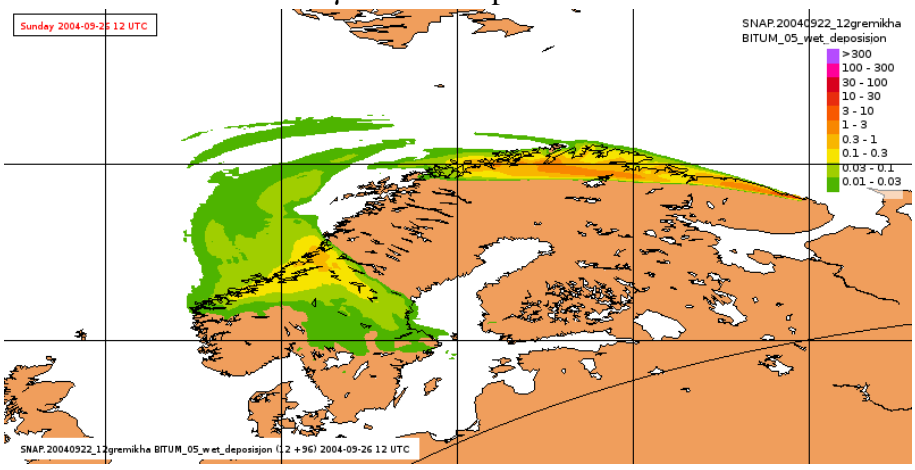

Bitumen 0.5 μm - total deposition after 96 hrs

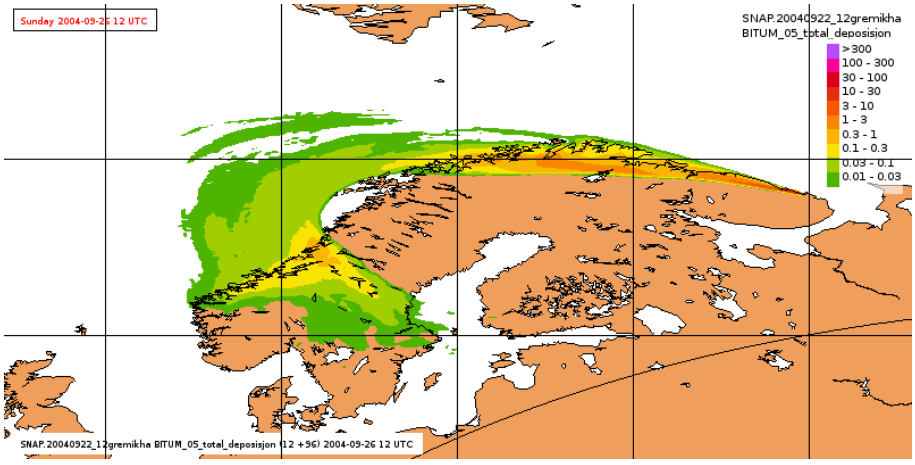

Bitumen 1 μm - dry deposition after 96 hrs

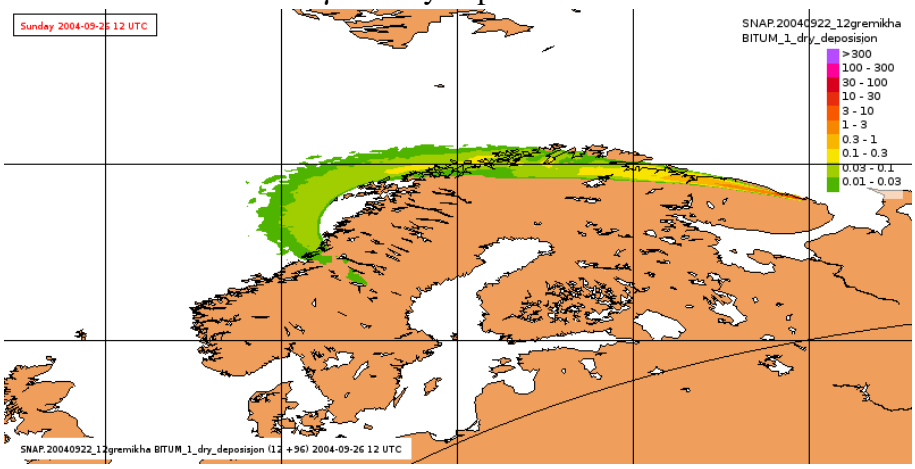

Bitumen 1 μm - wet deposition after 96 hrs

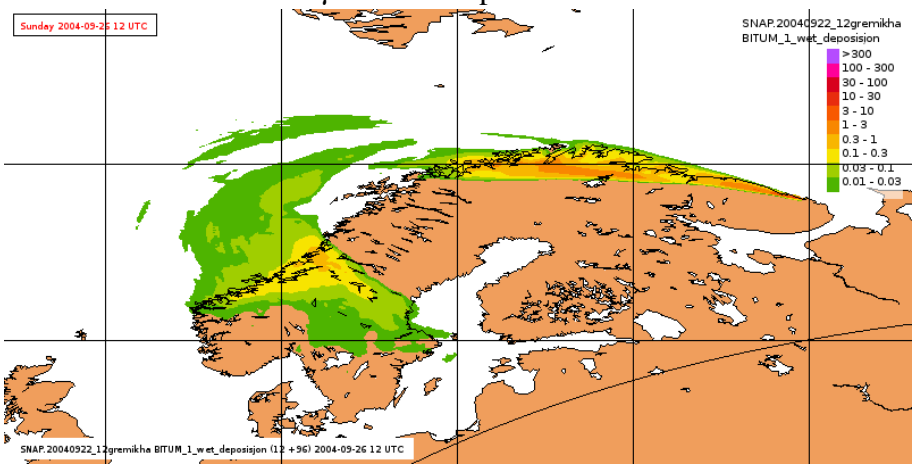

Bitumen 1 μm - total deposition after 96 hrs

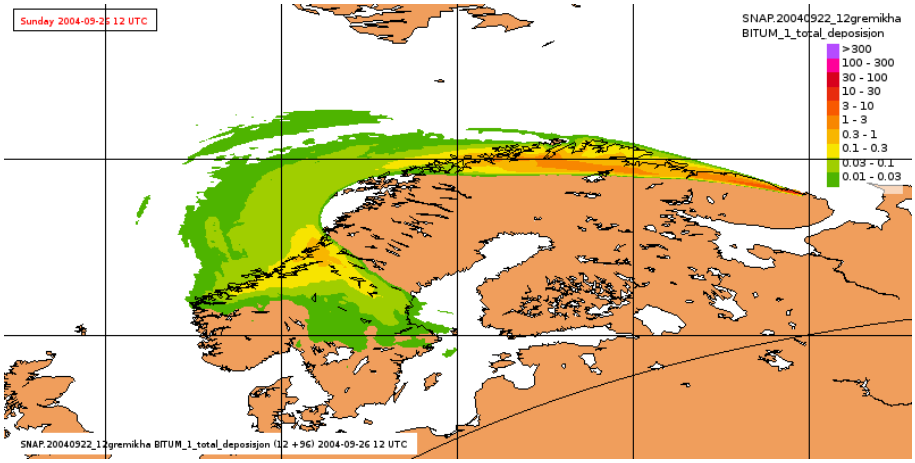

B. Deposition fields for the worst case scenario - individual components

Bitumen 5 μm - dry deposition after 96 hrs

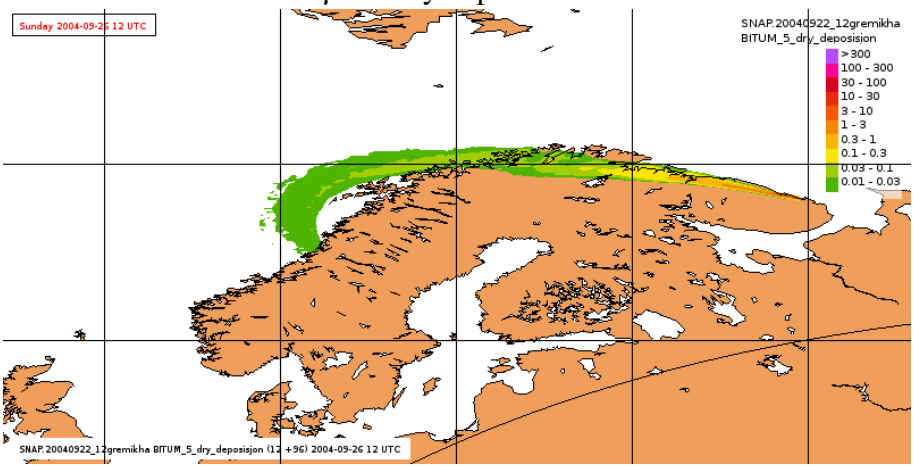

Bitumen 5 μm - wet deposition after 96 hrs

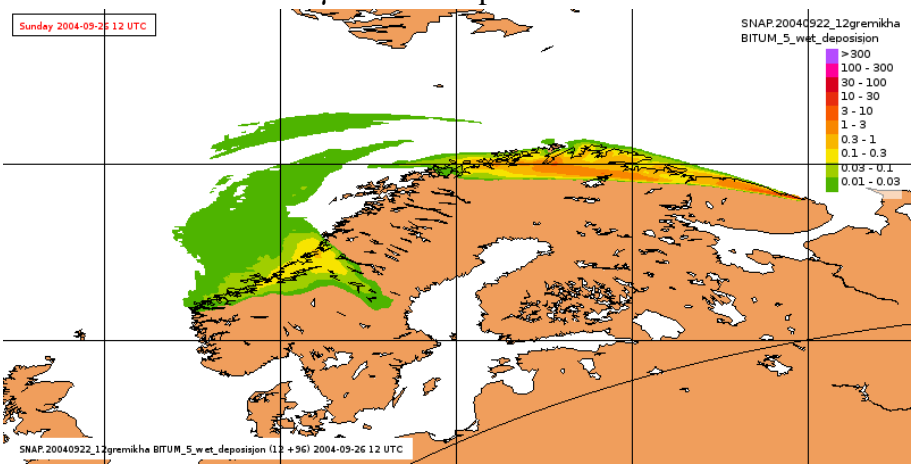

Bitumen 5 μm - total deposition after 96 hrs

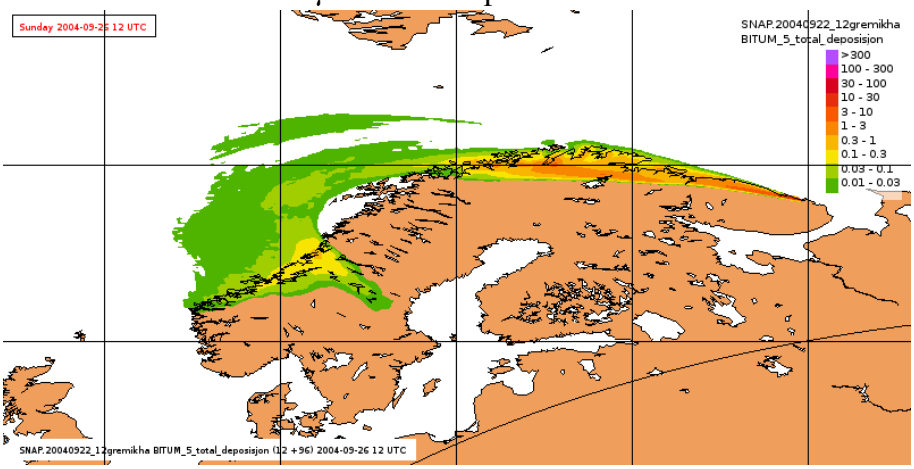

Bitumen 10 μm - dry deposition after 96 hrs

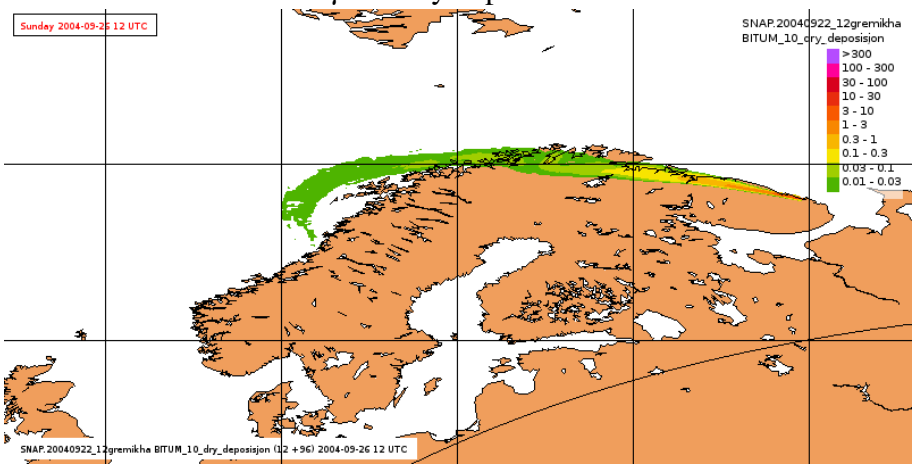

Bitumen 10 μm - wet deposition after 96 hrs

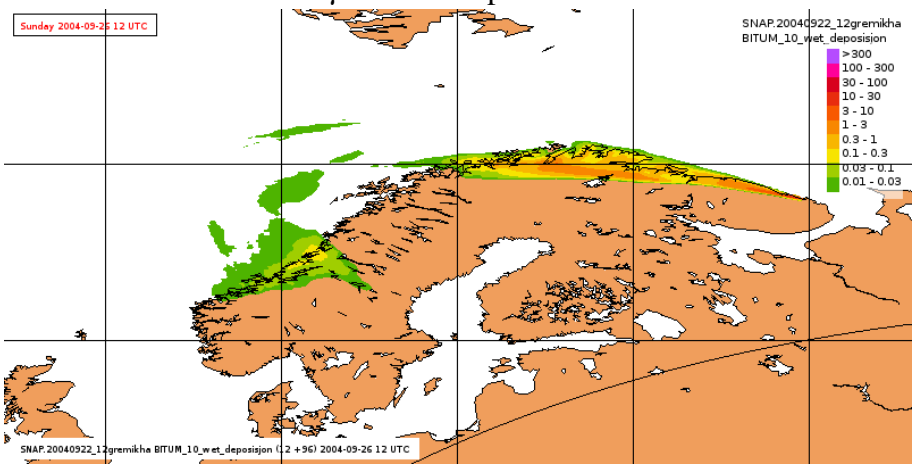

Bitumen 10 μm - total deposition after 96 hrs

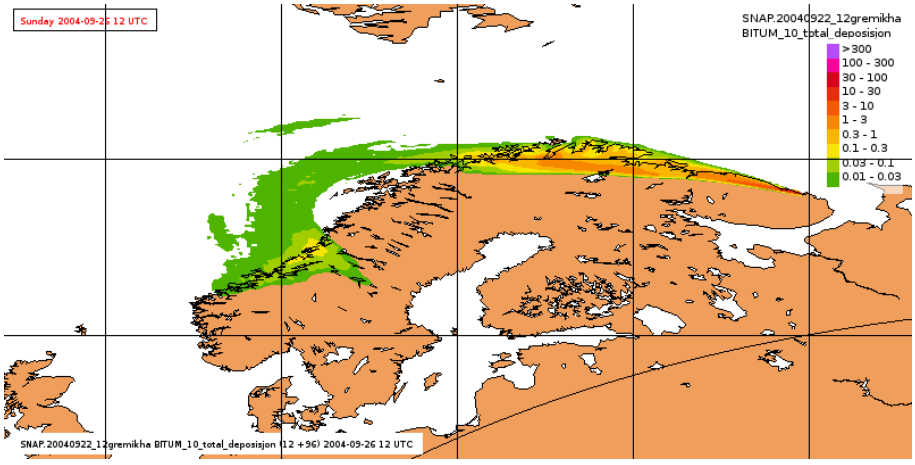

B. Deposition fields for the worst case scenario - individual components

Bitumen 20 μm - dry deposition after 96 hrs

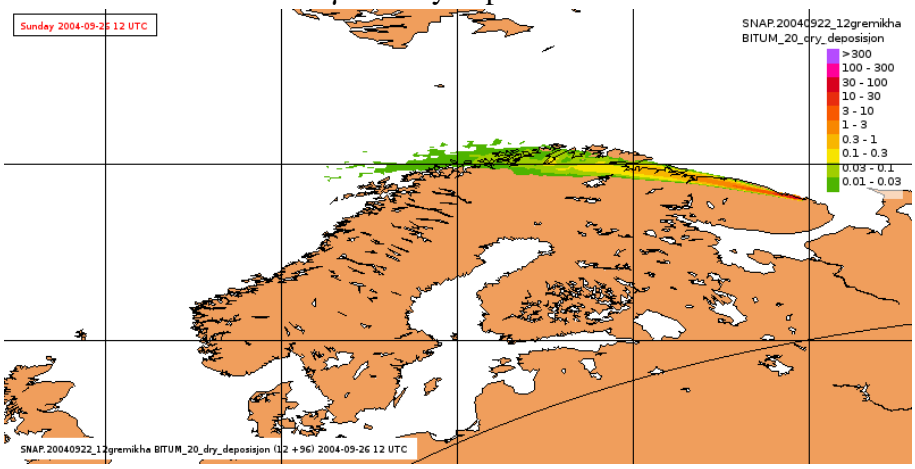

Bitumen 20 μm - wet deposition after 96 hrs

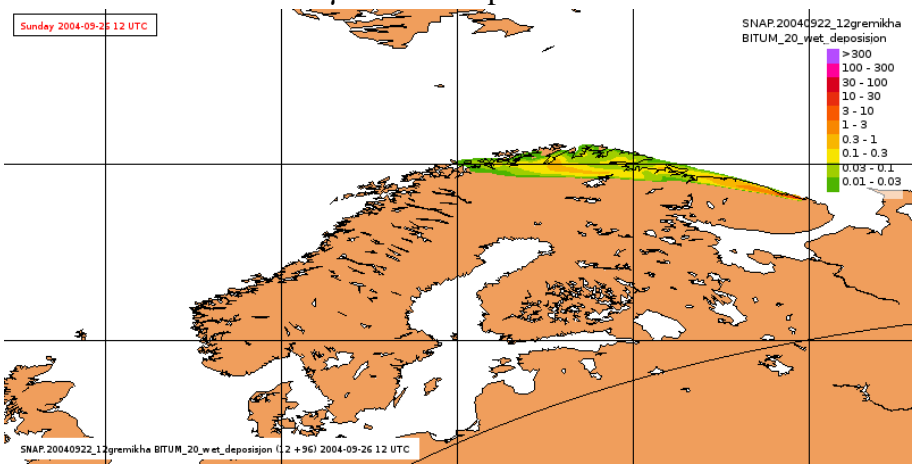

Bitumen 20 μm - total deposition after 96 hrs

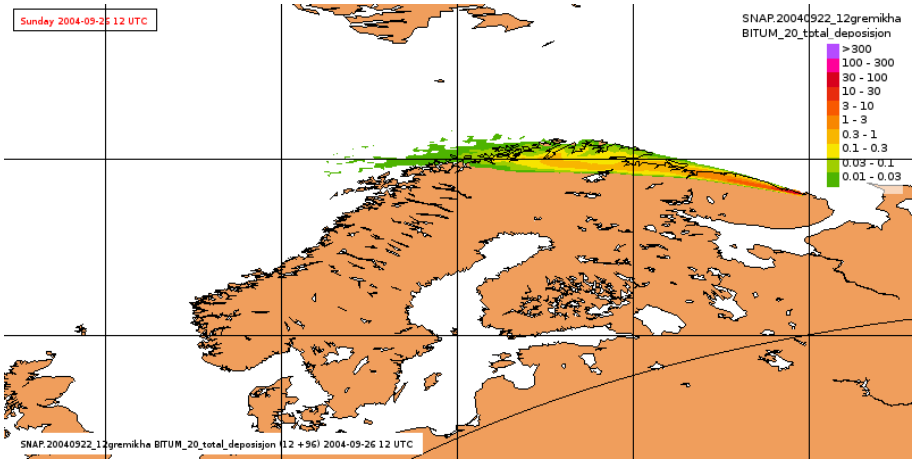

Bitumen 50 μm - dry deposition after 96 hrs

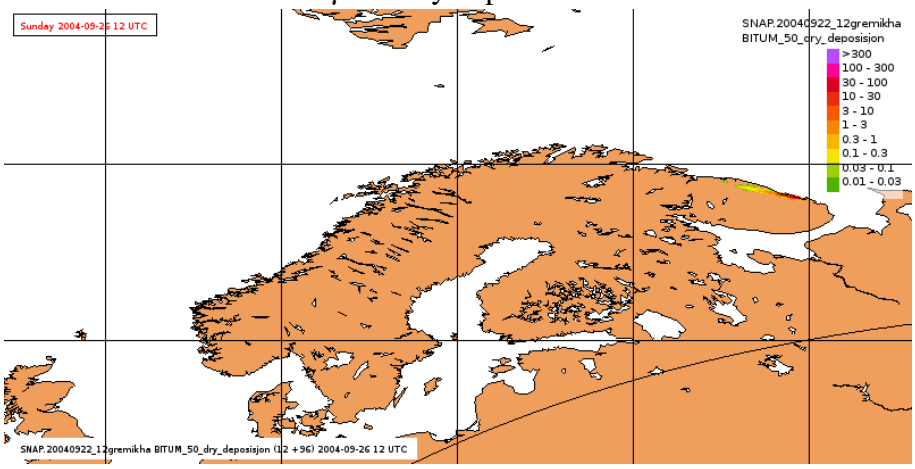

Bitumen 50 μm - wet deposition after 96 hrs

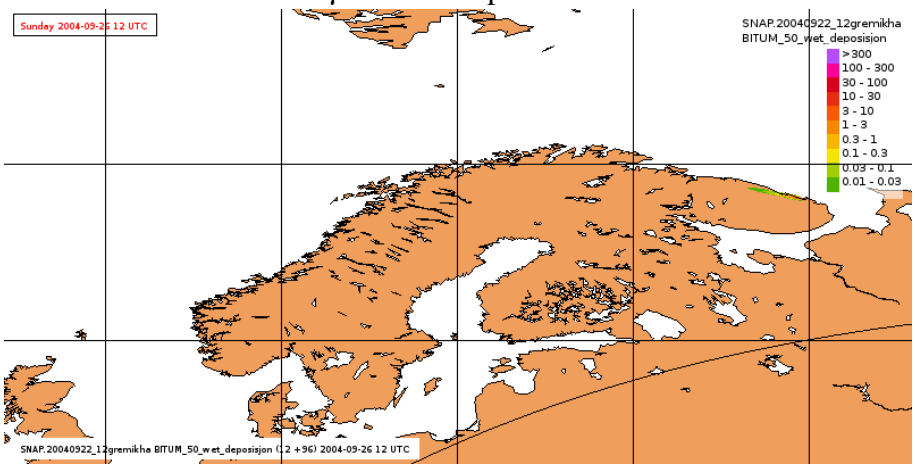

Bitumen 50 μm - total deposition after 96 hrs

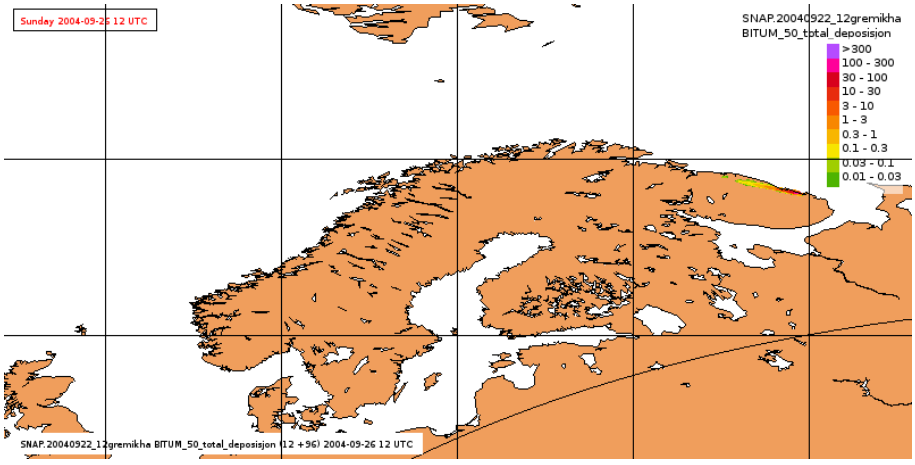

B. Deposition fields for the worst case scenario - individual components

Bitumen 100 μm - dry deposition after 96 hrs

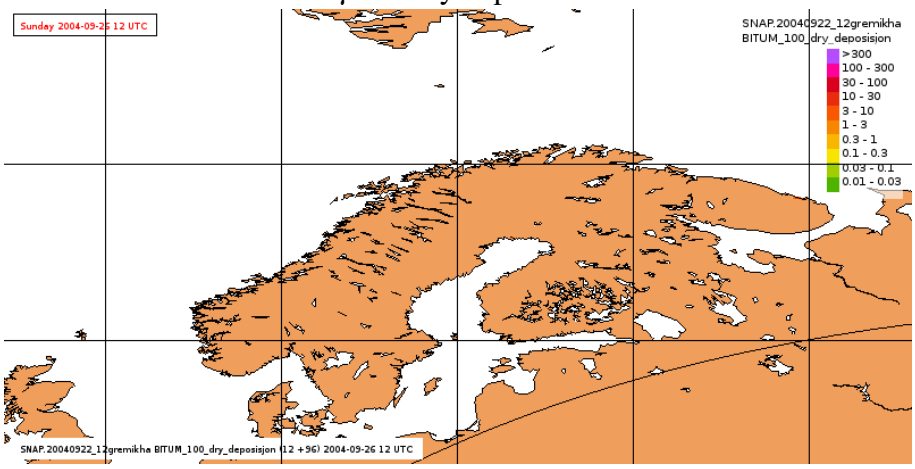

Bitumen 100 μm - wet deposition after 96 hrs

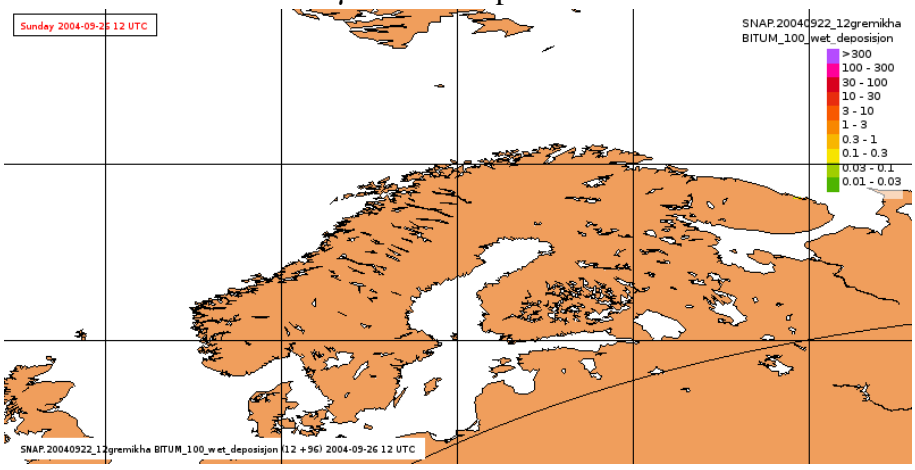

Bitumen 100 μm - total deposition after 96 hrs

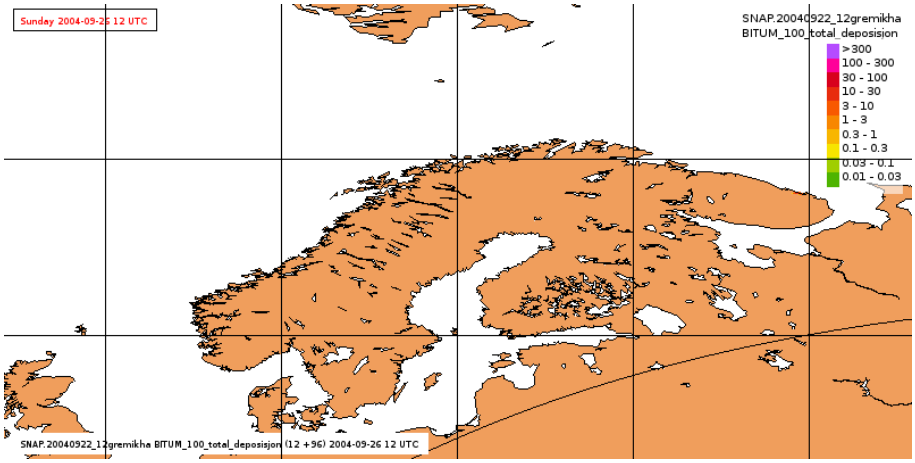

Metal 0.1 μm - dry deposition after 96 hrs

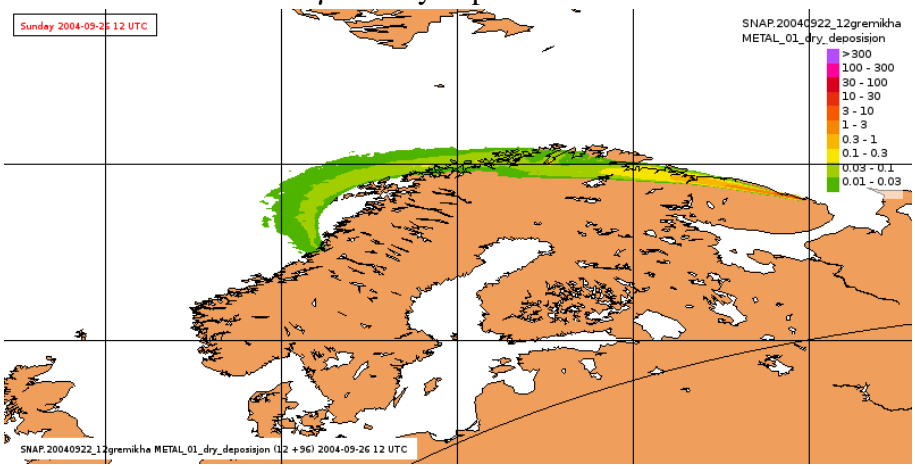

Metal 0.1 μm - wet deposition after 96 hrs

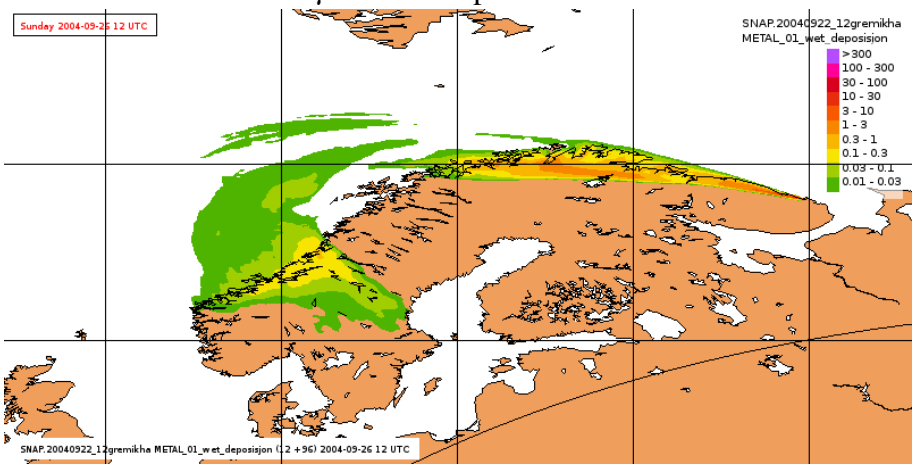

Metal 0.1 μm - total deposition after 96 hrs

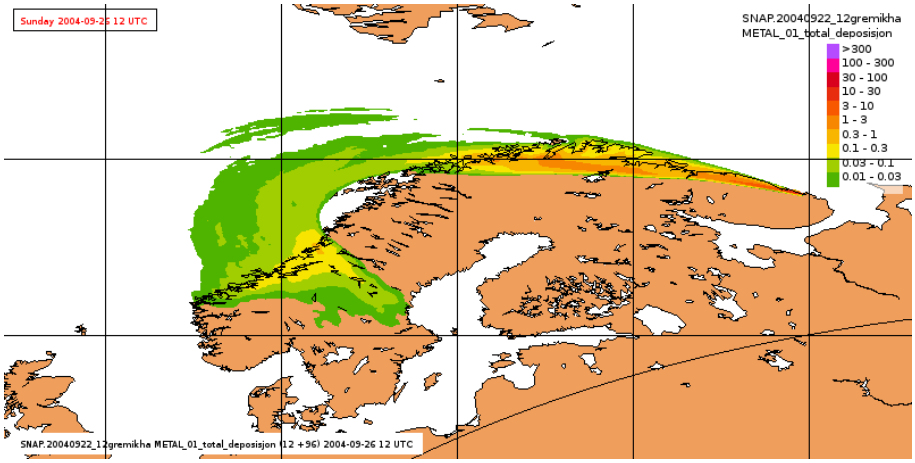

B. Deposition fields for the worst case scenario - individual components

Metal 0.5 μm - dry deposition after 96 hrs

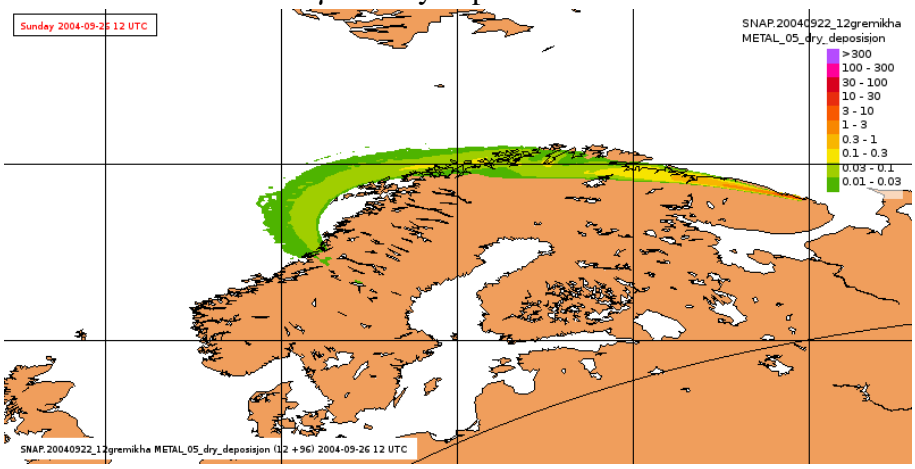

Metal 0.5 μm - wet deposition after 96 hrs

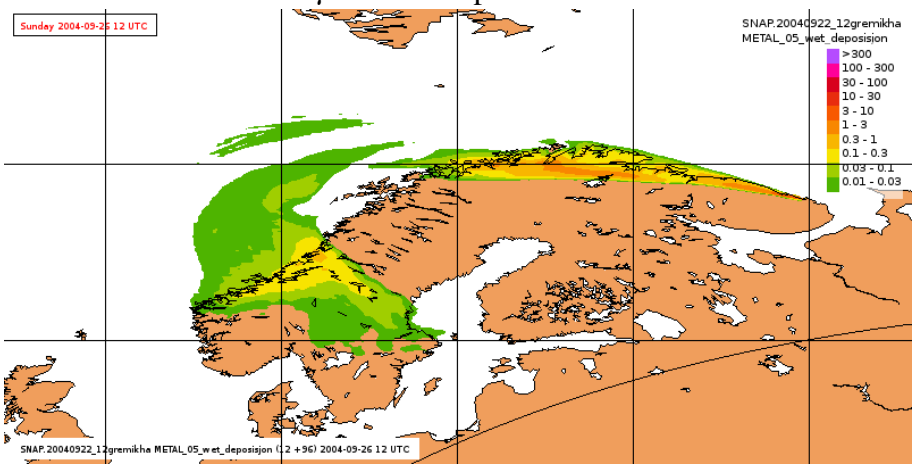

Metal 0.5 μm - total deposition after 96 hrs

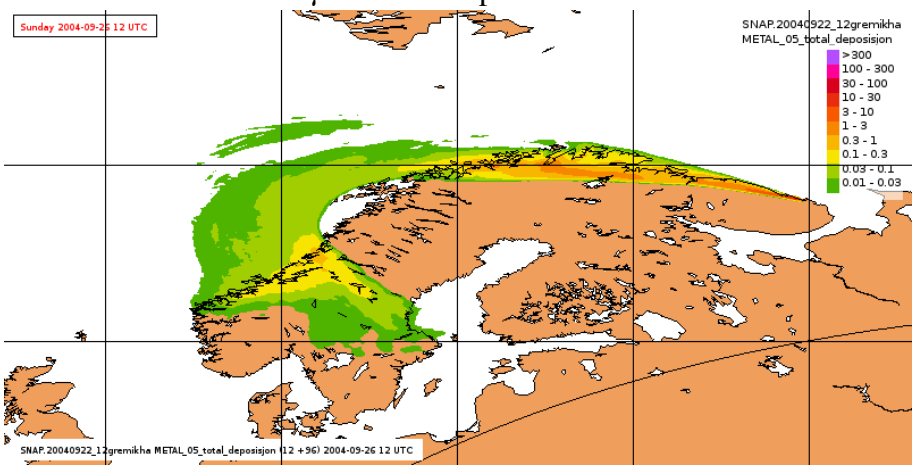

Metal 1 μm - dry deposition after 96 hrs

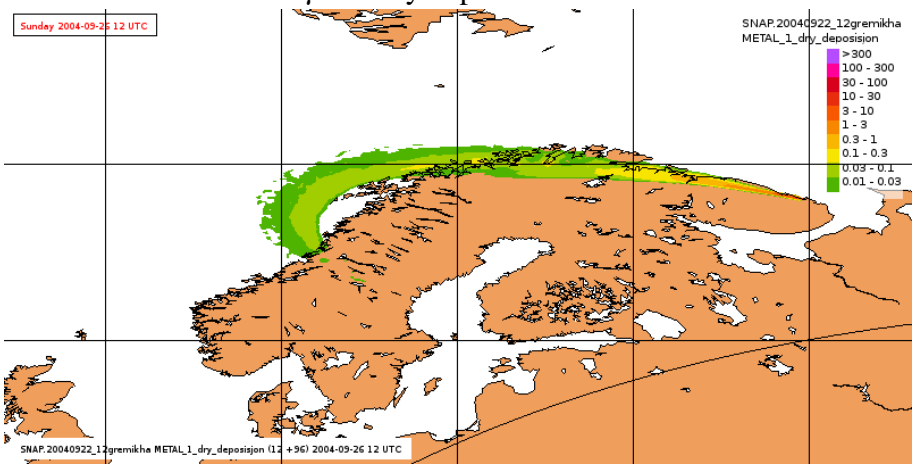

Metal 1 μm - wet deposition after 96 hrs

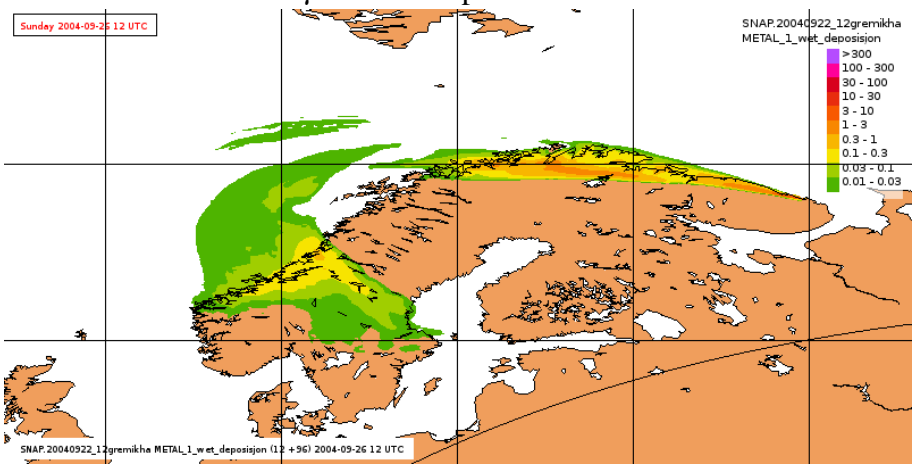

Metal 1 μm - total deposition after 96 hrs

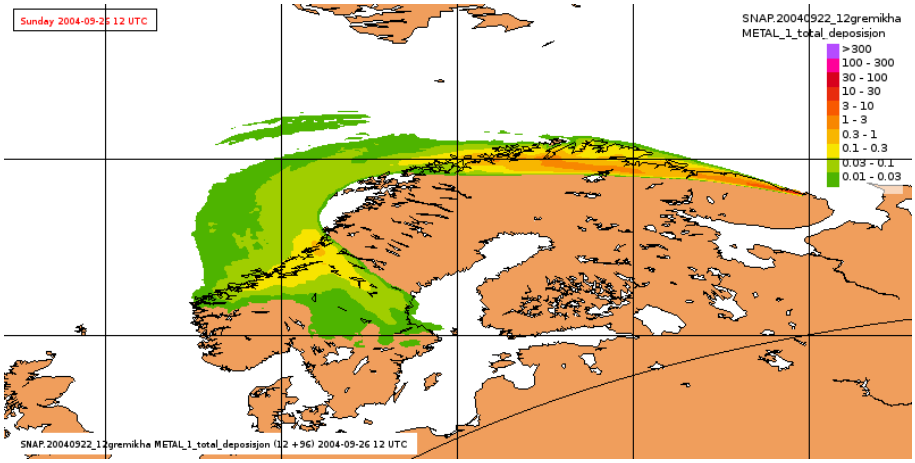

Metal 5 μm - dry deposition after 96 hrs

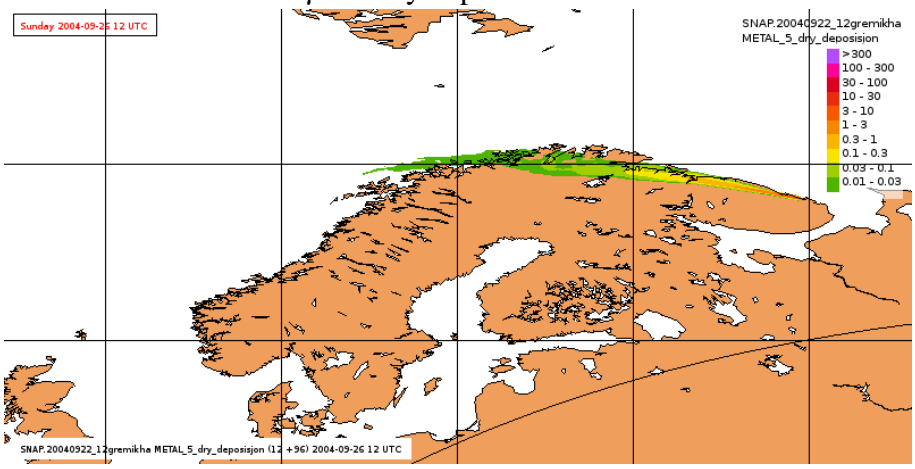

Metal 5 μm - wet deposition after 96 hrs

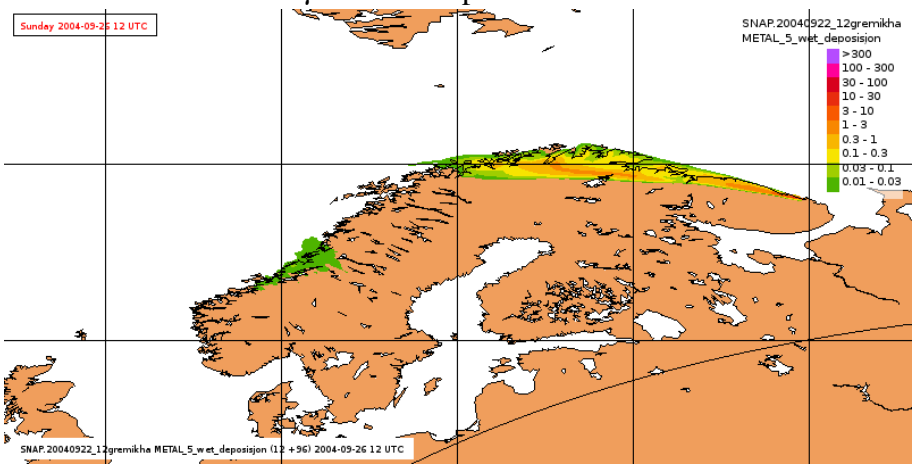

Metal 5 μm - total deposition after 96 hrs

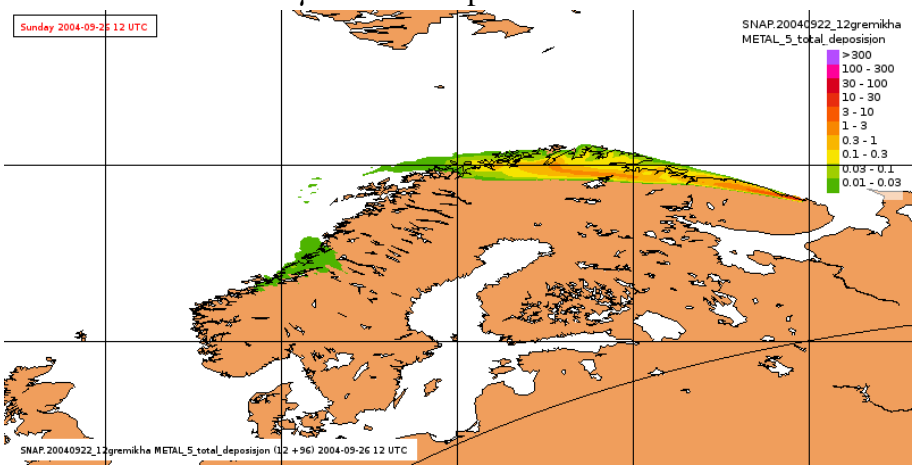

Metal 10 μm - dry deposition after 96 hrs

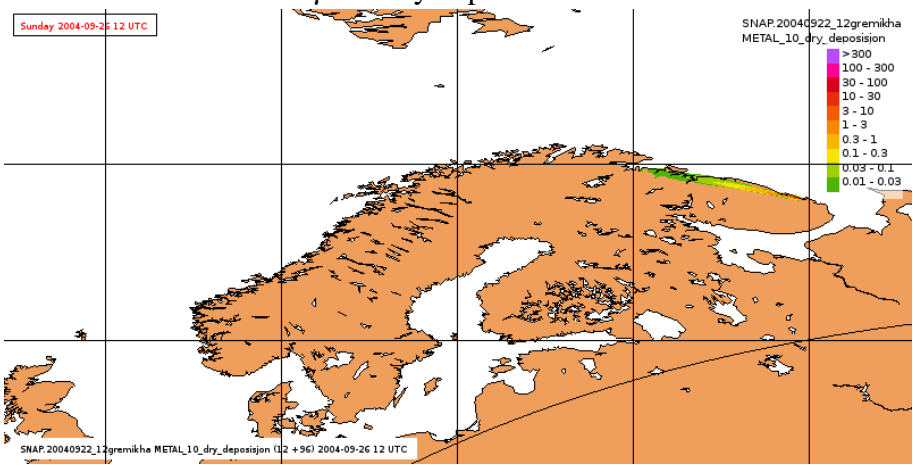

Metal 10 μm - wet deposition after 96 hrs

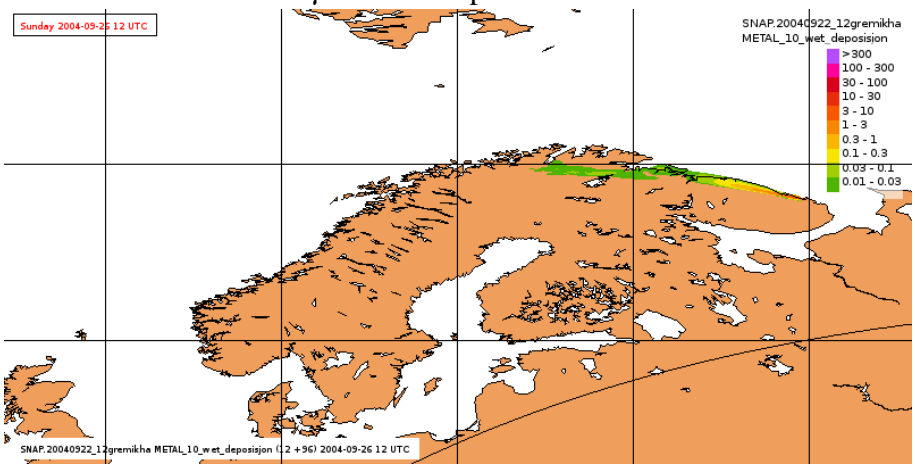

Metal 10 μm - total deposition after 96 hrs

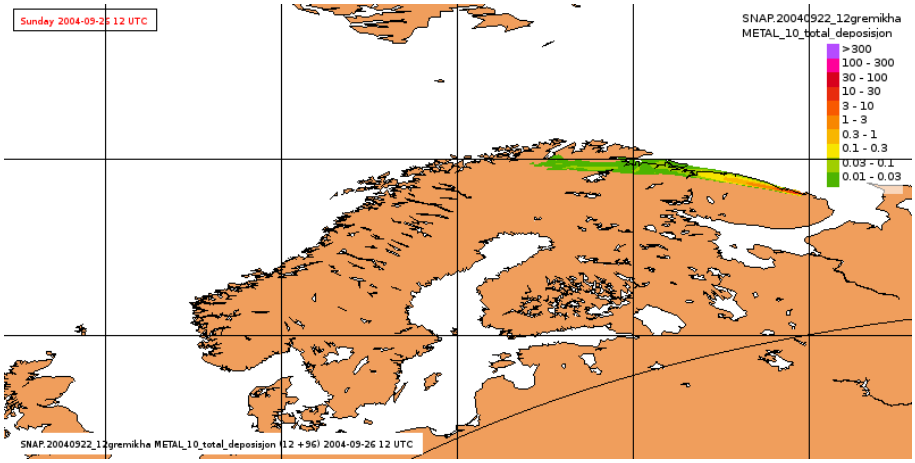

B. *Deposition fields for the worst case scenario - individual components*

Metal 20 μm - dry deposition after 96 hrs

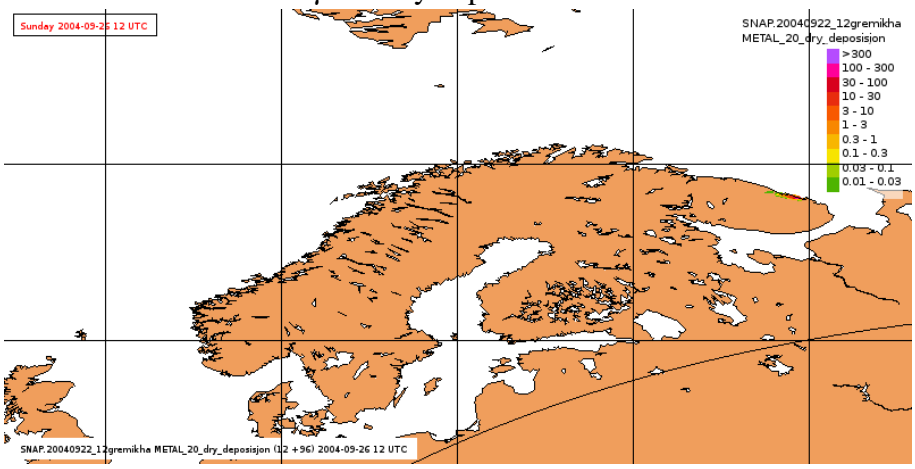

Metal 20 μm - wet deposition after 96 hrs

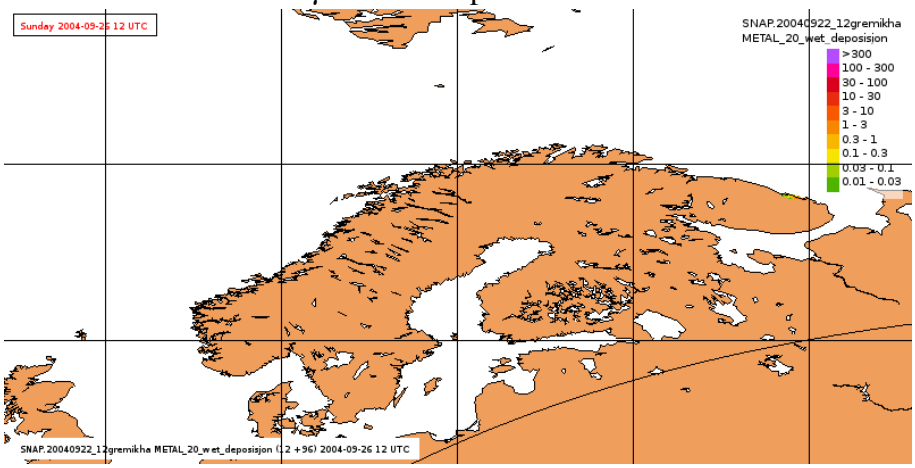

Metal 20 μm - total deposition after 96 hrs

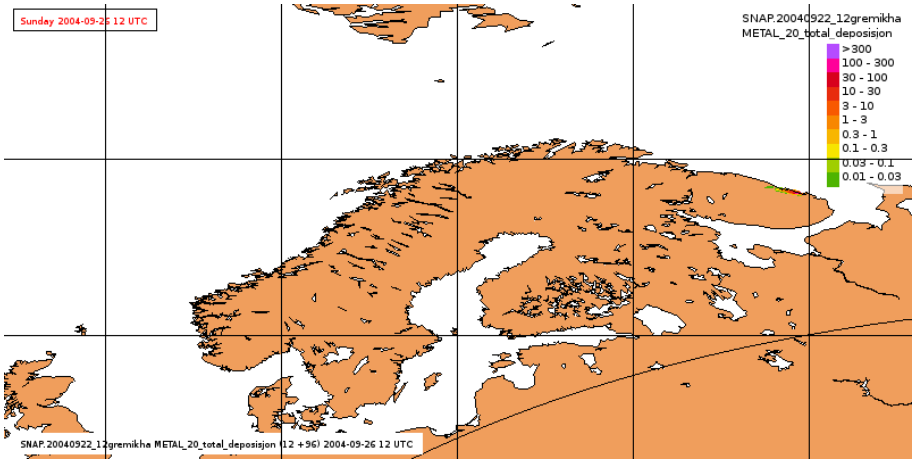

Metal 50 μm - dry deposition after 96 hrs

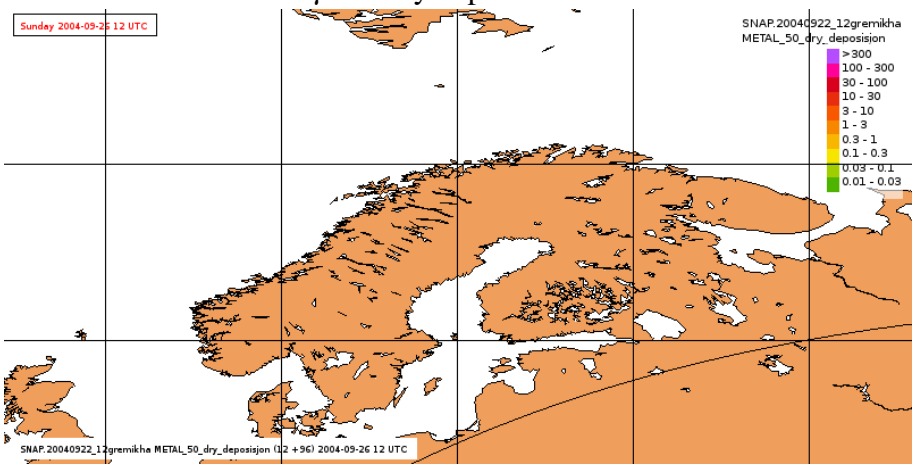

Metal 50 μm - wet deposition after 96 hrs

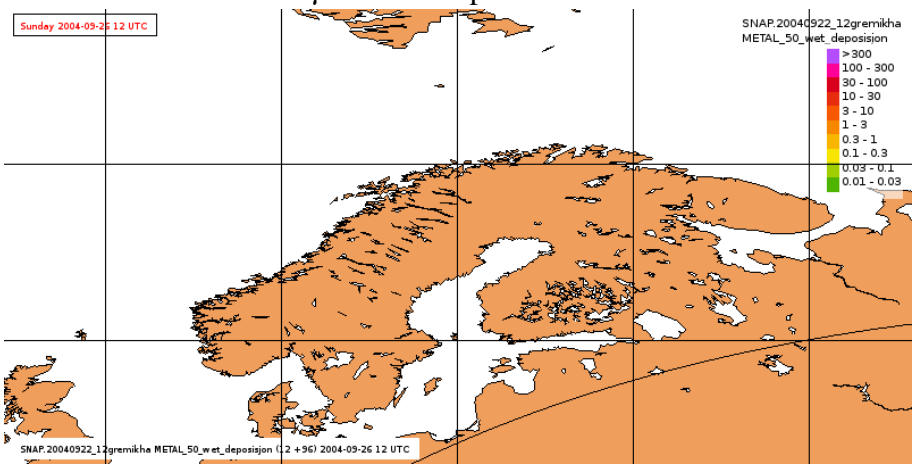

Metal 50 μm - total deposition after 96 hrs

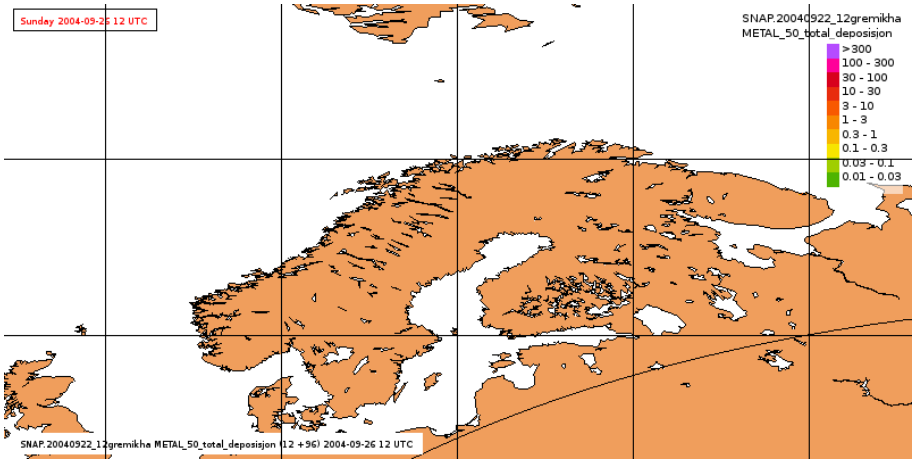

Metal 100 μm - dry deposition after 96 hrs

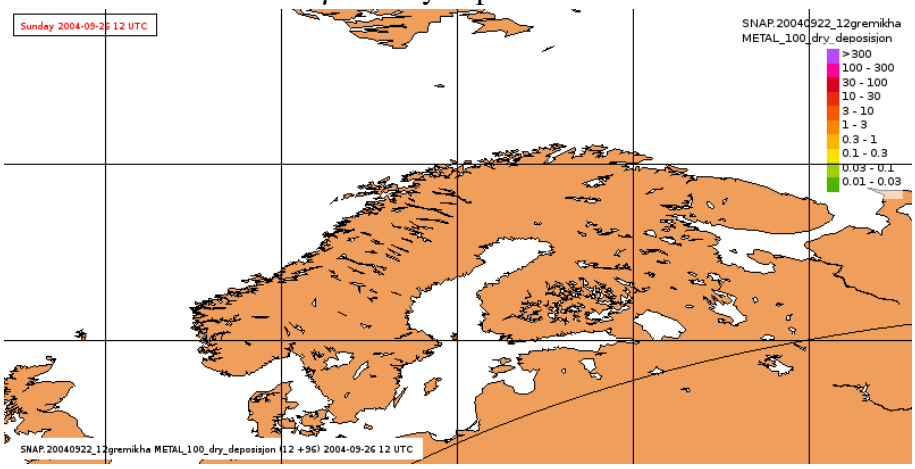

Metal 100 μm - wet deposition after 96 hrs

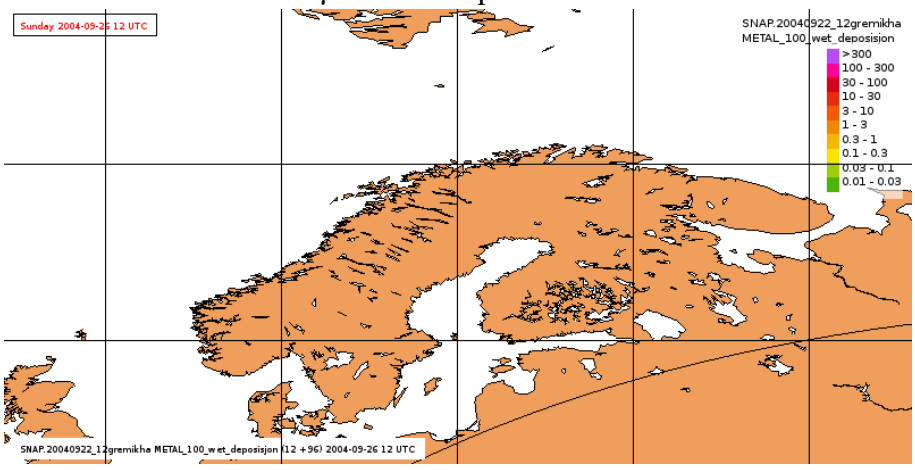

Metal 100 μm - total deposition after 96 hrs

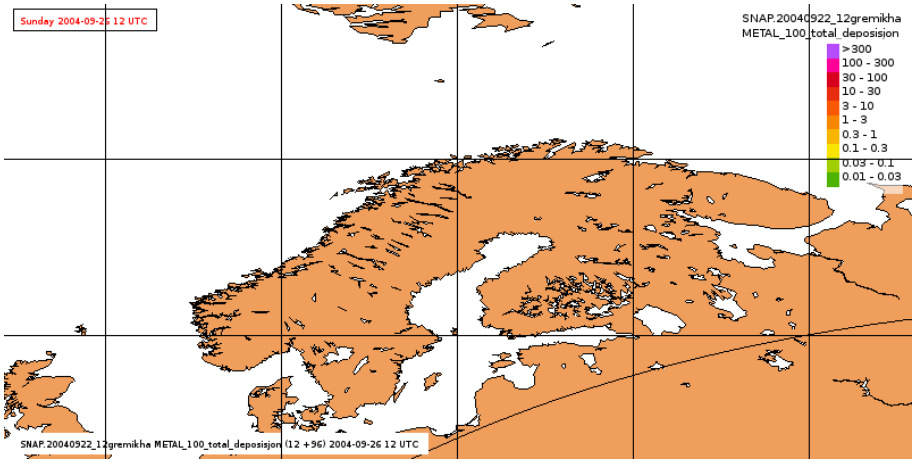

RU-106 0.1 μm - dry deposition after 96 hrs

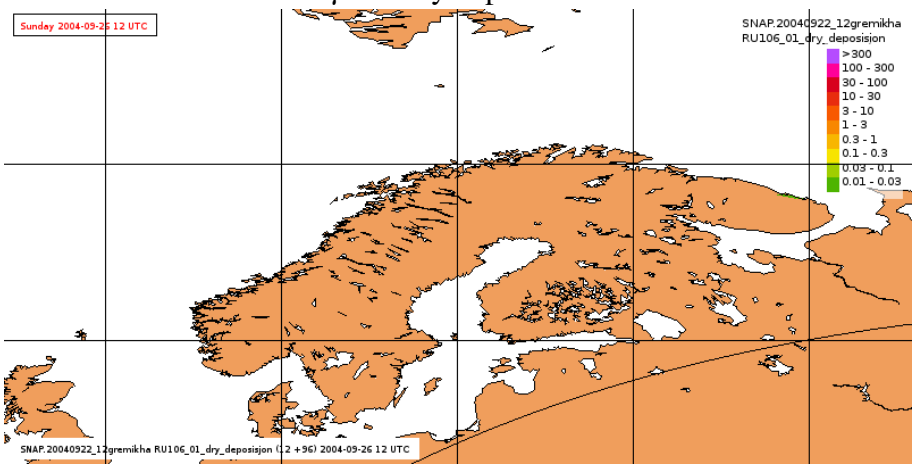

RU-106 0.1 μm - wet deposition after 96 hrs

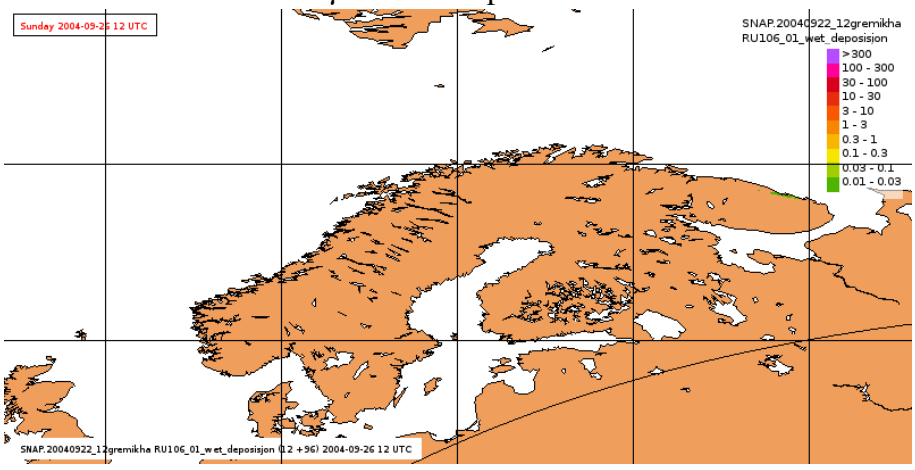

RU-106 0.1 μm - total deposition after 96 hrs

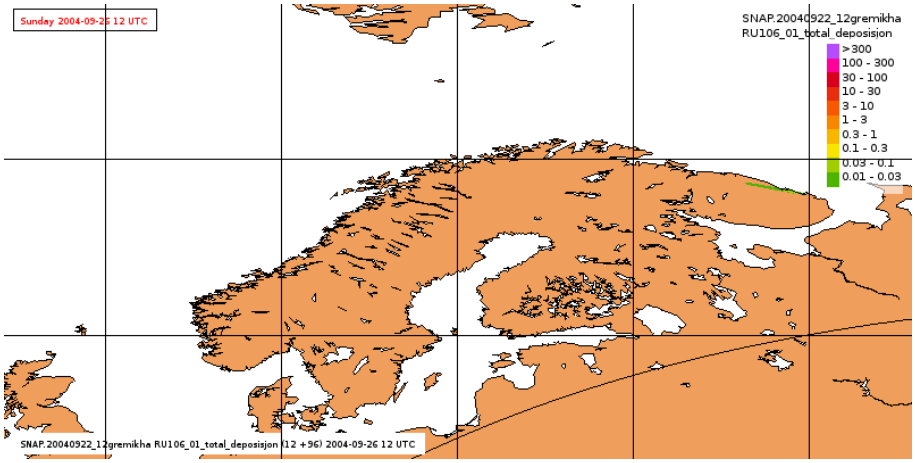

RU-106 0.5 μm - dry deposition after 96 hrs

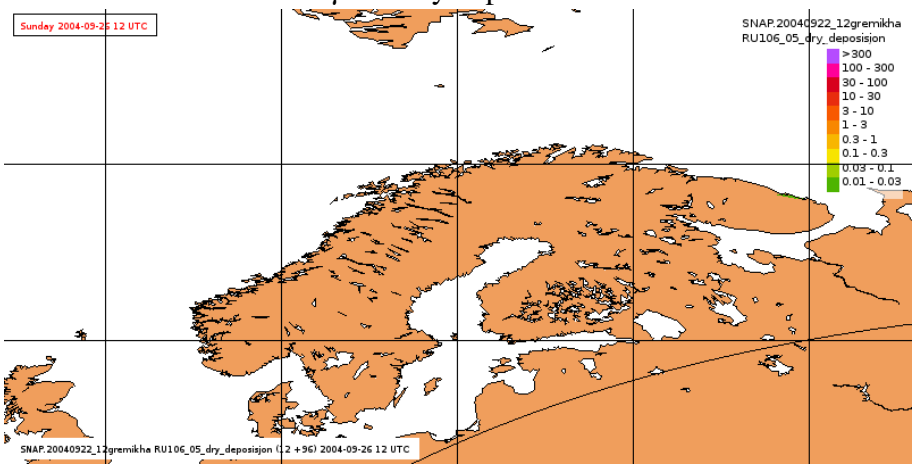

RU-106 0.5 μm - wet deposition after 96 hrs

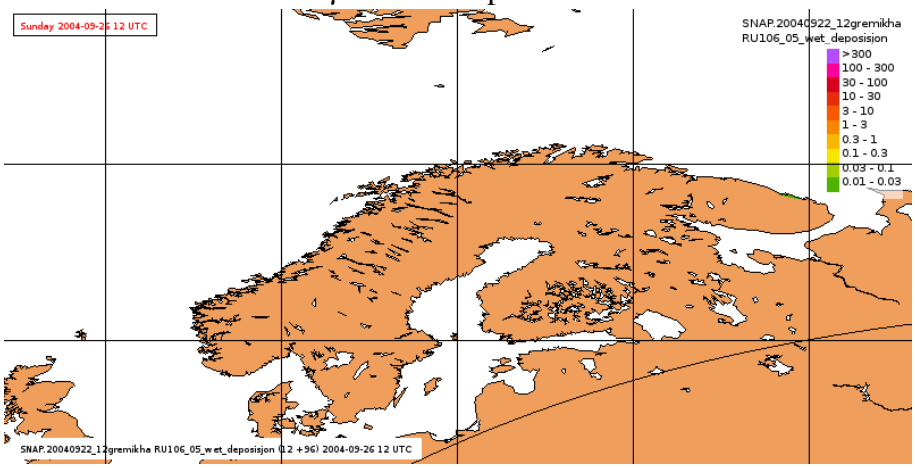

RU-106 0.5 μm - total deposition after 96 hrs

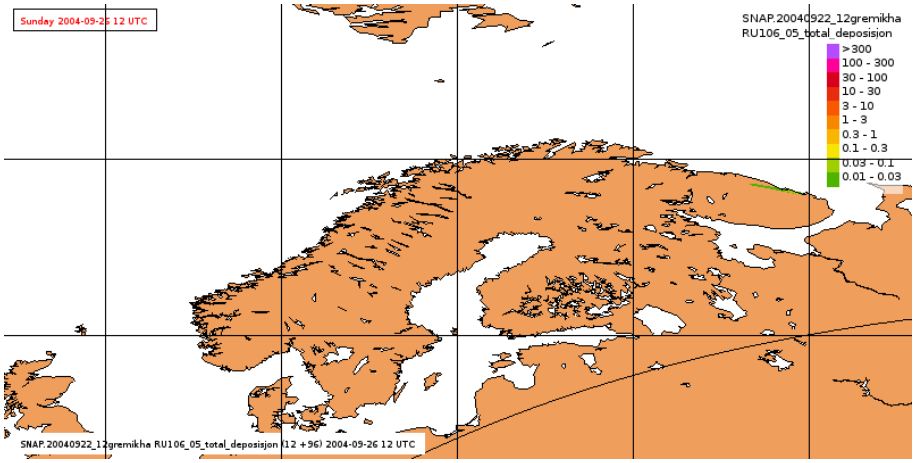

RU-106 1 μm - dry deposition after 96 hrs

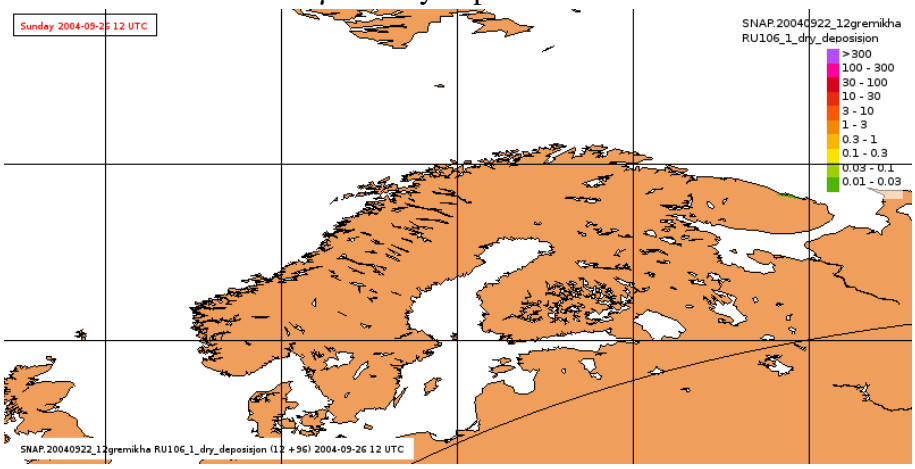

RU-106 1 μm - wet deposition after 96 hrs

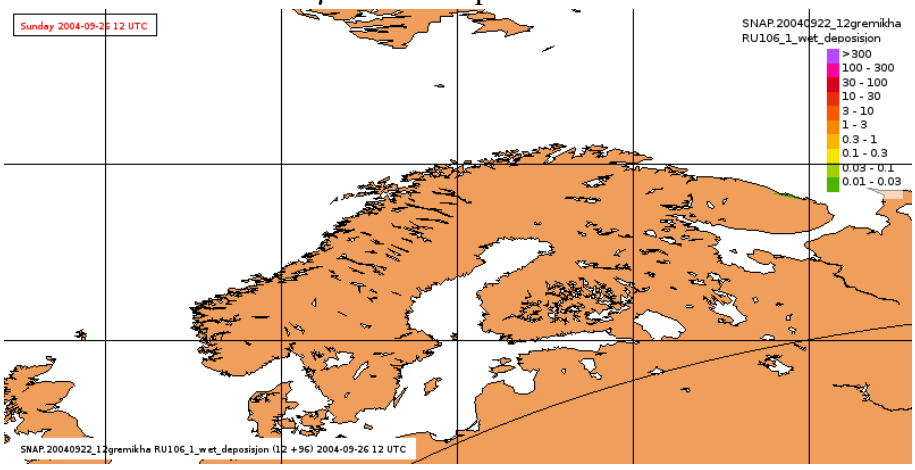

RU-106 1 μm - total deposition after 96 hrs

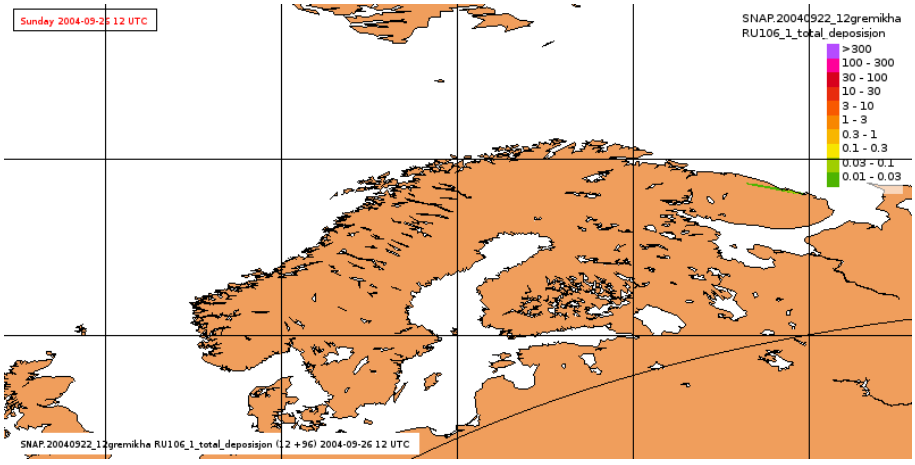

B. Deposition fields for the worst case scenario - individual components

RU-106 5 μm - dry deposition after 96 hrs

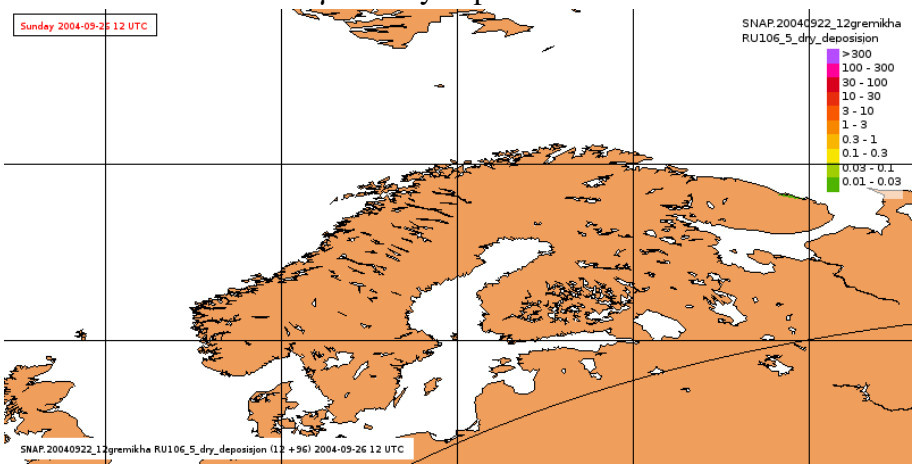

RU-106 5 μm - wet deposition after 96 hrs

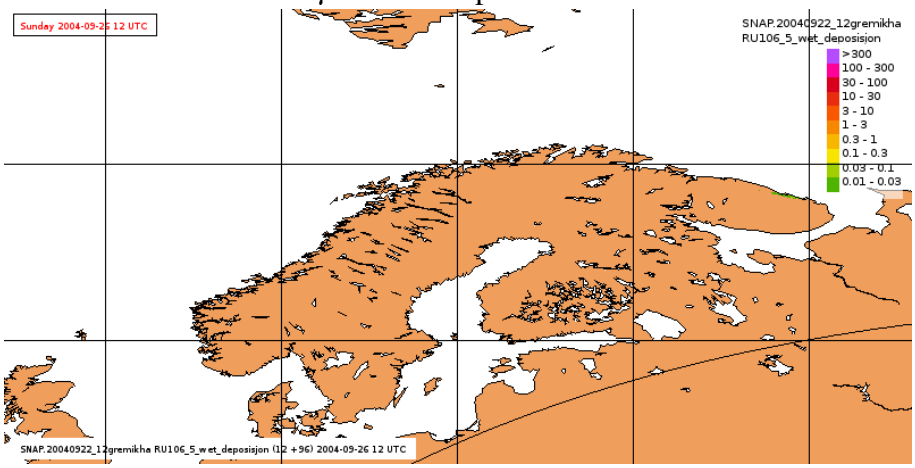

RU-106 5 μm - total deposition after 96 hrs

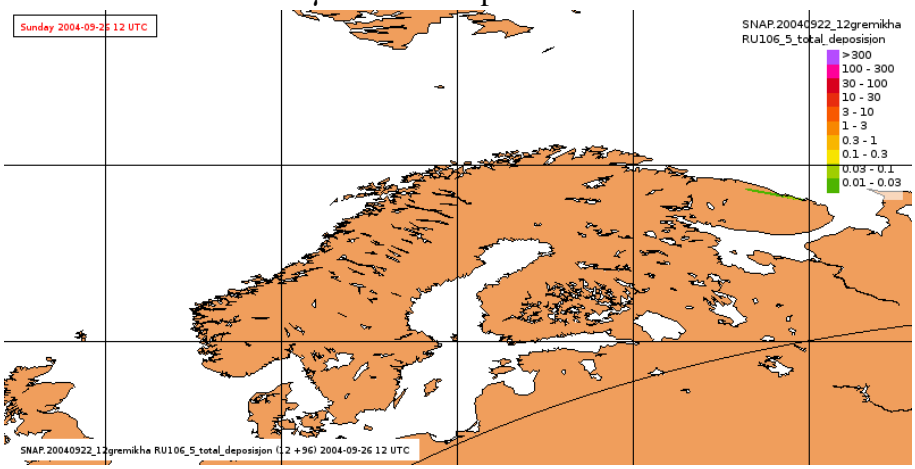

RU-106 10 μm - dry deposition after 96 hrs

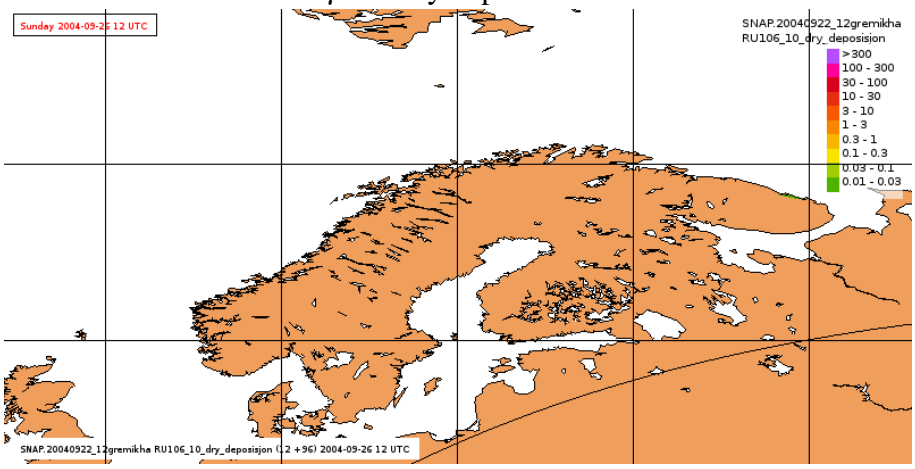

RU-106 10 μm - wet deposition after 96 hrs

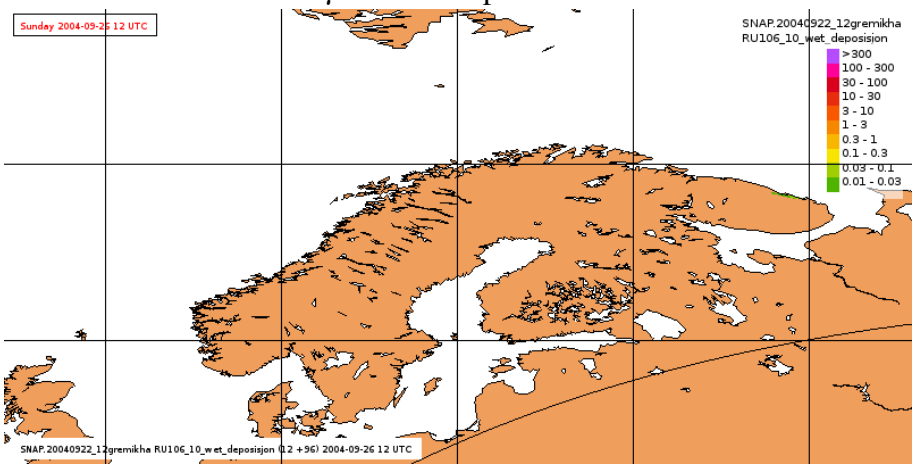

RU-106 10 μm - total deposition after 96 hrs

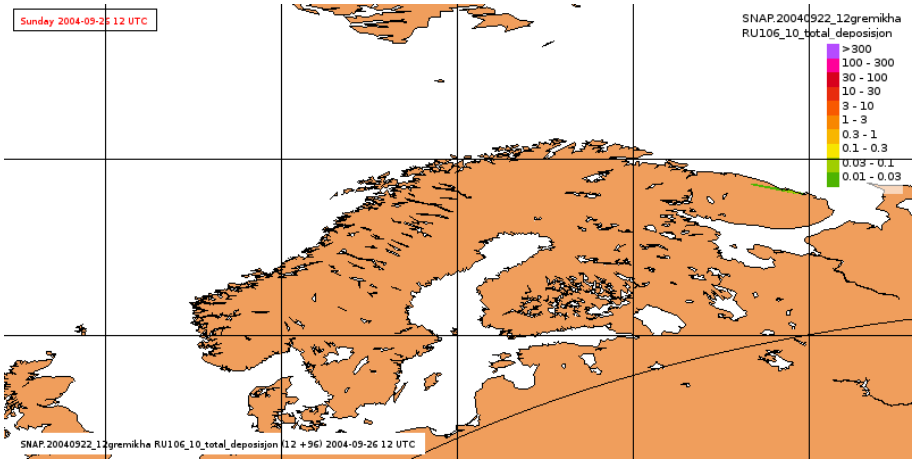

B. Deposition fields for the worst case scenario - individual components

RU-106 20 μm - dry deposition after 96 hrs

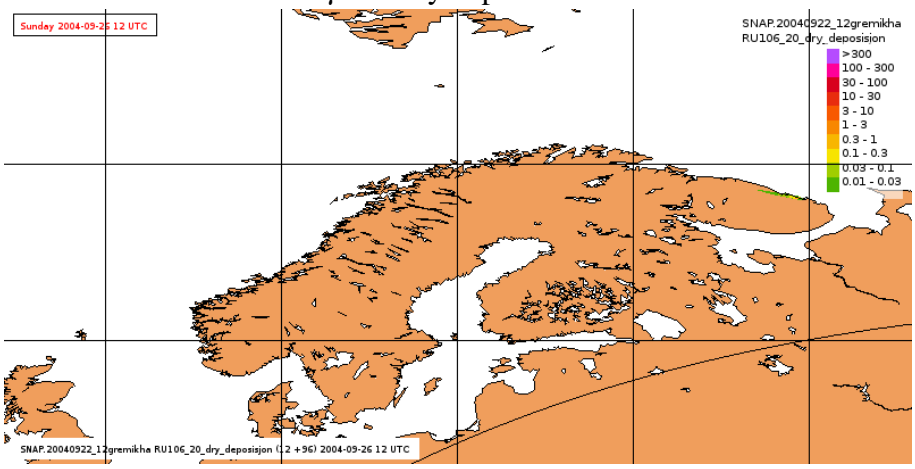

RU-106 20 μm - wet deposition after 96 hrs

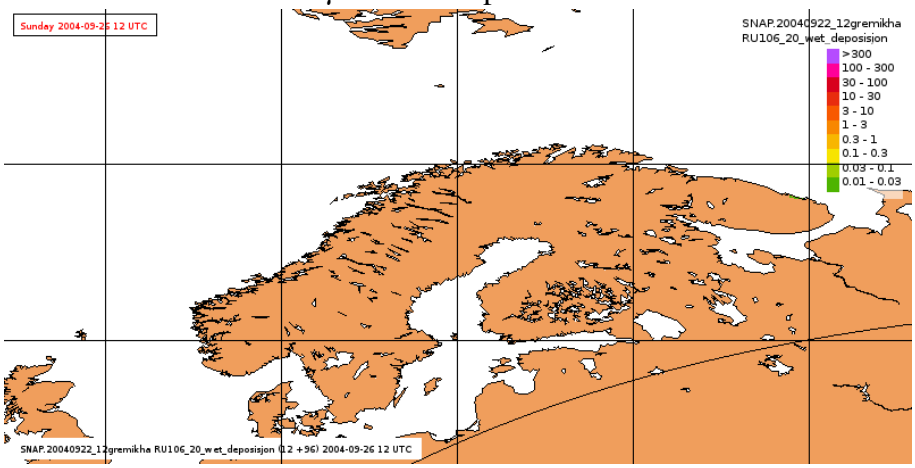

RU-106 20 μm - total deposition after 96 hrs

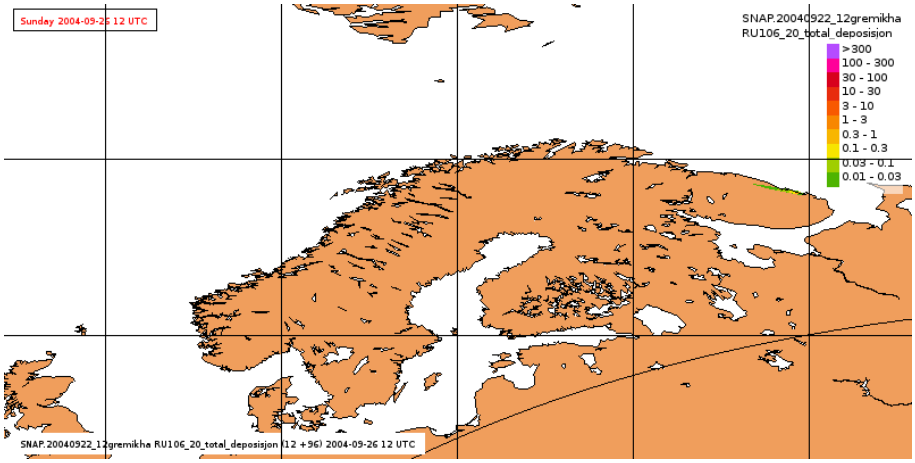

I-131 - dry deposition after 96 hrs

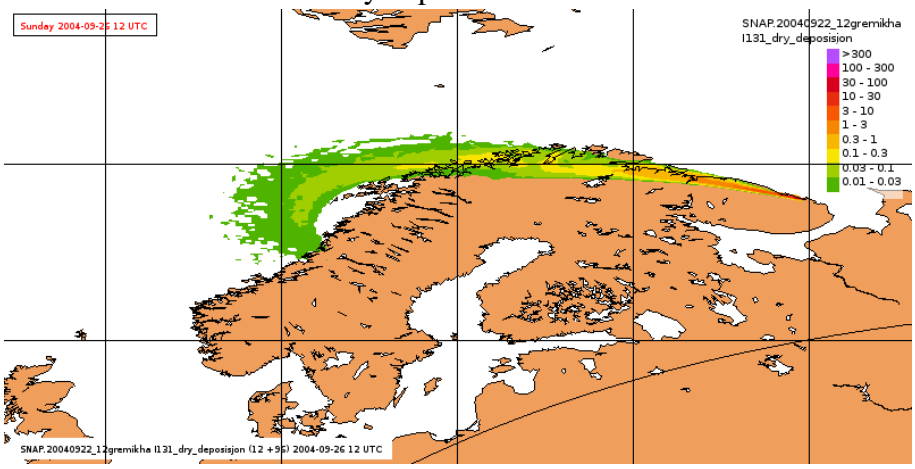

I-131 - wet deposition after 96 hrs

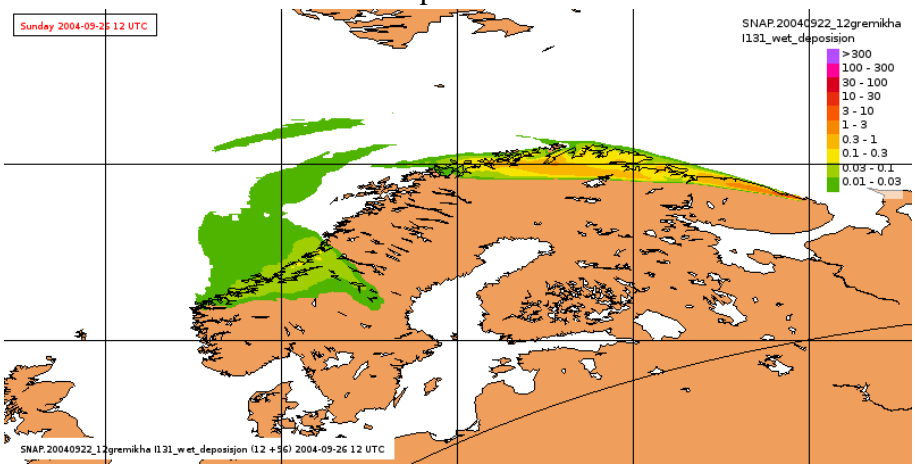

I-131 - total deposition after 96 hrs

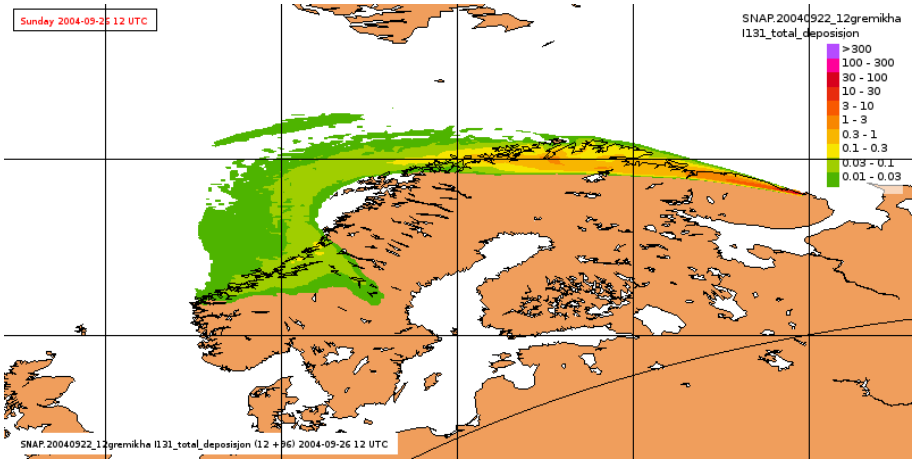

B. Deposition fields for the worst case scenario - individual components

I-133 - dry deposition after 96 hrs

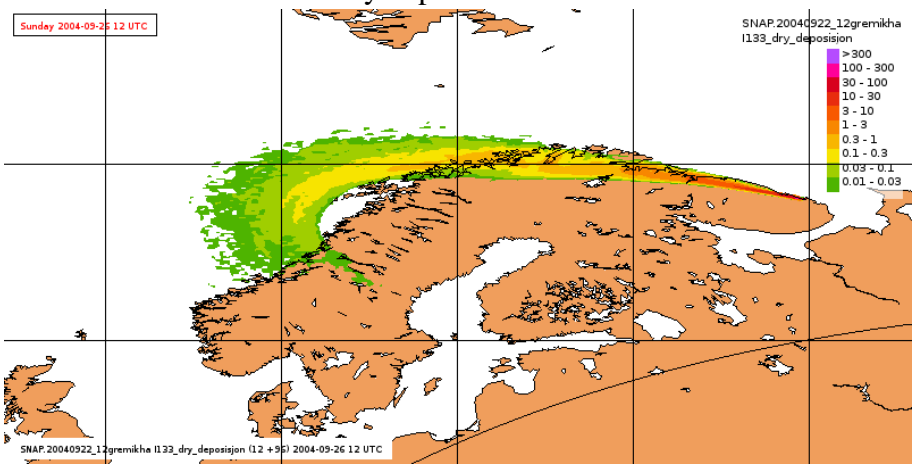

I-133 - wet deposition after 96 hrs

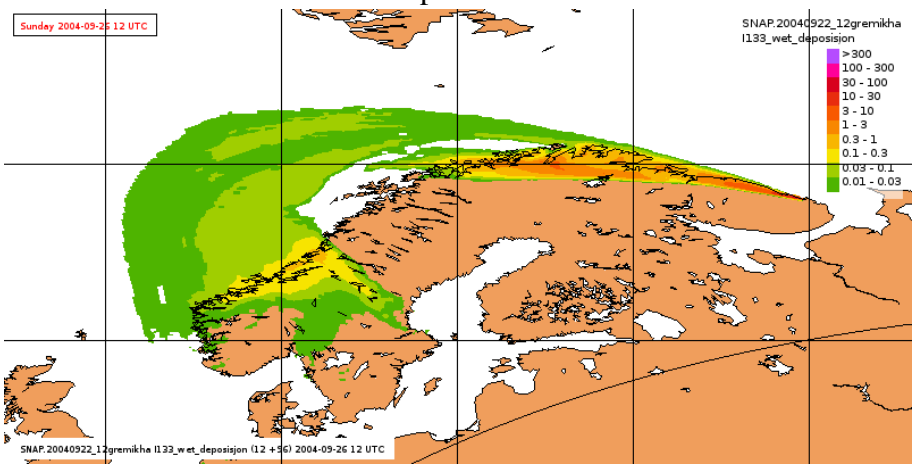

I-133 - total deposition after 96 hrs

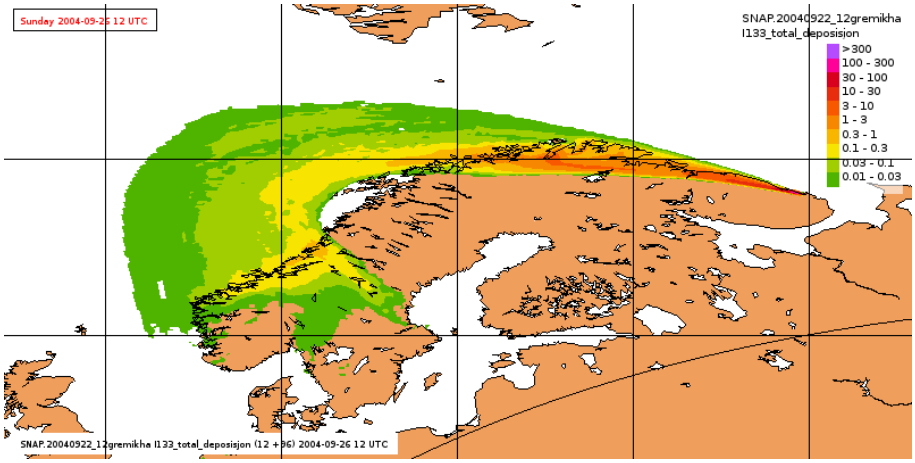

C. Evolution of the total deposition field for the worst case scenario

In this Appendix we show the maps of total deposition for the worst case scenario and accident at the final destination in Germikha Bay. The maps are shown for the period of 96 hours from the accident start with 3 hours interval. The same scale is used for all maps and the units are Bq m^{-2}.

C. *Evolution of the total deposition field for the worst case scenario*

3 hours after accident start

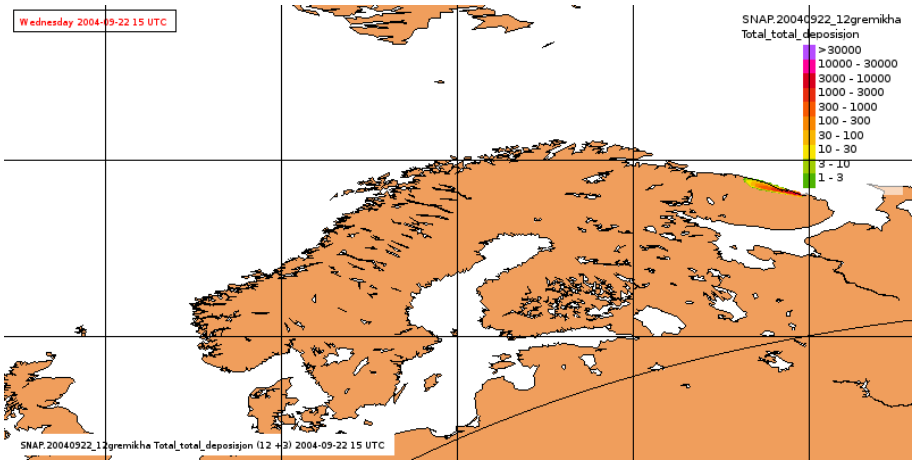

6 hours after accident start

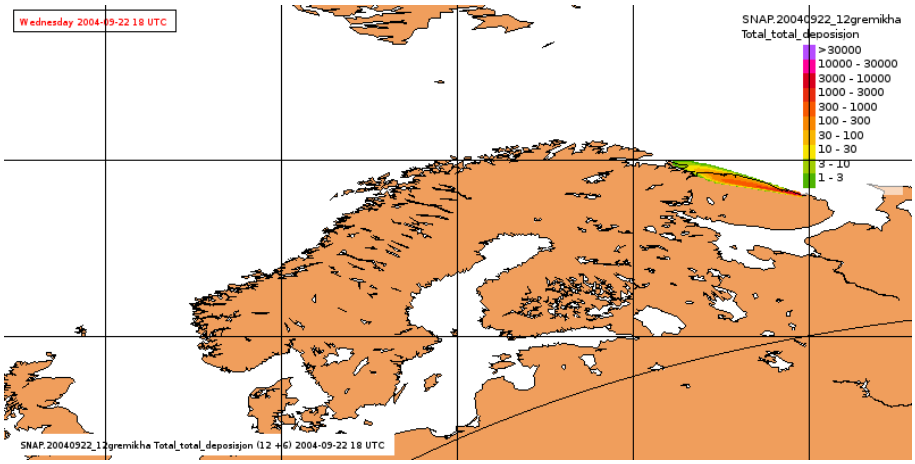

9 hours after accident start

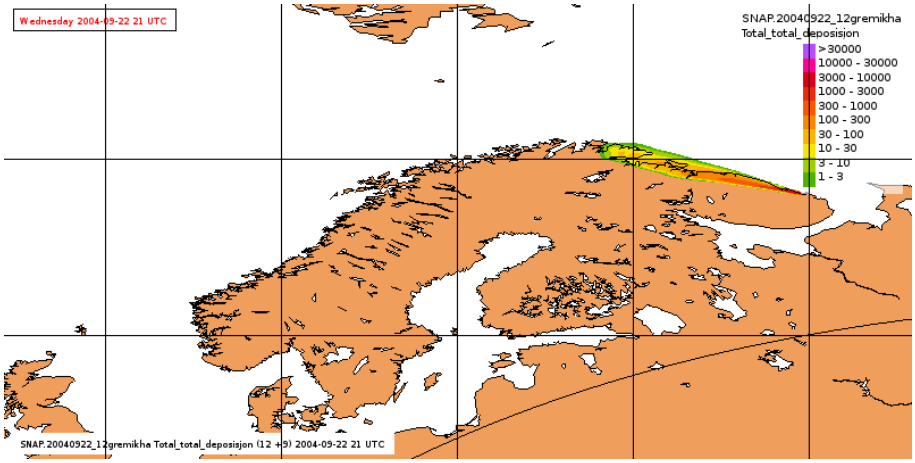

12 hours after accident start

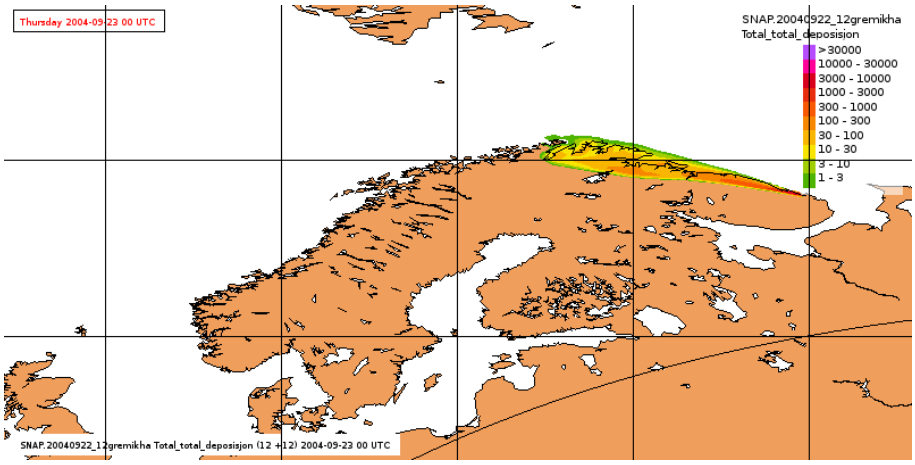

15 hours after accident start

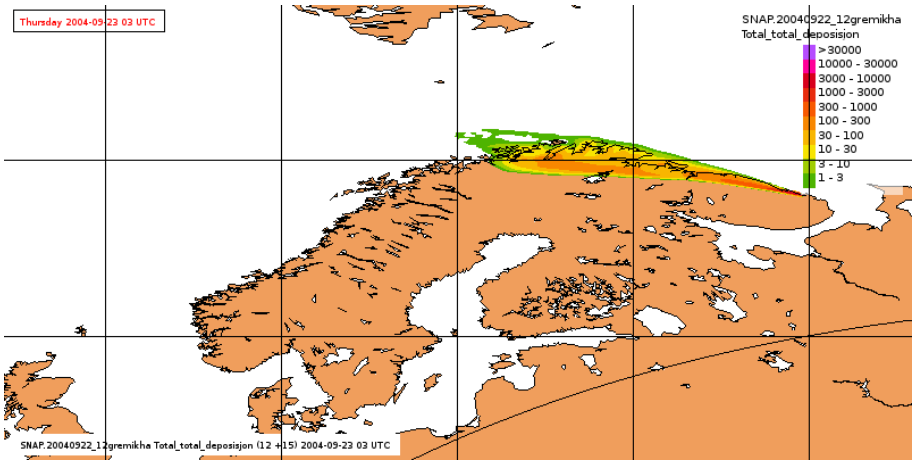

18 hours after accident start

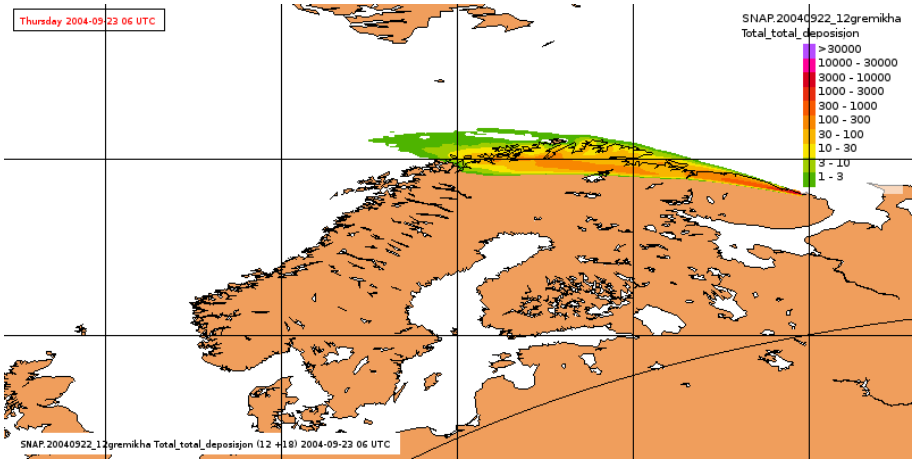

C. Evolution of the total deposition field for the worst case scenario

21 hours after accident start

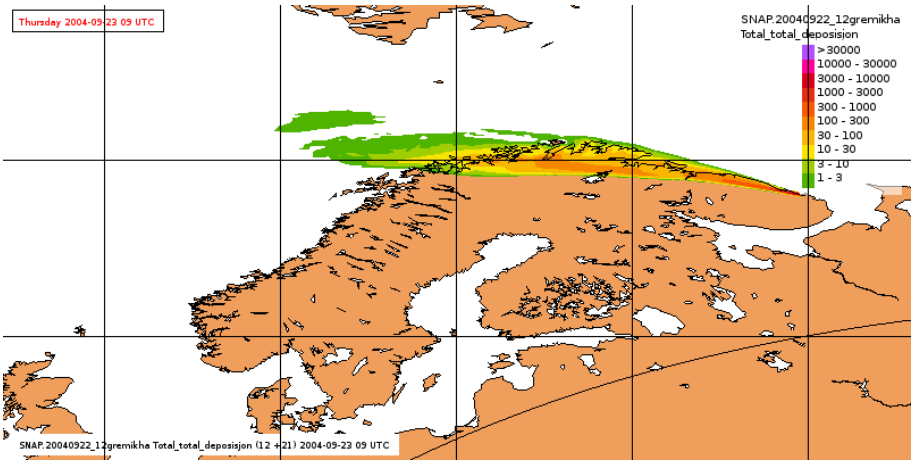

24 hours after accident start

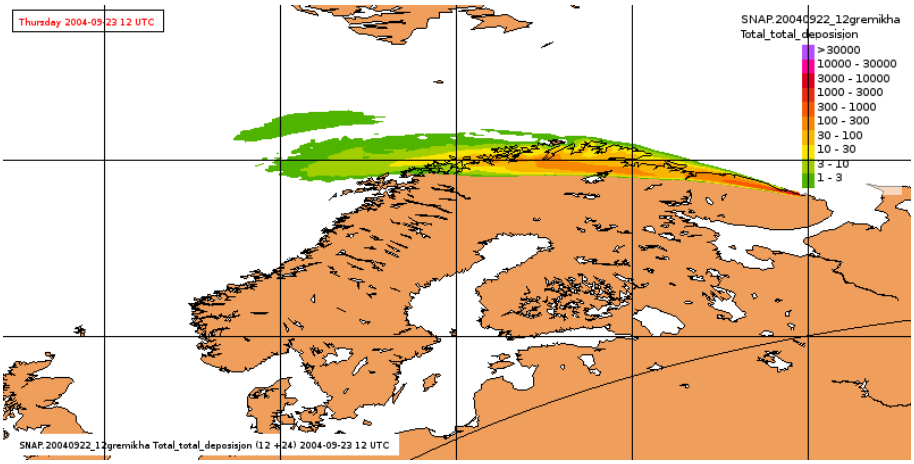

27 hours after accident start

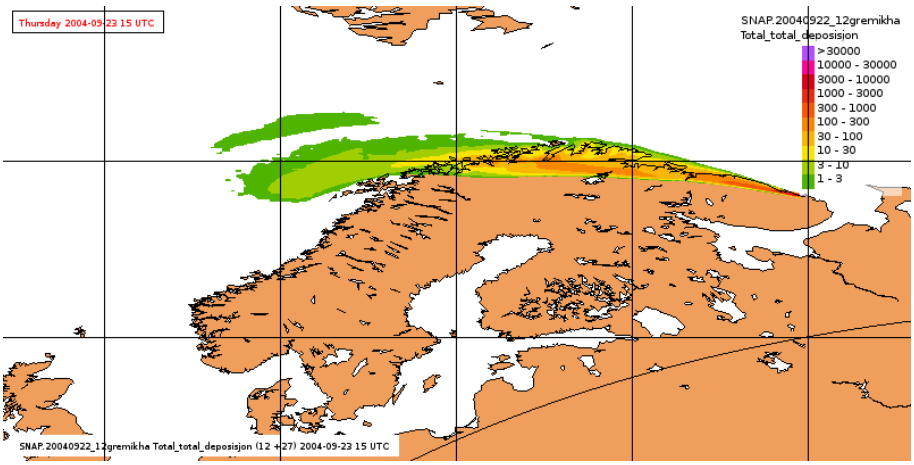

30 hours after accident start

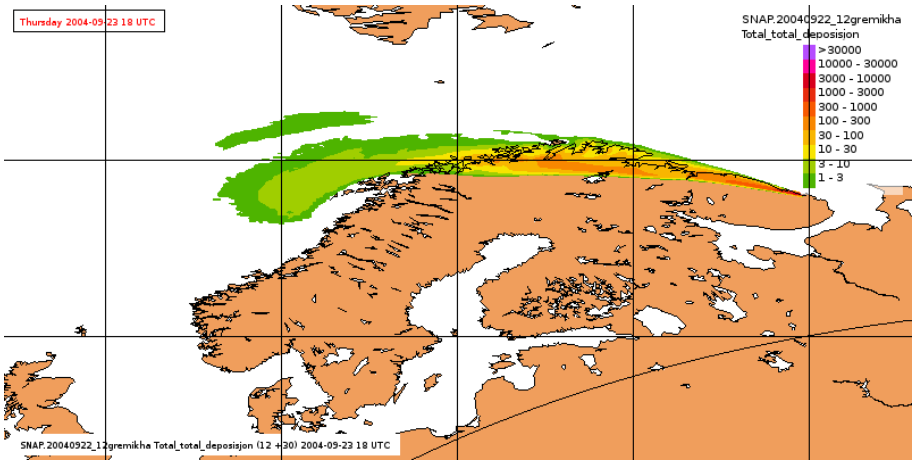

30 hours after accident start

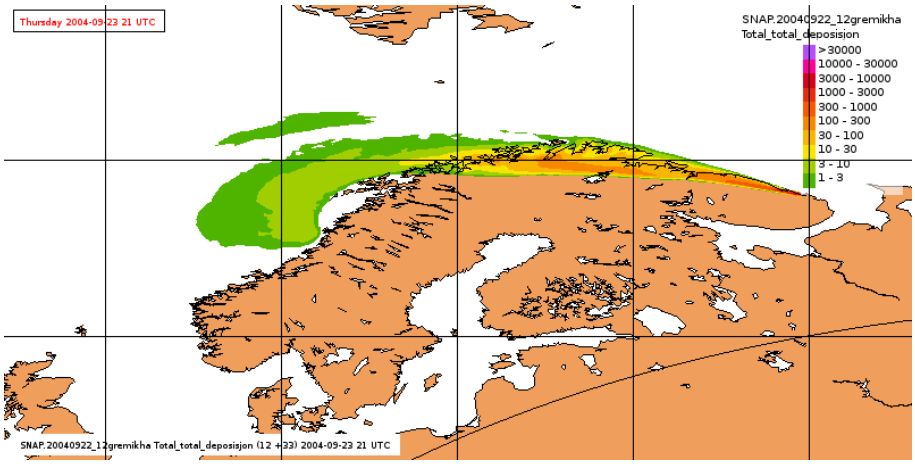

36 hours after accident start

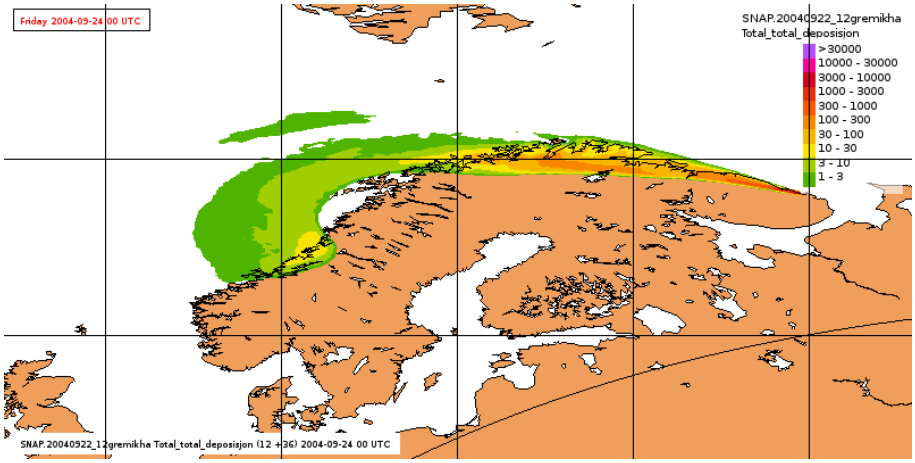

C. Evolution of the total deposition field for the worst case scenario

39 hours after accident start

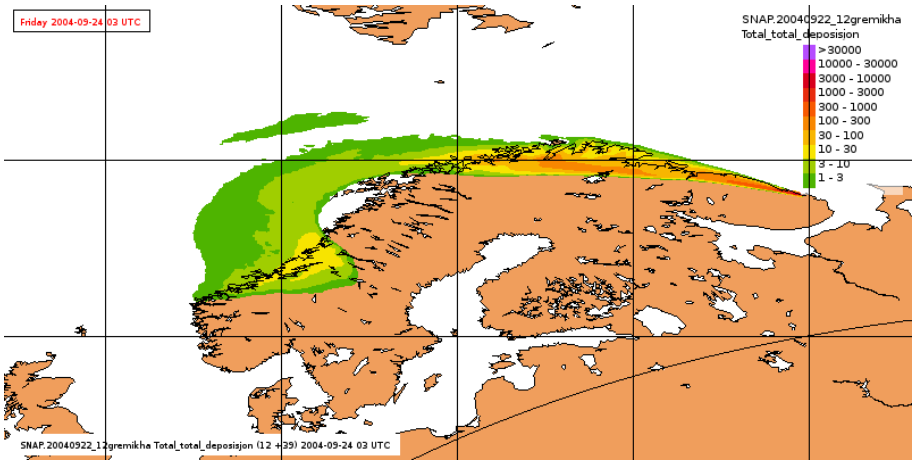

42 hours after accident start

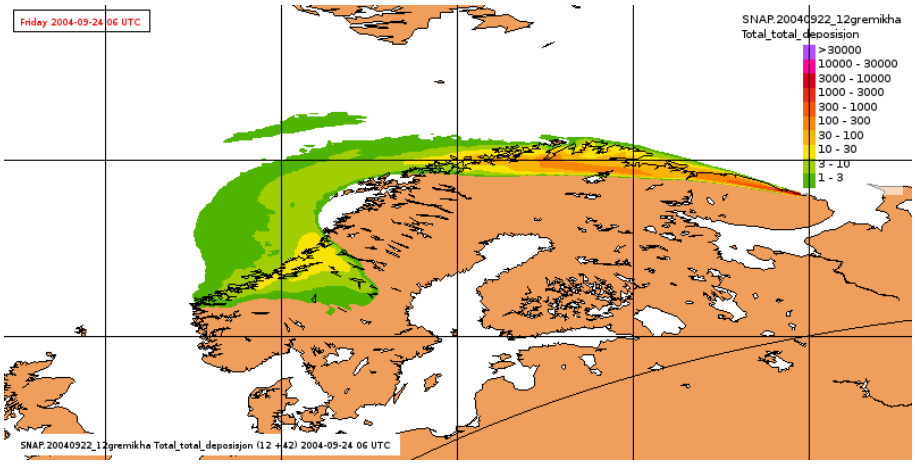

45 hours after accident start

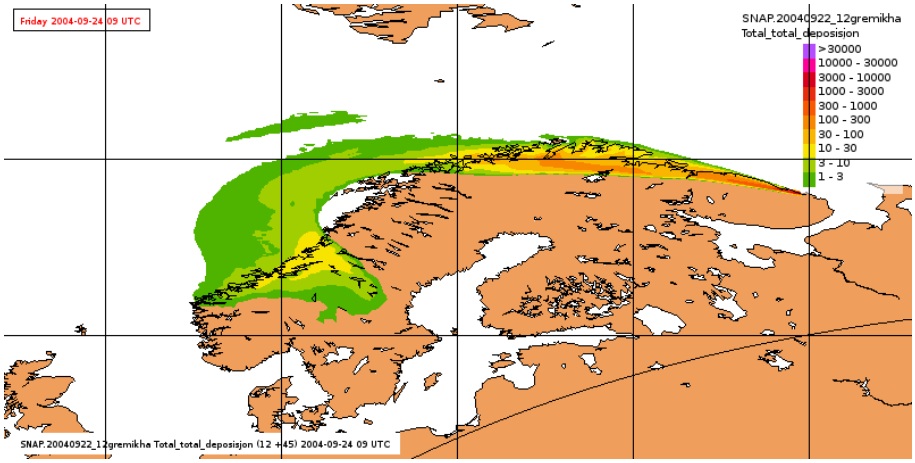

48 hours after accident start

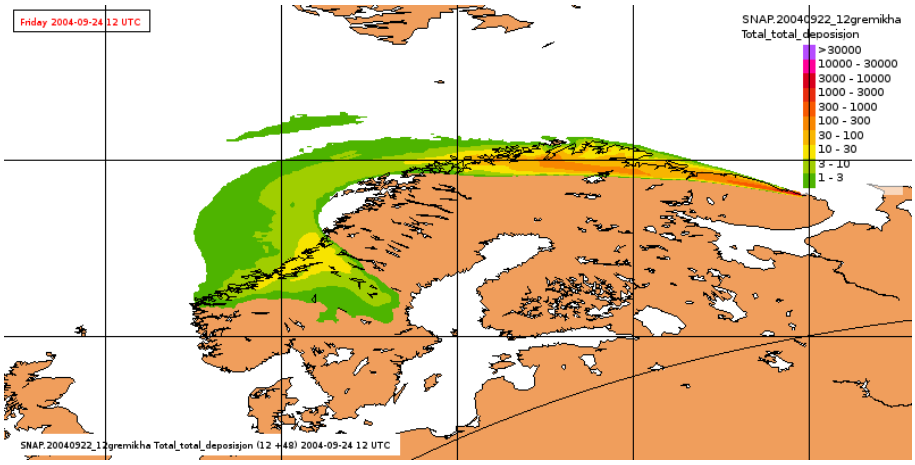

51 hours after accident start

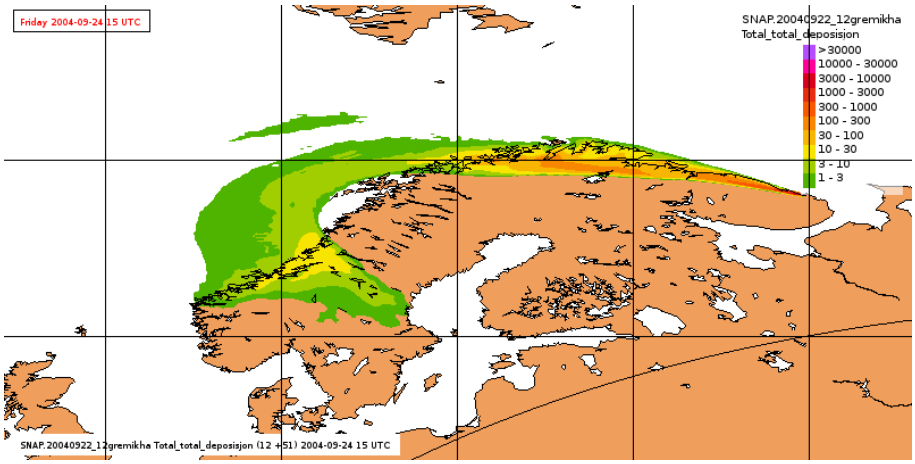

54 hours after accident start

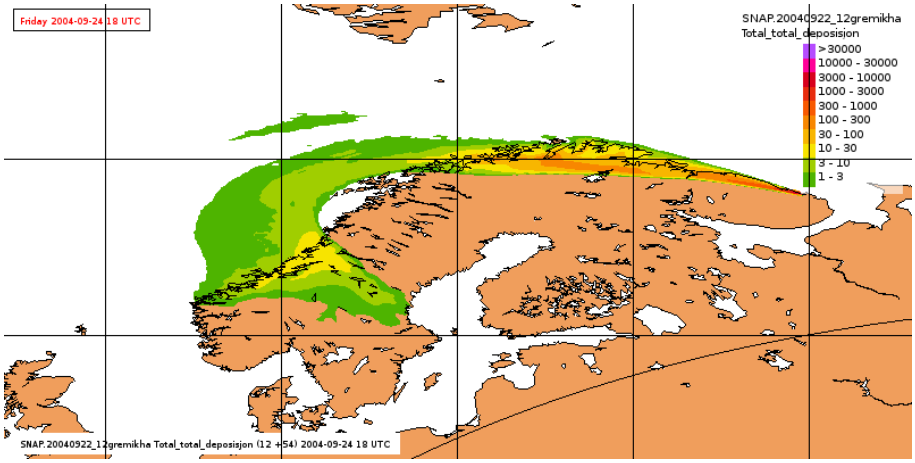

C. Evolution of the total deposition field for the worst case scenario

57 hours after accident start

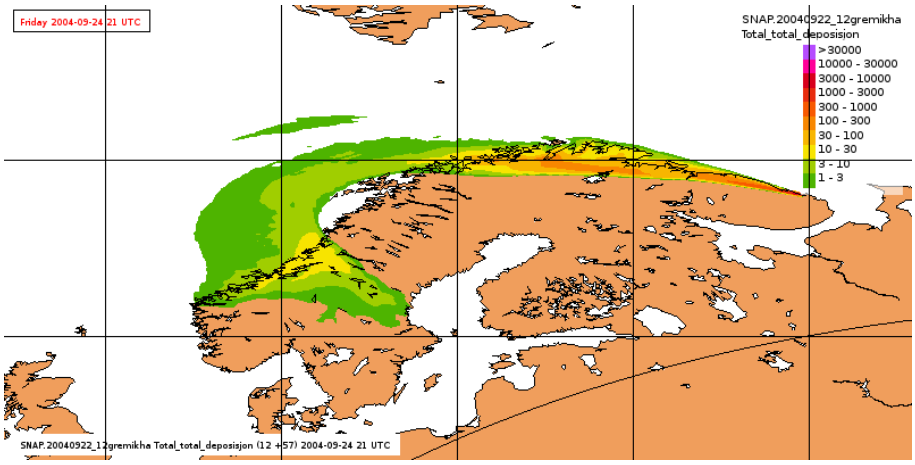

60 hours after accident start

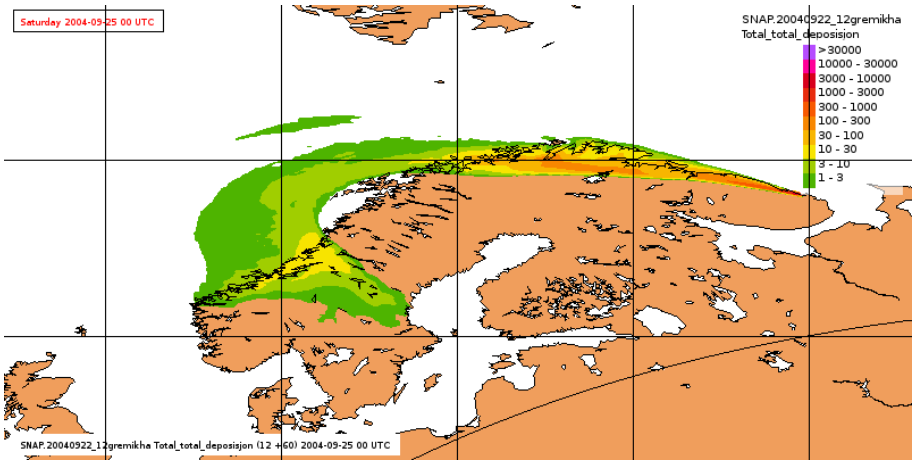

63 hours after accident start

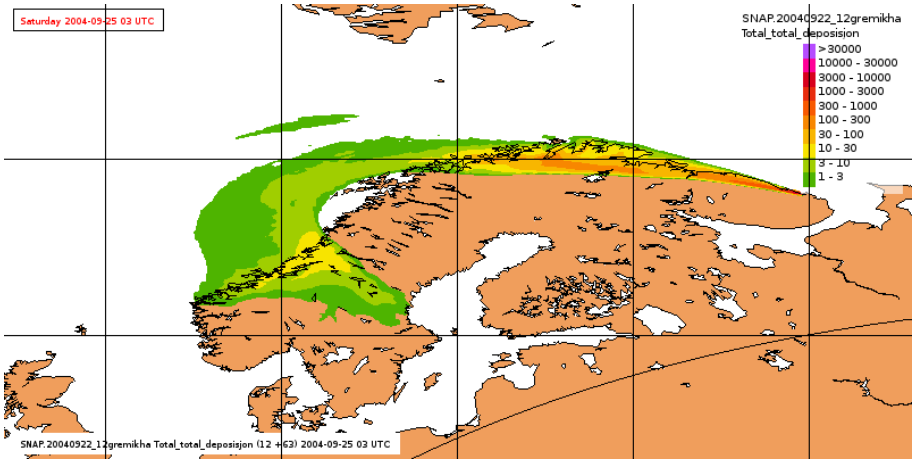

66 hours after accident start

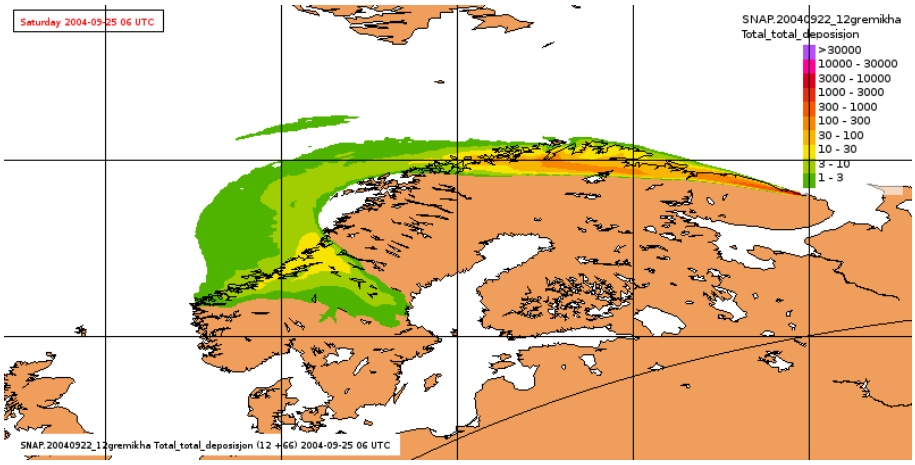

69 hours after accident start

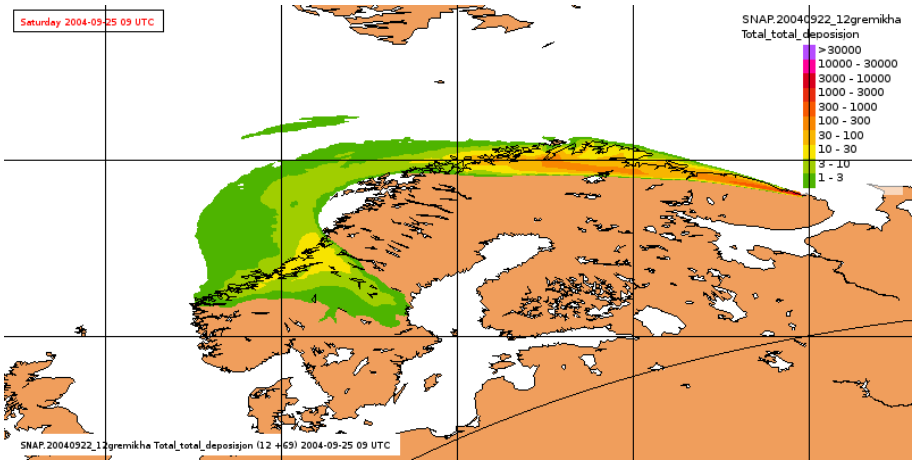

72 hours after accident start

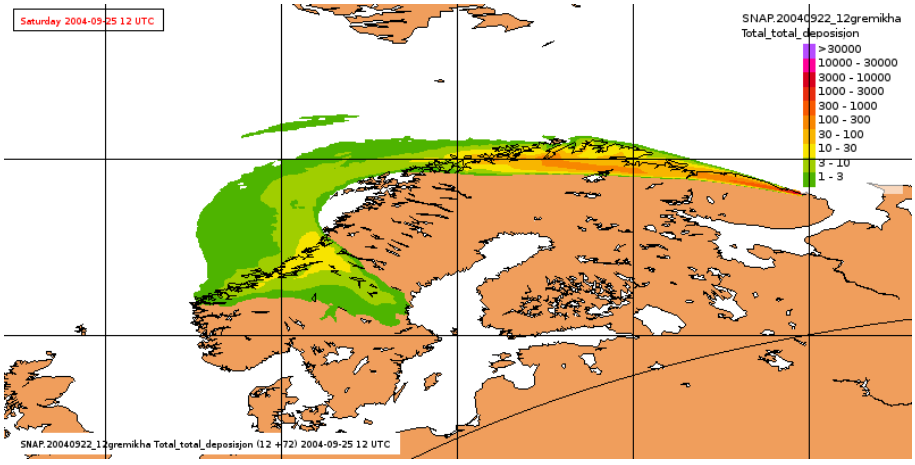

C. Evolution of the total deposition field for the worst case scenario

75 hours after accident start

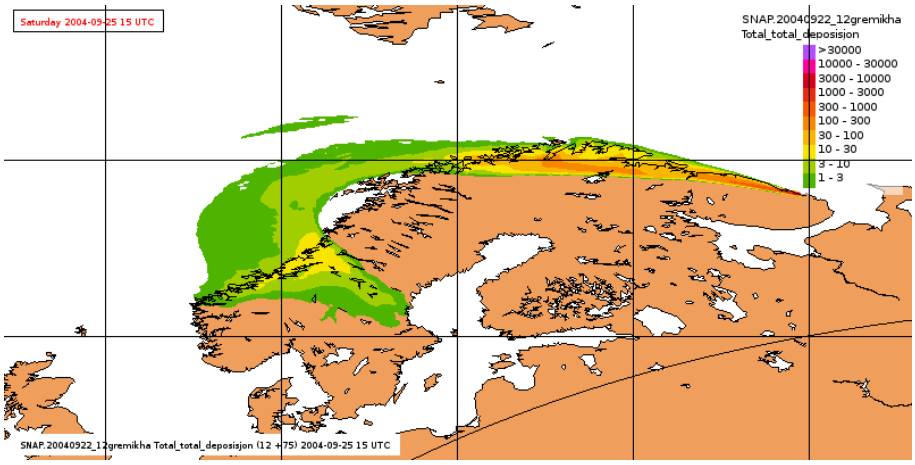

78 hours after accident start

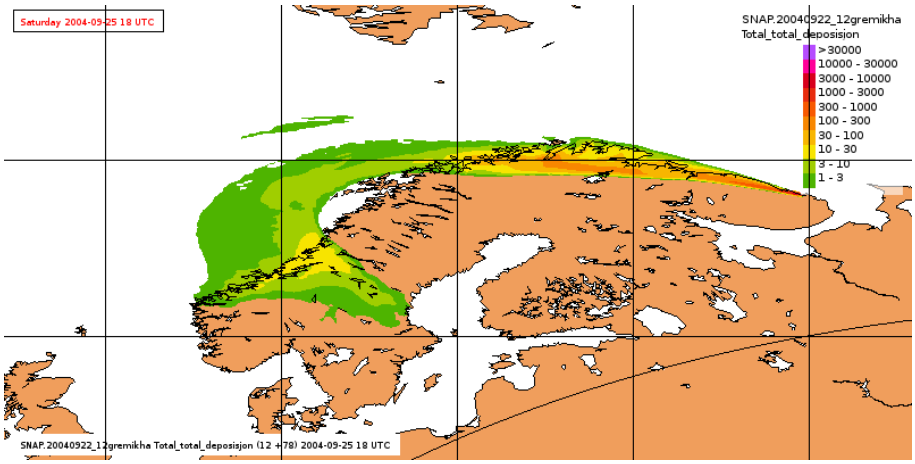

81 hours after accident start

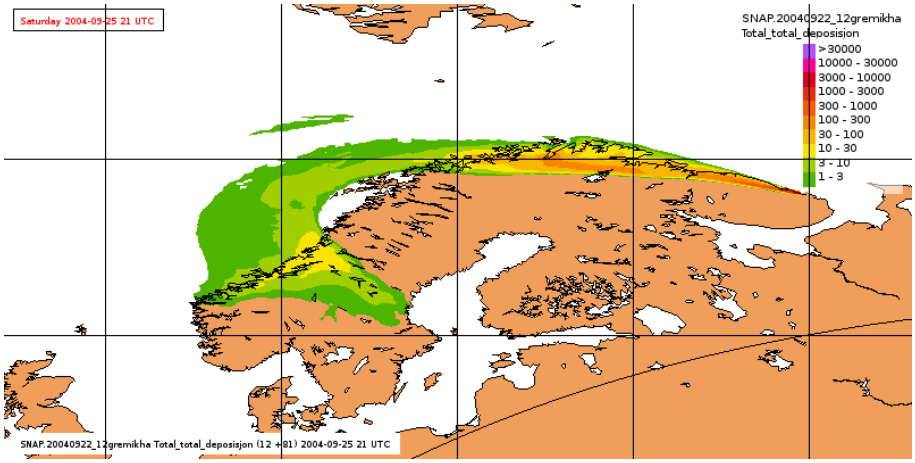

84 hours after accident start

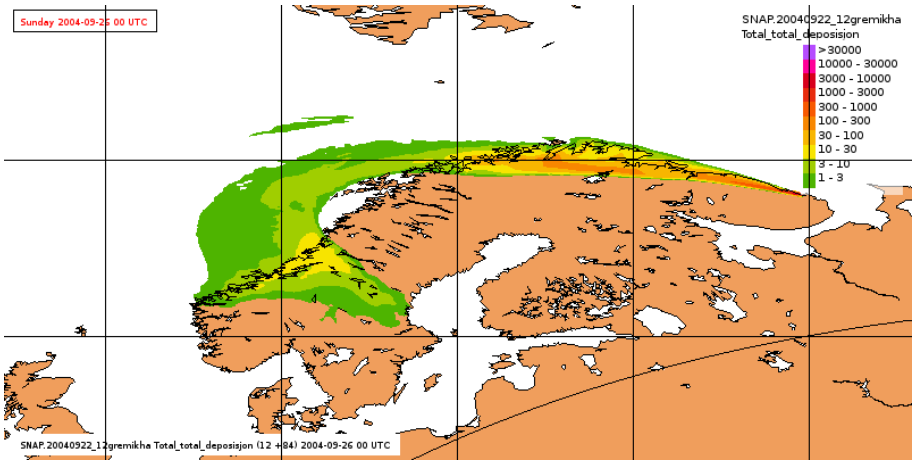

87 hours after accident start

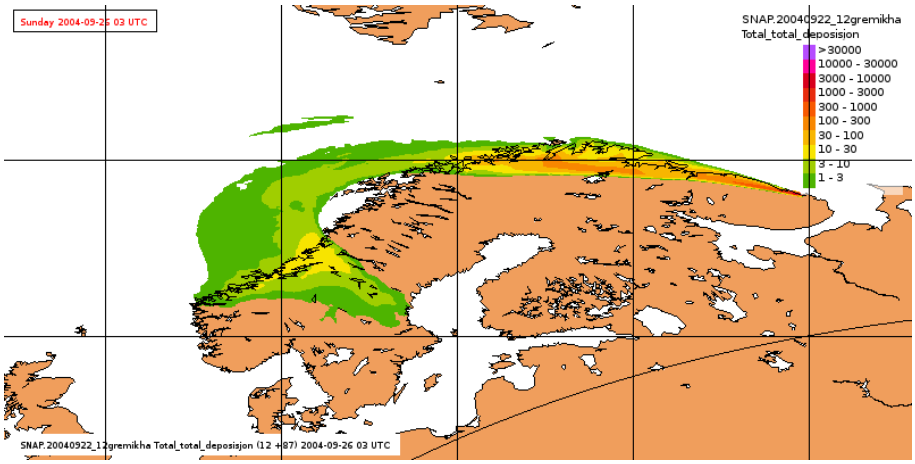

90 hours after accident start

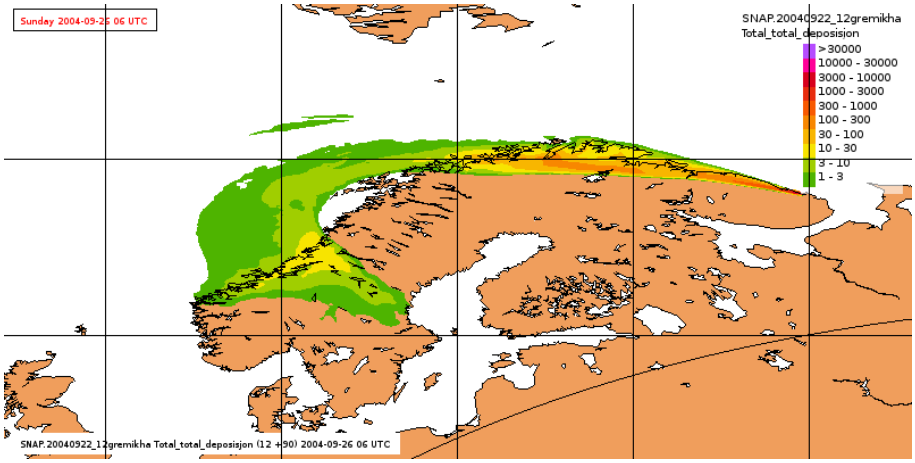

93 hours after accident start

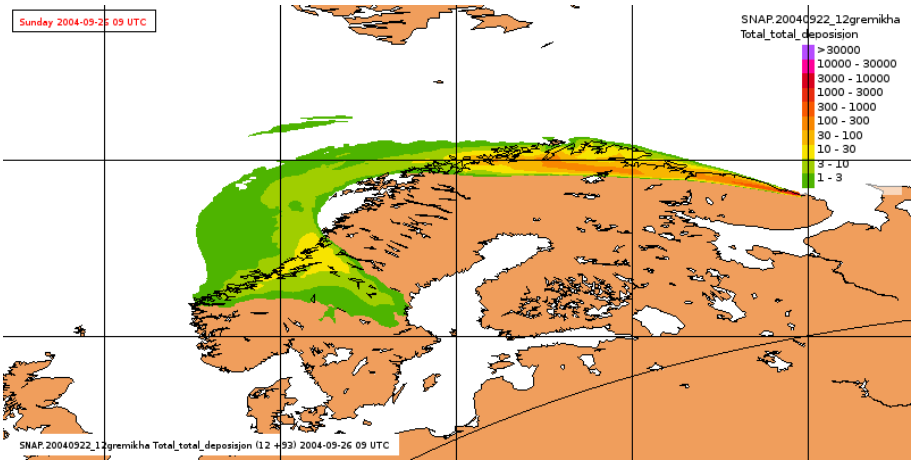

96 hours after accident start